

**Sustainable Gas Separation by Application of Natural Zeolites as  
Membranes and Adsorbents**

By  
Afrooz Farjoo

A thesis submitted in partial fulfillment of the requirements for the degree of

Doctor of Philosophy

in

Chemical Engineering

Department of Chemical and Materials Engineering

University of Alberta

©Afrooz Farjoo, 2016

## **Abstract**

The objective of this research was to develop new molecular sieve materials and to study their applications in membrane as well as adsorptive gas separation processes.

Membrane based processes have the potential to surpass the limitations of conventional gas separation techniques such as energy intensiveness, environmental concerns and possibly affordability. Natural zeolite membranes have recently been shown to demonstrate potential in separation of H<sub>2</sub> from H<sub>2</sub>/CO<sub>2</sub> mixtures or H<sub>2</sub>/light hydrocarbon mixtures and can be utilized to develop high performance molecular sieve membranes with advanced separation characteristics. In the previous work of this research team, disk membranes produced from dense natural clinoptilolite zeolite rocks showed high performance in gas separation. In this work, membranes from natural clinoptilolite powders are designed, studied and scaled up in disk and tubular configurations for gas separation applications. The membranes' permeation, separation performance and separation mechanisms were evaluated using different characterization methods and tests at several operating conditions.

The results showed that natural zeolite membranes such as compact disk or coated stainless steel tubular ones, have great potential for large-scale gas separation at high temperature and pressures. To evaluate the potential of membranes in industrial applications, single versus multi-component gas permeance was compared and discussed.

In another study, a new adsorbent for the adsorptive separation of ethylene from ethane as one of the most energy intensive separations was created by incrementally changing the pore size of clinoptilolite. The structure of a naturally occurring clinoptilolite was modified through ammonium exchange, calcination, and post-calcinations steam

treatment. The results demonstrated the potential to use steamed clinoptilolite and to increase the efficiency of the adsorptive separation of ethane/ethylene.

Results of this work suggest that natural zeolites can be employed as high performance membranes and be modified as unique adsorbents for enhanced gas separation purposes.

With further research, natural zeolites can be developed into economically viable membranes and adsorbents for several industrial applications.

## **Preface**

Most of the research conducted for this thesis is in collaboration with NOVA Chemicals Corporation (Center for Applied Research) in Calgary and it was led by the principal investigator, Dr. Steven M. Kuznicki, at the University of Alberta,

The technical apparatus referred to in chapter 5-7 were designed by this thesis author (Afrooz Farjoo) with the support of Weizhu An at the University of Alberta. The data analysis and conclusion are Afrooz Farjoo's work, as well as the literature review in chapters 1-2 and 4.

Chapter 3 of this thesis has been published as A. Farjoo, J. Sawada, and S. Kuznicki, "Manipulation of the pore size of clinoptilolite for separation of ethane from ethylene" *Journal of Chemical Engineering Science*, 2015, 138, 685-688. In this paper, Afrooz Farjoo was responsible for the data collection and analysis as well as the manuscript preparation. James Sawada contributed to manuscript correction and review. Dr. Steven M. Kuznicki was the supervisory author and the principal investigator that was also involved with concept formation and manuscript review.

Chapter 5 of this thesis has been accepted for publication in *Canadian Journal of Chemical Engineering* as A. Farjoo, S. Adamaref, A. Avila and S. Kuznicki, "H<sub>2</sub> separation using pressed clinoptilolite and mixed copper-membranes". In this paper, Afrooz Farjoo was responsible for the data collection and data analysis as well as the manuscript preparation. Adolfo Avila contributed to manuscript preparation and correction. Solmaz Adamaref contributed to part of the data collection and Dr. Steven M. Kuznicki was the supervisory author, the principal investigator, involved with concept development and the manuscript review.

Chapter 6 of this thesis has been accepted for publication in *Canadian Journal of*

Chemical Engineering as: Afrooz Farjoo, Steven Kuznicki, “H<sub>2</sub> separation using tubular stainless steel supported natural clinoptilolite membranes”, In this paper, Afrooz Farjoo was responsible for the data collection and analysis as well as the manuscript preparation. Dr. Steven. Kuznicki was the supervisory author, the principal investigator and was involved with concept development, and the manuscript review.

## **Acknowledgements**

I would like to thank my PhD supervisor, Dr. Steven M. Kuznicki, for his support and mentorship in every step of this research project.

I am also thankful for the assistance and input of Adolfo Avila, Tatyana Kuznicki, Weizhu An and James Sawada during this work.

A very special thank you goes to the Applied Research Centre at NOVA Chemicals Corporation in Calgary for the technical and financial support during all the phases of this research project.

# Table of Contents

<b>Introduction to Zeolites Molecular Sieves .....</b>	<b>1</b>
1.1 Zeolites Molecular Sieves.....	2
1.2 Natural Zeolites.....	4
1.2.1 Clinoptilolite and Heulandite.....	5
1.3 Synthetic Zeolites .....	7
1.4 References.....	8
<b>2. Fundamentals of adsorption and adsorptive gas separation processes .....</b>	<b>11</b>
2.1 The Theory of Adsorption.....	12
2.2 Fundamental Mechanisms of Gas Separation.....	13
2.2.1 Equilibrium Separation .....	13
2.2.2 Kinetic Separation.....	13
2.2.3 Steric Separation .....	14
2.3 Adsorptive Gas Separation Processes.....	14
2.3.1 Adsorbent Design.....	15
2.3.2 Pressure Swing Adsorption .....	15
2.3.3 Temperature Swing Adsorption.....	16
2.4 Henry's Law .....	17
2.5 Selectivity .....	18
2.6 Heat of Adsorption.....	18
2.7 Conclusion.....	19
2.8 References.....	20
<b>3. Manipulation of the Pore Size of Clinoptilolite for the Separation of Ethane from Ethylene.....</b>	<b>22</b>
3.1 Summary .....	23
3.2 Introduction.....	23
3.3 Materials and Methods.....	28
3.3.1 Sample Preparation.....	28
3.3.2 Sample Characterization .....	29
3.4. Results and Discussion.....	31
3.5 Conclusions.....	43
3.6 References.....	44
<b>4. Fundamentals of membranes and membrane gas separation .....</b>	<b>52</b>
4.1 Membrane technology.....	53
4.2 Membrane and membrane separation.....	54
4.3 Zeolite membrane on support .....	55

4.4 Permeation Mechanisms .....	56
4.5 Transport mechanism in zeolite membranes.....	62
4.6 Membrane evaluation and analytical methods.....	63
4.7 References.....	65
<b>5. Pressed clinoptilolite and copper-clinoptilolite disk membranes for hydrogen separation .....</b>	<b>71</b>
5.1 Summary.....	71
5.2 Introduction.....	71
5.3 Material and methods.....	74
5.3.1 Preparation and characterization of membranes .....	75
5.3.2 Mixed clinoptilolite-copper composite membranes.....	76
5.3.3 Gas Separation Tests.....	79
5.3.4 Membrane Screening based on the Relative Averaged Defect Size.....	81
5.4 Results and Discussion.....	82
5.4.1 Gas permeation through pressed clinoptilolite disks.....	82
5.4.2 Mixed clinoptilolite-copper composite membrane.....	87
5.4.3 Comparison of permeation results between both types of membrane disks.....	87
5.5 H <sub>2</sub> selectivity enhancement.....	91
5.6 Conclusions.....	93
5.7 References.....	94
<b>6. Composite Coated Stainless Steel Tubular Membranes for Gas Separation.....</b>	<b>103</b>
6.1 Summary.....	103
6.2 Introduction.....	104
6.3 Experimental.....	107
6.3.1 Materials.....	107
6.3.2 Preparation and Characterization of Membranes.....	108
6.4 Gas Separation Tests.....	111
6.5 Relative Average Defect Size .....	113
6.6 Results and Discussions .....	114
6.6.1 Single Layered Membranes.....	117
6.6.2 Double Layered Membranes.....	120
6.7 H <sub>2</sub> Selectivity Enhancement.....	126
6.8 Conclusion.....	128
6.9 References.....	130
<b>7. Single and multi-component transport through metal supported clinoptilolite membranes.....</b>	<b>140</b>
7.1 Summary.....	140
7.2 Introduction.....	140
7.2.1 Classification of gas mixtures.....	142

7.3 Experimental.....	143
7.3.1 Error propagation.....	145
7.4 Results and Discussion.....	146
7.5 Adsorption Parameters.....	153
7.6 Conclusion.....	156
7.7 References.....	158
<b>8. Conclusions and Future Work .....</b>	<b>162</b>
8.1 Conclusions.....	162
8.2 Recommendations for Future Work.....	164
Complete list of references.....	168

## List of Tables

Table 1-1 Kinetic Diameter of some gases molecules.....	3
Table 3-1 EDX data for the as received natural zeolite sample.....	32
Table 3-2 Unit cell volume based on the calculated unit cell constants.....	37
Table 3-3 IGC retention times for the adsorption of ethylene and ethane on raw, cation exchanged and steamed clinoptilolite.....	38
Table 3-4 Henry's Law selectivity for the raw and treated samples.....	41
Table 5-1 Energy-dispersive X-ray (EDX) data for the natural clinoptilolite sample (norm wt %). .....	75
Table 5-2 Comparison of H <sub>2</sub> permeability of different inorganic membranes.....	89
Table 5-3 Comparative Parameter for CLI and Cu-CLI disk membranes.....	91
Table 6-1 Energy-dispersive X-ray (EDX) data for the natural zeolite samples.....	107
Table 6-2 Particle size distribution analysis of the zeolite powder and coating slurry...	116
Table 6-3 Comparative parameter ( $\lambda = \alpha_v/\beta_{kz}$ ) for single layered and double layered tubing membranes.....	124
Table 7-1 Thermal conductivity of gases at 25 °C.....	145
Table 7-2 Uncertainty associated with each source of error.....	146
Table 7-3 Values of the adsorption parameters, for the various components at 70 °C, obtained from a fit with the Langmuir isotherm.....	156

## List of Figures

Figure 1-1 Unit cell structure of the HEU framework (Viewed alongside [001]) .....	6
Figure 2-1 Schematic picture of a pressure swing adsorption cycle.....	16
Figure 2-2 Schematic picture of a temperature swing adsorption cycle.....	17
Figure 3-1 TG analysis of the raw, NH <sub>4</sub> -exchanged/calcined and steamed at 600 °C clinoptilolites.....	33
Figure 3-2 XRD powder patterns for raw, NH <sub>4</sub> -exchanged/calcined and steamed clinoptilolite at different temperatures.....	34
Figure 3-3 Variation of <i>a</i> for as-received, NH <sub>4</sub> -exchanged /calcined and steamed samples at different temperatures.....	36
Figure 3-4 Variation of <i>b</i> for as-received, NH <sub>4</sub> -exchanged /calcined and steamed samples at different temperatures.....	36
Figure 3-5 Variation of <i>c</i> for as-received; NH <sub>4</sub> -exchanged /calcined and steamed samples at different temperatures.....	37
Figure 3-6 Adsorption isotherms for ethylene (red) and ethane (blue) on (a) as-received, (b) NH <sub>4</sub> -exchanged/calcined, (c) steamed at 300 °C, (d) steamed at 400 °C, (e) steamed at 500 °C and (f) steamed at 300 °C clinoptilolite at 25 °C.....	40
Figure 4-1 Different separation mechanisms in membrane.....	57
Figure 4-2 Mass transfer model for the permeation process through a zeolite in a zeolite pore.....	62
Figure 5-1 XRD patterns for natural clinoptilolite samples.....	76
Figure 5-2 a) SEM image of clinoptilolite powders, b) optical microscopy image of Cu-CLI (16x-64X), c) schematic of CLI membrane disks, and d) schematic of Cu-CLI membrane disks.....	78
Figure 5-3 XRD patterns of clinoptilolite, copper and copper oxides in Cu-CLI membrane after heat treatment up to 650 °C for 4 hours.....	79
Figure 5-4 Schematics of the set up for single gas permeation measurements.....	80
Figure 5-5 Single permeance of H <sub>2</sub> , C <sub>2</sub> H <sub>6</sub> and CO <sub>2</sub> through CLI membrane disks as a function of temperature.....	83

Figure 5-6 Single permeance of H <sub>2</sub> , C <sub>2</sub> H <sub>6</sub> and CO <sub>2</sub> through CLI membrane disks at different feed pressures.....	84
Figure 5-7 Permeance of H <sub>2</sub> , CO <sub>2</sub> and C <sub>2</sub> H <sub>6</sub> through CLI disk membrane disks as a function of a) kinetic diameter and b) molecular weight.....	86
Figure 5-8 CO <sub>2</sub> permeance through CLI and Cu-CLI membranes at different feed pressures.....	87
Figure 5-9 C <sub>2</sub> H <sub>6</sub> permeance through CLI and Cu-CLI membranes at different feed pressures.....	88
Figure 5-10 Comparative parameters ( $\alpha_v$ , $\beta_{kz}$ ) for CLI and Cu-CLI membranes, permeate pressure: 108.2 kPa, temperature: 25 °C.....	90
Figure 5-11 a) H <sub>2</sub> /CO <sub>2</sub> and b) H <sub>2</sub> /C <sub>2</sub> H <sub>6</sub> separation selectivities through CLI (solid bars) and Cu-CLI (shaded bars) membranes at different temperatures.....	92
Figure 6-1 Schematic picture of stainless steel support for zeolite membranes.....	108
Figure 6-2 Dip coating procedure using a syringe pump for slurry injection.....	109
Figure 6-3 Membrane formation process on a porous substrate by the capillary suction pressure.....	110
Figure 6-4 Schematic of the set-up for single gas permeation measurements.....	112
Figure 6-5 Gas transport passages through the membrane.....	113
Figure 6-6 XRD patterns of the natural zeolite clinoptilolite powders and the natural zeolite clinoptilolite membrane slurry. ....	115
Figure 6-7 Surface structure of the heat treated slurry taken by SEM.....	117
Figure 6-8 Cross-section of a stainless steel tube, coated with natural clinoptilolite slurry and TiO <sub>2</sub> .....	117
Figure 6-9 Permeance of individual gases through the single-layered membrane at different feed pressures.....	118
Figure 6-10 Permeance of H <sub>2</sub> , CO <sub>2</sub> and C <sub>2</sub> H <sub>6</sub> through single layered tubing membrane as a function of (a) kinetic diameter and (b) molecular weight.....	120
Figure 6-11 CO <sub>2</sub> (a), C <sub>2</sub> H <sub>6</sub> (b), H <sub>2</sub> (c) permeance through single and double layered membranes at different feed pressures.....	123
Figure 6-12 Comparative parameters for single and double-layered membranes.....	124

Figure 6-13 Permeance of individual gases through double-layered membrane at different temperatures.....	126
Figure 6-14 H <sub>2</sub> /CO <sub>2</sub> (a) H <sub>2</sub> /C <sub>2</sub> H <sub>6</sub> (b) separation selectivity through single layered (solid bars) and double layered (shaded bars) membranes at different pressures.....	128
Figure 7-1 Schematic of the set-up for gas permeation measurement.....	144
Figure 7-2 H <sub>2</sub> /C <sub>2</sub> H <sub>6</sub> separation factor in multi component and single gas permeation test through tubular mixed matrix membrane at different feed pressures.....	147
Figure 7-3 H <sub>2</sub> /C <sub>2</sub> H <sub>4</sub> separation factor in multi component and single gas permeation test through tubular mixed matrix membrane at different feed pressures.....	148
Figure 7-4 H <sub>2</sub> /CH <sub>4</sub> separation factor in multi component and single gas permeation test through tubular mixed matrix membrane at different feed pressures.....	148
Figure 7-5 Mixed (Blue), Ideal (Red), Knudsen (green), H <sub>2</sub> /C <sub>2</sub> H <sub>6</sub> separation selectivity through tubular mixed matrix membrane at different temperatures.....	150
Figure 7-6 Mixed (Blue), Ideal (Red), Knudsen (green), H <sub>2</sub> /C <sub>2</sub> H <sub>4</sub> separation selectivity through tubular mixed matrix membrane at different temperatures.....	151
Figure 7-7 Mixed (Blue), Ideal (Red), Knudsen (green), H <sub>2</sub> /CH <sub>4</sub> separation selectivity through tubular mixed matrix membrane at different temperatures.....	151
Figure 7-8 Adsorption isotherms for ethylene (red), ethane and methane on as received clinoptilolite at a) 25 °C, b) 100 °C, c) 200 °C, d) 300 °C and e) 400 °C.....	155

## **Chapter one**

---

### **Introduction to Zeolites Molecular Sieves**

## 1.1 Zeolites Molecular Sieves

Zeolite molecular sieves are microporous crystalline metal oxides that offer a unique arrangement for separating molecules according to their shape and size [1]. Zeolites are synthetic or natural crystalline aluminosilicates with three-dimensional framework structures and uniform pore sizes. Molecular sieve zeolites have been commercially utilized in several processes as catalysts, adsorbents, ion-exchange and purification agents. Classical zeolites and mixed coordination materials also identified as inorganic crystalline molecular sieves have broad industrial applications.

Classical zeolites' structures are four coordinated aluminum and silicon chains in the form of  $AlO_4$  and  $SiO_4$  tetrahedral units. Silica units are not charged and one negative charge is associated with aluminum units to sustain electron neutrality. The most recognized examples of commercial zeolites are: zeolite A, zeolite X and zeolite Y [2].

Originally the majority of zeolites were natural minerals and were formed when volcanic rocks and residues reacted with alkaline ground water or in particular post-depositional conditions for the duration of thousands to millions of years in low marine basins [3],[4]. Examples of natural zeolites are clinoptilolite, chabazite, mordenite, erionite, ferrierite and phillipsite, among them clinoptilolite and chabazite and are largely in use for industrial gas separation [5]. High thermal stability, abundance, and low price of the raw material, outweigh some features of natural zeolites such as non-uniformity and low purity. Adsorptive and transport properties in zeolites can be modified by ion exchange, structural changes or thermal treatment to enhance their separation potentials [6].

The micro-porous frameworks in mixed coordination molecular sieves have interconnected octahedra and tetrahedra. They also have rings of 4-coordinated

tetrahedral silicon atoms connected to parallel chains of 6-coordinated octahedral titanium atoms. While silica units are not charged, titanium chains are associated with the “-2” structural charge. One of the distinguished examples of mixed coordination molecular sieves is the Engelhard Titanium Silicate (ETS-4, ETS-10) [7].

The pore space in zeolites is in the range of 0.3 nm to 1.0 nm which is comparable with the kinetic diameter of gas molecules. This characteristic makes zeolite materials potential candidates in gas separations based on differences in molecular kinetic diameter which is identified as the restrictive cross sectional molecular dimension. Table 1-1 summarizes kinetic diameter for some of the gases used in this study.

**Table 1-1.** Kinetic Diameter of some gases molecules [2],[8],[9]

Gas	Kinetic Diameter (nm)
Helium (He)	0.26
Hydrogen (H <sub>2</sub> )	0.28
Nitrogen (N <sub>2</sub> )	0.36
Oxygen (O <sub>2</sub> )	0.34
Methane (CH <sub>4</sub> )	0.38
Ethane (C <sub>2</sub> H <sub>6</sub> )	0.41
Ethylene (C <sub>2</sub> H <sub>4</sub> )	0.44
n-butane (n-C <sub>4</sub> H <sub>10</sub> )	0.43
Carbon dioxide (CO <sub>2</sub> )	0.33

The steric effect originates from the molecular sieving characteristic of zeolites according to the uniform pore size in crystalline structure. Molecular exclusion is based on the diversity in molecular pore size. Only suitably shaped molecules can diffuse into

the adsorbent while other molecules are entirely excluded. Titanosilicate ETS-4 with a typical pore size in the range of 3-5Å that can be tailored to exclude methane with a kinetic diameter of 3.8 Å from nitrogen with a kinetic diameter of 3.6 Å [10].

## 1.2 Natural Zeolites

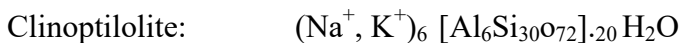
Zeolites have been known for over two centuries and initially their properties were not considered as unique ones. Commercial applications of natural zeolites are relatively recent and have received increasing research interest over the past decades. Current categorization and application of natural zeolite crystals have become an interdisciplinary study that involves physics, chemistry, petrology, geology and engineering [4]. The common natural zeolite frameworks' formula is as follows [4]:



The component of the formula in square brackets represents the tetrahedral framework of the zeolite with a negative structural charge [4]. Transferable cations are critical to balance the structure with negative charge. Cations in the above formula, split by commas in round brackets, show that they are transferable with one another [4]. A monovalent cation may exchange with another monovalent cation and the same approach applies for divalent cations. A single monovalent cation cannot substitute a single divalent one. Keeping charge neutrality requires two monovalent cations to substitute a single divalent cation. The compositions of naturally occurring zeolites vary extensively with the primary constraint of  $\text{Si} \geq \text{Al}$ , as it is possible to replace only each second silica with aluminum in the tetrahedral framework [2].

### 1.2.1 Clinoptilolite and Heulandite

The heulandite framework (HEU) is considered as one the most common naturally occurring zeolitic frameworks [10], [12]. The HEU framework has parallel 8- and 10-member rings with a cross channel that contains 8-member ring [13],[14]. The parallel 8- and 10- member rings have pore diameters of 4.1-4.7 Å and 4.4-7.2 Å respectively [13]. The 8 member-ring cross channel has a pore diameter of 4.0-5.5 Å [13]. Synthesizing HEU materials in the laboratory is technically challenging, therefore, less pure and as a result less expensive natural materials are used more commonly [14], [15]. Clinoptilolite is a natural zeolites from the heulandite category [16]. Clinoptilolite and heulandites, both share the HEU structural framework. In 1822, HEU was called after H. Heuland, the English mineralogist [4]. Clinoptilolite was known more than a century after heulandites in 1932 [17]. It was given the name “clinoptilolite” thanks to its distinguishing inclined edges and similarity to mordenite [17]. Currently, both heulandite and clinoptilite have industrial applications because of their low price and abundance while they still propose the unique features of zeolitic materials [4,11,17]. The formulas for clinoptilolite and heulandite are as follows [13]:



One approach to distinguish different types of zeolites such as clinoptilolite and heulandites is comparison of the cationic content [18]. Yet this measure is not necessarily valid when clinoptilolite and heulandite change into one another through different processes such as ion exchange. The Structural Commission of the International Zeolite

Association (IZA) assigns the HEU code to both of the clinoptilolite and heulandite framework structures, however heulandite acquired the HEU code earlier than clinoptilolite as it was found first [8].

Both Heulandite and clinoptilolite share the same HEU framework. IZA defines zeolite structures as clinoptilolite when the Si/Al ratio is larger than 4, and as heulandites when this ratio is less than 4 [8]. Clinoptilolite framework structure has a 2-dimensional system of intersecting channels that are 8- or 10- member rings [A (c-axis,  $4.4 \times 7.2\text{\AA}$ ), B (c-axis,  $4.7 \times 4.1\text{\AA}$ ) and C (a-axis,  $5.5 \times 4.0\text{\AA}$ )] [2]. Figure 1-1 shows the HEU unit cell structure.

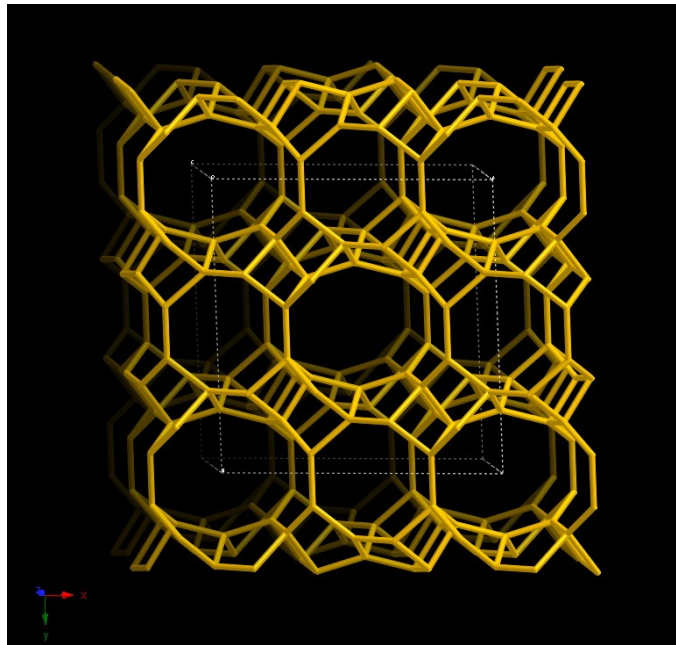


**Figure 1-1.** Unit cell structure of the HEU framework (Viewed alongside [001])

[Database of Zeolite Structures: [america.iza-structure.org/IZA-SC](http://america.iza-structure.org/IZA-SC)]

### **1.3 Synthetic Zeolites**

Zeolite A is believed to be the first synthetic zeolite that was formed in corrosive conditions through gradual crystallisation of silica-alumina gel. Zeolite A was first announced as a synthetic zeolite in 1948 by Milton [19].

Since 1948, more than 100 synthetic zeolites have been developed for many of which there is no natural comparable zeolite. Crystal sizes of synthetic zeolite are most likely smaller than their natural comparables, however there are more pure and uniform, making them unique candidates as catalysts or as adsorbents [1, 2, 19]. Synthesis processes in zeolites are described in detail by Cundy [1].

Natural or synthetic zeolites are employed commercially in catalytic reactions, adsorption, ion exchange and membrane separation applications [19].

This work focuses on developing novel molecular sieve materials and applying them in adsorptive gas separation in particular for energy intensive separations such as ethane and ethylene as well as developing inorganic ceramic membranes for gas separation processes. Chapter two reviews the fundamentals of adsorption and adsorptive gas separation processes. Chapter three describes the kinetic separation of ethylene and ethane and introduces a novel adsorbent for exclusive separation of ethane and ethylene.

After reviewing membranes and fundamentals of gas separation in membranes in chapter four, chapters five to seven focus on coated composite zeolite membranes in different configurations such as disk or tubular in addition to single against multi-component gas separation mechanisms in membranes. Finally, the dissertation is finished with chapter eight, which highlights the key outcomes of this research program and recommends the potential future work.

## 1.4 References

- [1] C. S. Cundy and P. a. Cox, "The hydrothermal synthesis of zeolites: Precursors, intermediates and reaction mechanism," *Microporous Mesoporous Mater.*, vol. 82, no. 1–2, pp. 1–78, 2005.
- [2] D.W. Breck, "Zeolite Molecular Sieves: Structure, Chemistry, and Use," no. John Wiley & Sons, Ltd, 1974.
- [3] M. W. Ackley, S. U. Rege, and H. Saxena, "Application of natural zeolites in the purification and separation of gases," *Microporous Mesoporous Mater.*, vol. 61, pp. 25–42, 2003.
- [4] G. Gottardi and E. Gallim, "*Natural Zeolites*", Germany: Springer-Verlag Berlin Heidelberg, 1985.
- [5] W. Ackley, Mark, S. U. Rege, and H. Saxena, "Application of natural zeolites in the purification and separation of gases", *Microporous Mesoporous Mater.*, vol. 61, pp. 25–42, Jul. 2003.
- [6] A. W. Thornton, T. Hilder, A. J. Hill, and J. M. Hill, "Predicting gas diffusion regime within pores of different size, shape and composition", *J. Memb. Sci.*, vol. 336, pp. 101–108, Jul. 2009.
- [7] Steven Kuznicki and Kathleen A. Thrush, "Large pored molecular sieves with charged octahedral titanium and charged tetrahedral aluminum", *US005244650A*, 1993.
- [8] L. B. Mccusker and D. H. Olson, "*Atlas of Zeolite Framework Types*". Elsevier,

2007.

- [9] S. M. Kuznicki, V. Bell, S. Nair, H. W. Hillhouse, R. M. Jacubinas, C. M. Braunbarth, B. H. Toby, and M. Tsapatsis, "A titanosilicate molecular sieve with adjustable pores for size-selective adsorption of molecules", *Nature*, vol. 412, no. 6848, pp. 720–4, Aug. 2001.
- [10] F. A. Mumpton, "*Mineralogy and Geology of Natural Zeolites*", Washington, D.C.: Mineralogical Society of America, 1977.
- [11] W. An, P. Swenson, L. Wu, T. Waller, A. Ku, and S. M. Kuznicki, "Selective separation of hydrogen from C1/C2 hydrocarbons and CO2 through dense natural zeolite membranes", *J. Memb. Sci.*, vol. 369, no. 1–2, pp. 414–419, Mar. 2011.
- [12] D. L. Bish and M. D.W., "Natural Zeolites: Occurrence, Properties, Application", *Rev. Miner. Geochemistry*, vol. 45, 2001.
- [13] D. Zhao, K. Cleare, C. Oliver, C. Ingram, D. Cook, R. Szostak, and L. Kevan, "Characteristics of the synthetic heulandite-clinoptilolite family of zeolites", *Microporous Mesoporous Mater.*, vol. 21, no. 4–6, pp. 371–379, 1998.
- [14] S. Satokawa and K. Itabashi, "Crystallization of single phase (K, Na) - clinoptilolite," *Microporous Mater.*, vol. 8, pp. 49–55, 1997.
- [15] A. Ansón, S. M. Kuznicki, T. Kuznicki, T. Haastrup, Y. Wang, C. C. H. Lin, J. A. Sawada, E. M. Eyring, and D. Hunter, "Adsorption of argon, oxygen, and nitrogen on silver exchanged ETS-10 molecular sieve", *Microporous*

*Mesoporous Mater.*, vol. 109, no. 1-3, pp. 577-580, 2008.

- [16] W. T. Schaller and U. S. Geological, "The Mordenite-Ptilolite Group; Clinoptilolite, a New Species", *Mineral. Soc. Am.*, vol. 8, pp. 128-134, 1923.
- [17] A. Julbe, "Zeolite membranes-synthesis, charactersitic and application" in "*Intorduction to zeolite science and practices*", Elsevier B.V., 2007.
- [18] A. Dyer, "*An Introduction to Zeolite Molecular Sieves*", John Wiley, Chichestar, 1988.
- [19] R. Szostak, "*Handbook of Molecular Sieves: Structures*", New York: Van Nostrand Reinhold, 1992.

## **Chapter Two**

---

### **Fundamentals of adsorption and adsorptive gas separation processes**

## 2.1 The Theory of Adsorption

Adsorption is an impulsive thermodynamic process taking place when liquid or gas molecules build up on the surface of a solid adsorbent and form a film of atoms or molecules identified as adsorbate. In gas adsorption process on porous materials such as zeolite molecular sieves, the gas phase is essentially concentrated in the interior channels of the porous framework where surface adsorption may also happen.

Adsorption that is associated with the diffusion of a substance into the solid materials is a result of surface energy and is different from absorption. In adsorption, a gas molecule close to a solid surface experiences low potential energy as a consequence of interaction with atoms or molecules in the solid phase. As a result, the gas molecules have a tendency to concentrate in solid region where the molecular density in the area of the surface is significantly larger than the gas phase [1], [2].

The effectiveness of the surface forces depends on the nature of the adsorbate and the adsorbent. If the forces are comparatively weak (only Van der Waals interactions) complemented with polar or quadrupolar groups by electrostatic forces (e.g. dipole or quadrupole interactions, etc), it is recognized as physical adsorption [1]. If the interaction forces are strong and involve a major extent of electron transfer, it is recognized as chemical adsorption which is restricted to a monolayer, while in physical adsorption, multiple molecular layers can also be formed [2].

Gas adsorption is commonly used in chemical processing applications for gas separation and purification. Examples of solid adsorbents in adsorptive gas separation are activated carbons, zeolite molecular sieves, activated alumina, silica gels, and synthetic resins.

## **2.2 Fundamental Mechanisms of Gas Separation**

Adsorptive separation of gas mixtures on porous solids such as zeolites is mainly by one of the below major separation mechanisms or a combination of some of them [4], [5]:

- Equilibrium Separation
- Steric Separation
- Kinetic Separation

### **2.2.1 Equilibrium Separation**

Equilibrium separation is the most common mechanism of adsorptive gas separation. It is based on the differences in the interaction between the competitive adsorbates and the adsorbent controlled by thermodynamics and electrostatics laws.

Equilibrium selectivity and capacity are the key features associated with equilibrium separation. While the equilibrium selectivity is the separation factor at equilibrium conditions, the capacity of the adsorbent depends on two corresponding factors of surface area and porosity.

An example of equilibrium separation is oxygen production from air by means of Li-LSX zeolite [6]. Li-LSX with considerably higher affinity for nitrogen than oxygen separates a pure flow of oxygen when air passes through the zeolite bed as adsorbent.

### **2.2.2 Kinetic Separation**

Kinetic separation is based on the difference in the adsorption rate than equilibrium affinities when one adsorbate group adsorbs quicker than the competitors. The rate of physical adsorption is typically controlled by diffusion restrictions rather than the real rate of equilibration on a surface. Therefore, many equilibrium gas separation processes

are not exclusively equilibrium-based but include a kinetic component associated with mass transfer which is known as “quasi-equilibrium” [7], [8].

Carbon molecular sieves (CMS) correspond to a class of adsorbents that separate molecular groups through the kinetic phenomenon. Kinetic separation is achievable with CMS since it has a range of pore sizes. Such a distribution of pores allows different gases to diffuse at different rates while completely avoiding exclusion of other gases in the mixture. Another example of kinetic separation using carbon molecular sieves is the production of nitrogen from air. The diffusion of oxygen is 30 times faster than nitrogen diffusion in CMS even if the capacity of CMS is comparatively no more than just a fraction of most zeolites. It might appear more reasonable to use CMS for the production of nitrogen from air [9],[10].

### **2.2.3 Steric Separation**

The steric effect is based on the theory that only suitably oriented and small molecules can diffuse into the pores of the adsorbent, whereas other molecules, either because of size or geometry are entirely excluded. Steric separation is originated from the molecular sieving property of zeolites. This is a feature of zeolitic adsorbents since these materials are crystalline and the size of the micropores are determined by the crystal structure. Control of pore size in zeolites can be achieved through cation-exchange method [11], framework anion replacement [12] or structural contraction through de-alumination and steaming processes [13].

## **2.3 Adsorptive Gas Separation Processes**

Adsorptive gas separation processes are classified by their method of regeneration

process. Pressure swing adsorption (PSA) and temperature swing adsorption (TSA) are the more commonly employed processes for gas separation. However, other processes employ purge swing cycles or reactive sorption. Most adsorptive processes use fixed beds while some utilize moving fluidized beds or rotary wheels [14].

### **2.3.1 Adsorbent Design**

Adsorbent in adsorptive gas separation processes offers a particular surface for the selective adsorption of specific gas molecules [10]. A high selectivity is the principal requirement, while a high capacity is also essential to conclude the size of the adsorbent bed and the regeneration process. Since the overall performance of an adsorptive gas separation process depends on both equilibrium and kinetic factors, adsorbent design ought to consider equilibrium properties such as selectivity and capacity as well as the diffusion rates.

### **2.3.2 Pressure Swing Adsorption**

As thermodynamics favor adsorption at higher operating pressures, a pressure swing adsorption cycle is one in which desorption takes place at a pressure much lower than adsorption cycle. Its primary application is for mass separations where contaminants are present at high concentrations. Systems with weakly adsorbed groups are particularly suitable for PSA cycles. Examples of PSA separation are air separation and upgrading of fuel gases.

Pressure swing adsorption (shown in Figure 2.1) can be further categorized into three categories: classical PSA, vacuum swing adsorption (VSA), and vacuum-pressure swing adsorption (VPSA). The main distinction between these three processes is the operating pressure choice. A classical PSA cycle swings between a high super-atmospheric (e.g.

above 1 atm) and a lower super-atmospheric pressure. A VSA cycle swings from a super-atmospheric pressure to a sub-atmospheric (e.g. below 1 atm) pressure. VPSA cycles swing quickly and immediately above and below atmospheric pressure, as a result, it is the most efficient of all the above mentioned PSA categories.

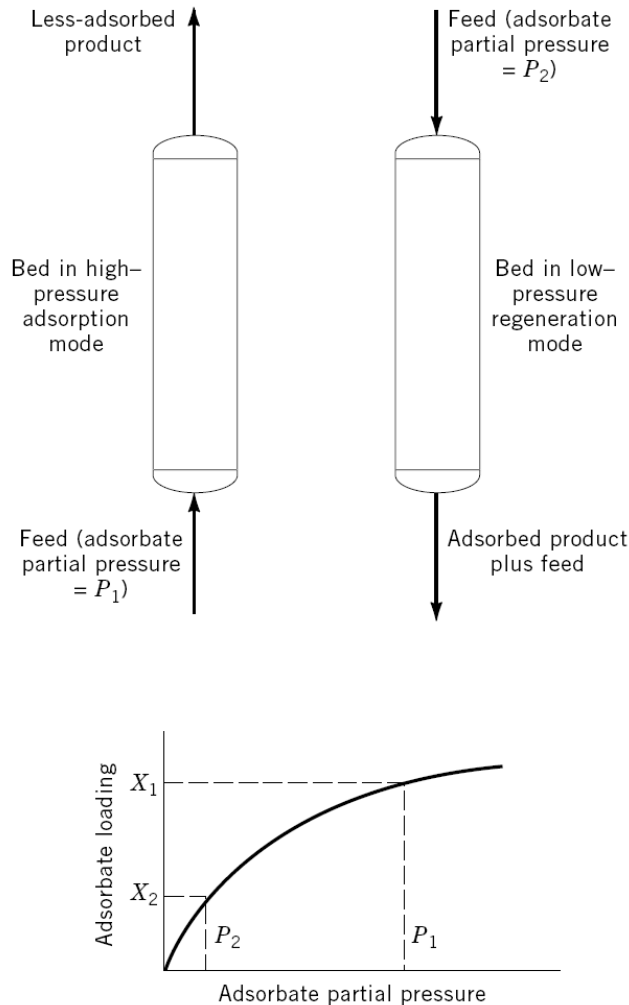


**Figure 2-1.** Schematic picture of a pressure swing adsorption cycle [2].

### 2.3.3 Temperature Swing Adsorption

As thermodynamics favor adsorption at lower operating temperatures, a temperature swing adsorption cycle is a process in which desorption takes place at a temperature

much higher than adsorption. Its main application is for separation at low concentrations (trace-separation) where low concentration of contaminants exists. Systems with strongly-adsorbed groups are particularly suitable for TSA cycles. The applications of TSA (shown in Figure 2-2) separation include sweetening, desiccation, pollution control and carbon dioxide removal [14].

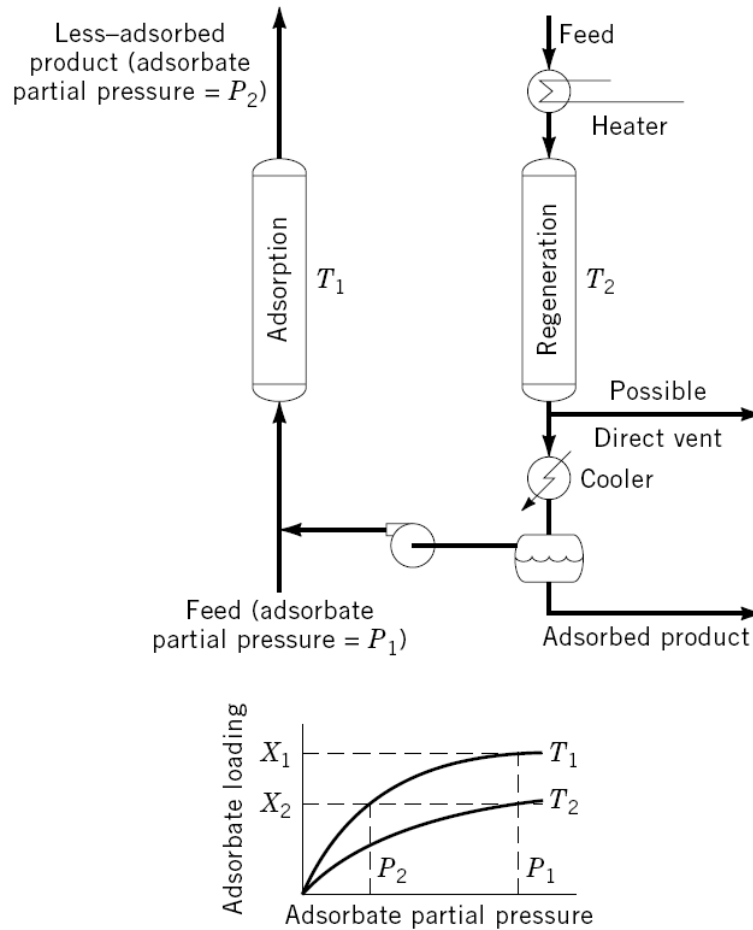


**Figure 2-2.** Schematic picture of a temperature swing adsorption cycle [2].

## 2.4 Henry's Law

The adsorbed layer at the surface of adsorbents thermodynamically might be considered as an individual phase. Equilibrium with the nearby gas or liquid is described by the laws

of thermodynamics. Physical adsorption in the gas phase is an exothermic in which equilibrium favors adsorption at low temperatures and desorption at high temperatures. At adequately low pressures, the equilibrium typically approaches a linear trend known as the Henry's law [15]:

$$v = KP \quad (1)$$

Where the proportionality constant (K) is the Henry's law constant and it decreases with rising temperature. The temperature reliance of the Henry's law constant can be described in terms of the Van't Hoff formula[15]:

$$K = A \cdot \exp\left(-\frac{\Delta H}{RT}\right) \quad (2)$$

Where A is the pre-exponential factor,  $\Delta H$  is the heat of adsorption, R is the gas constant, and T is the absolute temperature.

## 2.5 Selectivity

The separation factor or selectivity in adsorptive gas separation is described as adsorbent's preference to the completing the adsorbates. The limiting selectivity ( $\alpha$ ) or selectivity of gas A over gas B in the Henry's law region, is identified as the ratio of the Henry's law constants of gas A and gas B:

$$\alpha_{(A/B)} = \frac{K_A}{K_B} \quad (3)$$

## 2.6 Heat of Adsorption

Physical adsorption processes are in nature exothermic, as the entropy change ( $\Delta S$ ) and

the free energy change ( $\Delta G$ ) are both negative for the duration of the adsorption process. Therefore, thermodynamics would require the enthalpy change ( $\Delta H$ ), or the heat of adsorption to be negative or exothermic.

The isosteric heat of adsorption,  $\delta H_{iso}$ , is determined from the slope of the adsorption isostere which is a constant adsorbate loading on the graph of  $\ln P$  vs.  $1/T$  by Clausius-Clapeyron equation [15]:

$$\frac{d \ln P}{d\left(\frac{1}{T}\right)} = \frac{\delta H_{iso}}{R} \quad (4)$$

Where,  $R$  is the gas constant,  $P$  is the adsorbate absolute pressure, and  $T$  is the absolute temperature.

## 2.7 Conclusion

Performance of an adsorptive gas separation process depends on material development as the separating agent and adsorption operating conditions that determines the mechanism. Development of new microporous materials is crucial to the chemical processing industry, energy intensive gas separations and the innovation of next-generation adsorptive gas separation applications.

## 2.8 References

- [1] D. M. Ruthven, "Principle of adsorption and adsorption processes." John Wiley & Sons, Inc., 1984.
- [2] Y. Wu, H. Chen, D. Liu, Y. Qian, and H. Xi, "Adsorption and separation of ethane / ethylene on ZIFs with various topologies : Combining GCMC simulation with the ideal adsorbed solution theory ( IAST )," *Chem. Eng. Sci.*, vol. 124, pp. 1–10, 2014.
- [3] R. Szostak, "*Handbook of Molecular Sieves: Structures*", New York: Van Nostrand Reinhold, 1992.
- [4] A. Wender, A. Barreau, C. Lefebvre, A. Lella, A. Boutin, P. Ungerer, and A. H. Fuchs, "Adsorption of n-alkanes in faujasite zeolites: molecular simulation study and experimental measurements," *Adsorption*, vol. 13, no. 5–6, pp. 439–451, 2007.
- [5] A. Ansón, S. M. Kuznicki, T. Kuznicki, T. Hastrup, Y. Wang, C. C. H. Lin, J. A. Sawada, E. M. Eyring, and D. Hunter, "Adsorption of argon, oxygen, and nitrogen on silver exchanged ETS-10 molecular sieve," *Microporous Mesoporous Mater.*, vol. 109, no. 1–3, pp. 577–580, 2008.
- [6] M. W. Ackley, R. F. Giese, and R. T. Yang, "Clinoptilolite : Untapped potential for kinetic gas separations," vol. 12, no. April, pp. 780–788, 1992.
- [7] D. M. Ruthven and S. C. Reyes, "Adsorptive separation of light olefins from paraffins," *Microporous Mesoporous Mater.*, vol. 104, pp. 59–66, 2007.
- [8] M. M. A. Freitas and J. L. Figueiredo, "Preparation of carbon molecular sieves for

- gas separations by modification of the pore sizes of activated carbons,” *Fuel*, vol. 80, no. 1, pp. 1–6, 2001.
- [9] R. T. Yang, "*Adsorbents: Fundamentals and Applications*". John Wiley and Sons, 2003.
- [10] W. An, P. Swenson, A. Gupta, L. Wu, T. M. Kuznicki, and S. M. Kuznicki, “Improvement of H<sub>2</sub>/CO<sub>2</sub> selectivity of the natural clinoptilolite membranes by cation exchange modification,” *J. Memb. Sci.*, vol. 433, pp. 25–31, 2013.
- [11] C. C. H. Lin, J. A. Sawada, L. Wu, T. Haastrup, and S. M. Kuznicki, “Anion-Controlled Pore Size of Titanium Silicate Molecular Sieves,” *J. Am. Chem. Soc.*, no. 131, pp. 609–614, 2009.
- [12] P. Bartl and W. F. Holderich, “A study of the dealumination methods for zeolite L,” *Microporous Mesoporous Mater.*, vol. 38, no. 38, pp. 279–286, 2000.
- [13] G. E. Keller, R. A. Anderson, and C. M. Yon, "*Handbook of Separation Process Technology*", John Wiley & Sons, 1987.
- [14] D. R. Gaskell, "*Introduction to the Thermodynamics of Materials*", Fifth Edit. Taylor and Francis Books Inc.: London., 2003.

## **Chapter Three**

---

# **Manipulation of the Pore Size of Clinoptilolite for the Separation of Ethane from Ethylene**

This chapter has been published in Chemical Engineering Science Journal, 2015 138, 658- 688

### **3.1 Summary**

Naturally occurring zeolites are uniquely useful for small molecule separations due to the effective size of their pores. While the crystal structure of clinoptilolite has large 12-ring pores, the effective pore size of the zeolite excludes molecules larger than  $\sim 0.4$  nm. In this work, the structure of a naturally occurring clinoptilolite was modified through ammonium exchange, calcinations, and post-exchange steam treatment. The ammonium exchange removed some fraction of structural cations, which caused the framework to expand, while steam treatment at  $600$  °C caused a contraction in the structure. The effective pore size of the modified clinoptilolite allowed it to adsorb ethylene and exclude ethane in a dynamic adsorption experiment. By incrementally changing the pore size of clinoptilolite, a new rate-based adsorbent for the adsorptive separation of ethylene from ethane was created.

### **3.2 Introduction**

The separation of ethylene from ethane is carried out on a large scale commercially through cryogenic distillation process. However, for ethane/ethylene separation this process is energy intensive because their boiling points are close (ethane:  $-89$  °C and ethylene:  $-103.7$  °C). In a typical ethylene production plant, a large number of distillation stages and a high reflux ratio are required in order to achieve polymer-grade products, and the process must be operated at low temperatures and high pressures. For example, ethane/ethylene separation is typically performed at  $-25$  °C and 23 bar in a distillation column with over 100 trays [1]. The cracking equipment represents only about 25% of the cost of the process, while remaining 75% is associated with the compression, heating,

dehydration, recovery and refrigeration systems [2]. For the purification of light gases with a relatively low volatility difference, separation by adsorption rather than by distillation can be more energy efficient which is becoming more essential with the rising cost of energy [3], [4].

With increasing global demand for polymers, an increased focus in the production of ethylene is anticipated [5-8] which places further emphasis on decreasing the energy required to produce chemicals. Adsorptive separation using molecular sieves is attractive because it reduces the compression requirements of the process. However, to create an acceptable replacement for distillation the primary difficulty associated with using molecular sieves is their limited selectivity toward ethylene. Low selectivity for the ethylene will negatively affect the purity and recovery of ethylene from the process.

Conventional molecular sieves such as NaX and CaX show a preference for ethylene compared to ethane. However, the selectivity was not high enough to produce high purity ethylene without introducing process complexity and product recycle into the separation process [9], [10]. Other zeolites such as 4A and 5A were also examined. In experimental and modeling study by Mofarahi et al. (2012), zeolite 5A was used for ethylene/ethane separation in pressure swing adsorption processes. The lower the temperature for ethylene composition at a specified pressure, the greater was the ethylene separation by zeolite 5A. This zeolite offered good selectivity up to 50 °C [12], [13]. Romero-Perez et al. (2010) studied kinetic and equilibrium adsorption of CO<sub>2</sub>, C<sub>2</sub>H<sub>4</sub> and C<sub>2</sub>H<sub>6</sub> on zeolite 4A and showed that the gases could be adsorbed reversibly. Unlike CO<sub>2</sub>, the adsorption rate of C<sub>2</sub>H<sub>4</sub> and C<sub>2</sub>H<sub>6</sub> increased with increasing temperature indicating activated diffusion as the rate-controlling process [14]. In the above studies, by using zeolites

(zeolite A), exchanged with divalent cations (calcium) improvements in separation of ethylene from ethane or methane were observed over a wide range of temperatures. The strength of the interaction between the divalent cations in 5A and CaX zeolites and the ethylene double bond was responsible for the stronger selectivity of 5A and CaX zeolites. To improve the zeolites' selectivity toward ethylene the influence of transition metals was explored. The double bond of the olefin can form  $\pi$ -complexes with some transition metals and a difference in adsorption affinity between olefin and paraffin can be achieved [15]. In a study by Miltenburg et al. (2006), NaX crystals with a Si/Al ratio of 1.3 were modified by dispersing CuCl into large NaX crystals. According to single component isotherms of ethane and ethylene on CuCl/NaX, CuCl containing adsorbents are highly selective to the olefin. This strong affinity is completely associated with the  $\pi$ -complex formation of ethylene with  $\text{Cu}^+$  in CuCl and allows a more sustainable process [9]. However, while adsorbents based on Cu (I) are appealing because of their high capacity and specificity toward ethylene, their chemical reactivity toward acetylene component present in trace amounts in a cracked ethane stream makes them impractical to see commercial adoption due to the safety risks [16], [17].

Natural zeolites such as clinoptilolite, chabazite (CHA) or mordenite (MOR) are promising candidates for the separation of ethane from ethylene because their pore size is much smaller than their framework would suggest. For example, while the heulandite framework (HEU) has 12-membered rings, its effective pore size for naturally occurring material is less than 0.4 nm [18]. Clinoptilolite shares the heulandite framework but differs chemically by virtue of its higher Si/Al ratio [19] which imparts a higher degree of thermal and hydrothermal stability to the framework. Having unique small pore structure along with chemical composition, clinoptilolite appears to be one of the most favourable zeolites for gas separations, followed by chabazite and mordenite [20-24].

The pore size of clinoptilolite is comparable to the molecular diameter of a range of small gases, which allows it to act as a “kinetic” molecular sieve and discriminate against molecules based on their size and relative diffusion rates into the framework. Natural zeolites such as clinoptilolite have demonstrated unique performance in commercial kinetic gas separations including O<sub>2</sub> production from air as well as removal of trace levels of N<sub>2</sub>O from air. For application of natural zeolites in air separations, natural zeolites underperformed synthetic zeolites, while clinoptilolite and chabazite outperformed commercially available synthetics in N<sub>2</sub>O removal from air [25]. The purification of natural gas landfill gas and coal gas are kinetic bulk separation applications for natural zeolites. Clinoptilolite allows smaller molecules such as H<sub>2</sub>, CO<sub>2</sub> and N<sub>2</sub> to diffuse in quickly while hindering the diffusion of slightly larger molecules such as methane, ethane or ethylene [25- 28].

As the pore size of clinoptilolite is too small to accommodate either ethane or ethylene, if the pore size of clinoptilolite could be modified to discriminate ethane and ethylene, then

the selectivity would be greater than conventional zeolites without carrying the risks of introducing transition metals into a reactive hydrocarbon stream. This approach is used in this work to modify the pore size of clinoptilolite was to first ammonium exchanging the sieve, calcine the NH<sub>4</sub>-clinoptilolite, and finally steam the zeolite over a range of temperatures to selectively etch out the aluminum. The steaming treatment affects the extent of dealumination and the Si(nAl) units in a tetrahedral aluminosilicate lattice [29],[30], which alters the framework dimensions. Steaming of the structure, dealuminates and increases the ratio of Si/Al and as a result a more stable framework was obtained [31] . Ammonium exchange, calcination and steaming were the steps taken to enrich the structure with silica. As Al–O bond is slightly larger than the Si–O bond, by de-alumination contraction of the structure and reduction of the unit cell constants of the lattice is expected to occur [32-37]. Because the pore size of clinoptilolite is so close to the molecular diameter of small hydrocarbons, a small change in zeolite framework due to dealumination may cause a significant change in the adsorption characteristics of the sieve.

### **3.3 Materials and Methods**

Naturally occurring clinoptilolite was supplied by St. Cloud Mining Company (USA, New Mexico) with the Si/Al molar ratio of 4.13. There are impurities such as quartz in most of the clinoptilolite deposits. These factors reduce the uptake of ions such as ammonium onto natural clinoptilolite [38]. However, based on the supplier's characterization report, the clinoptilolite in this work is of high purity having more than 99 % clinoptilolite without any measurable levels of impurities of chabazite, quartz or smectite.

#### **3.3.1 Sample Preparation**

Modified zeolite was prepared by exchanging 100 g of granular clinoptilolite in an ion exchange column with an ammonium chloride solution. Ion exchange columns have the maximum efficiency for replacement of structural cations by ammonium present in the stripping solution [39-41]. The exchanged ions are eluted from the system and cannot re-equilibrate with the zeolite, which maximizes the  $\text{NH}_4^+$  content in the sieve compared to the other methods of exchange. An electric heating belt attached to the column was used to maintain a constant temperature of  $80\text{ }^\circ\text{C} \pm 2\text{ }^\circ\text{C}$  during the experiment and the column was insulated to reduce heat loss. Based on cation exchange capacity (CEC) of 1.85 mEq/g, 100 g of clinoptilolite was exchanged with an aqueous solution of ammonium chloride prepared by adding 55 g of ammonium chloride in 2 L of de-ionized water. The solution was introduced to the top of the column at a constant rate of 5.5 cc/min and the flow out of the exit of the column was restricted to ensure the flow rate out matched the flow rate into the column. After ion exchange sample was washed thoroughly with de-ionized water and dried at  $80\text{ }^\circ\text{C}$  overnight, the dried material was calcined in static air to

decompose the ammonium ions inside a programmable muffle furnace at atmospheric pressure to 500 °C with the heating rate of 5 °C/min for 11 h.

After calcination steaming treatment at four different temperatures (300 °C, 400 °C, 500 °C and 600 °C) was done. Steaming with water vapour at each temperature was carried out on 20 grams of the ion exchanged samples for 2 h while the samples were placed in quartz tubes and heated with the heating rate of 5 °C/min to the pretreatment temperature inside a programmable tubing furnace under a flow of a nitrogen–steam mixture at a flow rate of 30 mL/min. The nitrogen gas was humidified by passing it through an insulated glass container filled with 200 mL of deionized water placed on an electric heater kept constant at 100 °C. As steam rose out of the container it mixed with the nitrogen flow and was then admitted to the quartz tube. To compare the properties of all samples including the as-received one, 20 g of ammonium-exchanged zeolite was calcined but not steamed.

### **3.3.2 Sample Characterization**

The X-ray diffraction (XRD) patterns were collected to track any possible changes in crystalline morphologies and atomic composition of the materials as well as quantification of crystalline phases using a Rigaku Geigerflex 2173 (Rigaku Corporation, Tokyo, Japan) with a vertical goniometer equipped with a D/Tex detector and a Fe filter. The elemental analysis of the adsorbents was performed using a Zeiss EVO MA 15 (Zeiss, Gottingen, Germany) equipped with a Bruker Silicon Drift Detector for Energy Dispersive X-Ray analysis (EDX). Samples were run using a top-pack mount from 5 to 90° on a continuous scan at a speed of 2°-2 $\theta$  per min with a step size of 0.02°.

Thermal gravimetric analysis (TGA) was performed on the as-received and modified samples to reveal each sample's weight loss with temperature after exposure to ion

exchange and different heat steaming treatments. Data were also used to determine the optimal activation temperature of adsorbents before using them in IGC gas separation test. IGC is a method for characterizing the physicochemical properties of materials as it determines the pore size of the zeolite and affinity of the interaction between a solid and a gas phase. In this study, the as received zeolite, ion exchanged and steamed treated samples was tested with IGC method to determine how ion exchange and dealumination might change the affinity of the adsorbents in gas separation based on applied structural changes. A Q500 (TA Instruments) thermo gravimetric analyzer was used for TGA. The samples were heated at 10 °C/min in argon from 25 °C to 700 °C.

Inverse gas chromatography (IGC) profiles were used to examine the relative affinity of the various samples toward ethane and ethylene. IGC analysis was performed on a Varian 3800 Gas Chromatograph (GC) equipped with a thermal conductivity detector (TCD). Test adsorbents were packed into 10” copper columns with an OD of 0.25”. The columns were filled with 3 g of pelletized adsorbent (20–50 mesh). Carrier gas was helium with flow rate of 30 mL/min. Columns were activated at 350 °C for 4 h under a helium flow of 50 mL/min. At this temperature, the adsorbed water was removed and sieve was considered activated for gas separation tests. Probe gas was introduced by 1 mL pulse injections into the column.

The affinity of the zeolite for a probe gas is proportional to its retention time and the selectivity for the sieve is the ratio of the retention times (adjusted for the dead time of the column) of to probe gases. The selectivity of the adsorbent ( $\alpha$ ) in the Henry’s law region (limiting selectivity) is defined as the ratio of the Henry’s law constants of the pure gas components.

$$\alpha (\text{ethylene/ethane}) = \frac{(T_{\text{Ret}} - T_{\text{Dead}})_{\text{Ethylene}}}{(T_{\text{Ret}} - T_{\text{Dead}})_{\text{Ethane}}} \quad (1)$$

The IGC experiments are dynamic adsorption experiments and the gas has a finite amount of time to diffuse into the sieve before the carrier gas elutes it. The isotherm measurements are expected to allow the gas as much time as required to diffuse into the framework and thus represents the adsorptive characteristics of the sieve at equilibrium.

Ethane and ethylene adsorption isotherms on as received, ion-exchanged and steamed clinoptilolite samples (0–120 kPa) were measured at 30 °C with a Micromeritics ASAP 2020C in its chemisorption configuration. Samples were activated under a flow of 200 ml/min of N<sub>2</sub> to 350 °C and held isothermally for 15 min. The samples were evacuated (10<sup>-4</sup> Pa) for 60 min before being cooled to 30 °C under vacuum. Samples were dosed with fixed quantities of gas until a pressure of 1.14 bar was reached.

### 3.4. Results and Discussion

*EDX.*

EDX result of the as-received zeolite is shown in Table 3-1. Calculated Si/Al ratio equals to 4.13 and the level of trace impurities is below 1 wt%.

**Table 3-1.** EDX data for the as received natural zeolite sample

	<b>EDX Data</b>								
	Na	K	Ca	Mg	Fe	Al	Ti	Si	Si/AL
<b>Clinoptilolite</b>	0.553	0.361	0.047	0.063	0.0601	1	0.0036	4.124	4.125

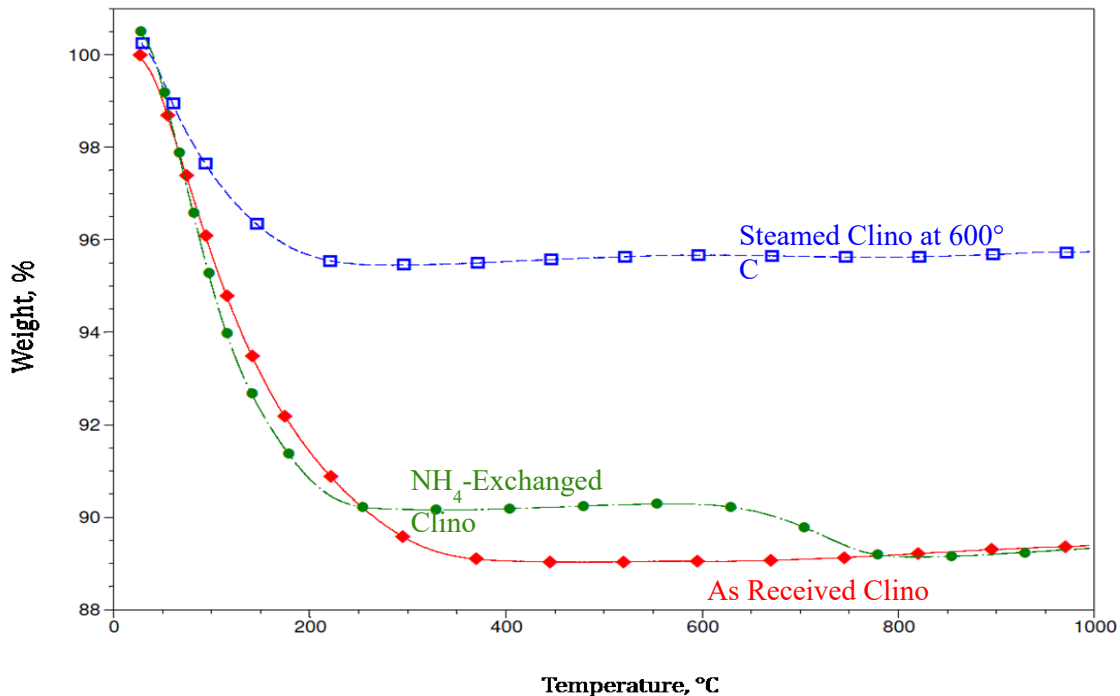
*TGA.*

Figure 3.1 shows TGA profiles of the weights of the samples as the temperature increases. For these samples the profiles can be indicative of the amount of volatile material trapped inside the pores such as either surface or structural water. The secondary loss in  $\text{NH}_4$  exchanged/calcined clinoptilolite profile implies ammonium ion decomposition after the samples were exposed to temperatures higher than  $500\text{ }^\circ\text{C}$ . The TGA analysis for the as-received zeolite showed 4.5% water typical of aluminosilicate molecular sieves that was largely complete by  $350\text{ }^\circ\text{C}$ .

The ammonium-exchanged sample steamed at  $600\text{ }^\circ\text{C}$  showed only a single weight loss event that was complete by  $200\text{ }^\circ\text{C}$  and  $\sim 11\%$  weight loss. The reduction of the dewatering temperature and the lack of a high-temperature weight loss indicated that the majority of the cations in the framework were replaced by protons and the steaming process, by  $600\text{ }^\circ\text{C}$ , dealuminated the crystal structure.

Hydrophobicity of the samples after exposure to different steaming treatments changed water capacity and influenced the water adsorption. Steam treating the samples was expected to be accompanied by dealumination and siliceous zeolite exhibit hydrophobic character [29-35], [42], [43]. For dealuminated/hydrophobic sieves, steamed at  $600\text{ }^\circ\text{C}$ , the pore accommodated less water confirmed by the TGA profile [44-46]. Since by ammonium exchanging the zeolite Al/Si ratio is not changed and in terms of hydrophilicity, the hydrophilicity of the zeolite is the same as before and no obvious change is observed in the profile. The unsteamed sample was previously calcined in air at  $500\text{ }^\circ\text{C}$  yet the

sample shows a discrete weight loss of about 11 % centered on about 700 °C which suggesting the framework contain strong resulting acid sites.



**Figure 3-1.** TG analysis of the raw, NH<sub>4</sub>-exchanged/calcined and steamed at 600 °C clinoptilolites.

*XRD.*

Figure 3.2 presents the XRD results for the as received, ion exchanged and steam treated samples. The XRD results of the as synthesized zeolite do not show any unassigned reflections other than those expected from clinoptilolite. After the various treatments the powder patterns for the treated materials were almost indistinguishable from the parent sieve, which confirms the hydrothermal stability of clinoptilolite.

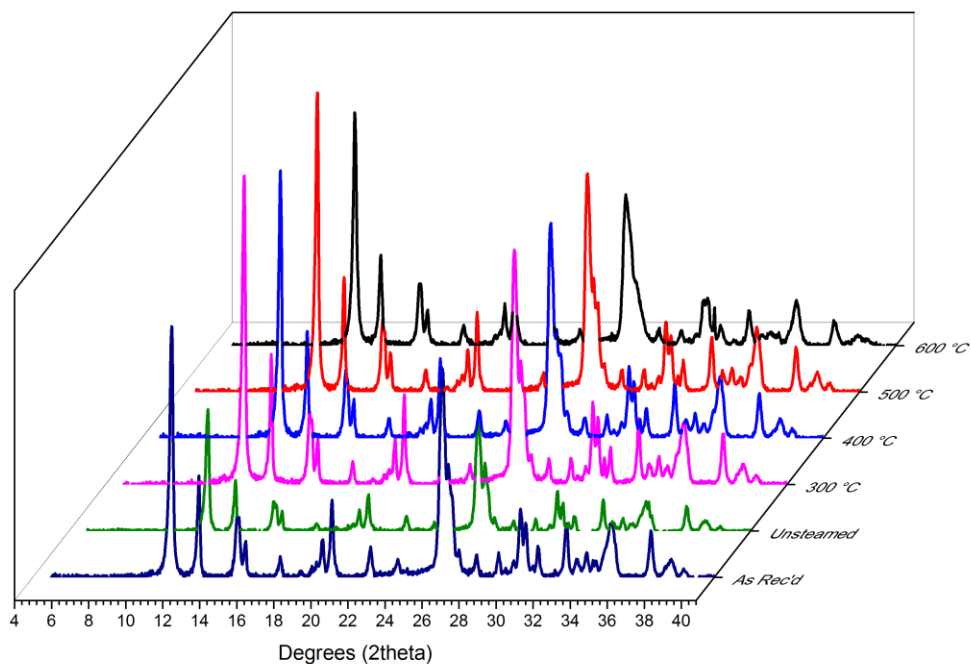


**Figure 3-2.** XRD powder patterns for raw,  $\text{NH}_4^-$ -exchanged/calcined and steamed clinoptilolite at different temperatures.

The ammonium exchanged sample displayed that ion exchange procedures had no significant impact on the clinoptilolite crystal structure, the peak widths and locations match for the raw and ion exchanged zeolites, which was expected because, for hydrated zeolite frameworks, ion exchange and calcination did not change the unit cell dimensions. As the samples were steamed, the crystalline structure of the framework was almost identical. Moreover, the position of the reflections changed, indicating that the dimensions of the unit cell of the zeolite had changed. Although, increase of the steaming temperature up to 600 °C resulted in slightly smaller peaks, however, XRD results confirmed that the modified zeolite had survived the steaming treatment and possessed the same clinoptilolite structure as reported in literature [47],[48].

Contraction of the unit cell dimensions was attributed to the removal of aluminum from the framework connected with the forming of non-framework aluminum groups [31]. Since the average value for a tetrahedral Al-O bond is 1.74 Å, and the average value for a tetrahedral Si-O bond is 1.60 Å, therefore a relation exists between the unit cell constant of the steamed structures and the aluminum content of framework or the steaming temperature. As the framework aluminum concentration in a zeolite decreased, the lattice parameters were expected to decrease [49]. To determine if dealumination took place the lattice parameters of the zeolites were calculated from the XRD patterns. The zeolite unit cell has three lattice length parameters, referred to as *a*, *b*, and *c*. Figures 3.3, 3.4 and 3.5 present the calculated value for *a*, *b* and *c* axis respectively. The angles for the (200, 020, and 002) reflections at 11.52, 12.98, and 15.52  $\theta$ , were used to determine the unit cell size (Å). The pore system for clinoptilolite lies in the (110) plane so changes in the dimensions of either *a* or *b* axes would be expected to influence the pore size. Changes in the *c* direction should have no effect on the size of the pore. Figures 3.3, 3.4 and 3.5 show that the framework did not change isotropically. The *a*-axis was more sensitive to the steaming conditions than *b*-axis and the *c*-axis and was relatively insensitive to the different treatments. The sieve did not change its unit cell size as a function of ion exchange. Above 400 °C, the framework contracted while the *a*-axis returned to the dimension typical of the as-received material through the *b*-axis and showed a step change at 600 °C to a value significantly lower than any other sample. Due to the slight contraction of the framework by steaming treatment, the accessibility of the internal parts of zeolite structure to larger molecules should be reduced.

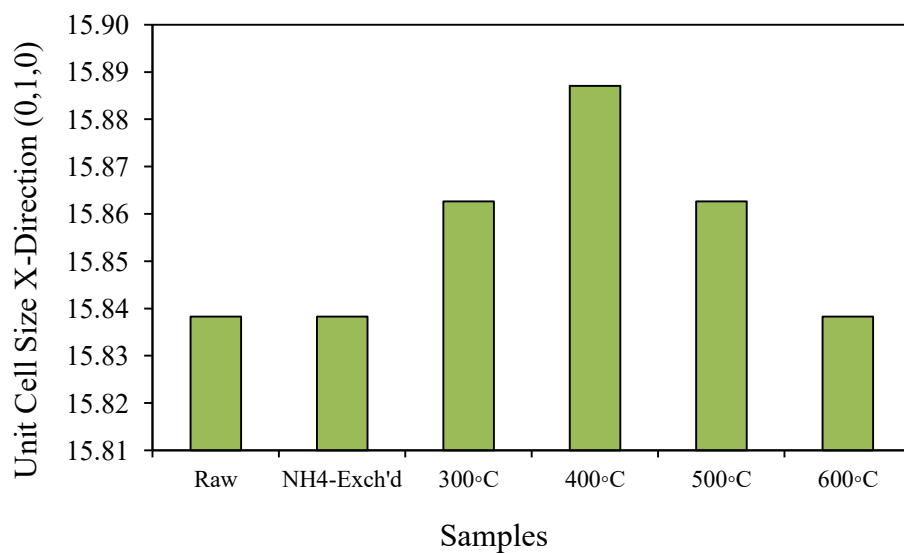


**Figure 3-3.** Variation of  $a$  for as-received,  $\text{NH}_4$ -exchanged /calcined and steamed samples at different temperatures.

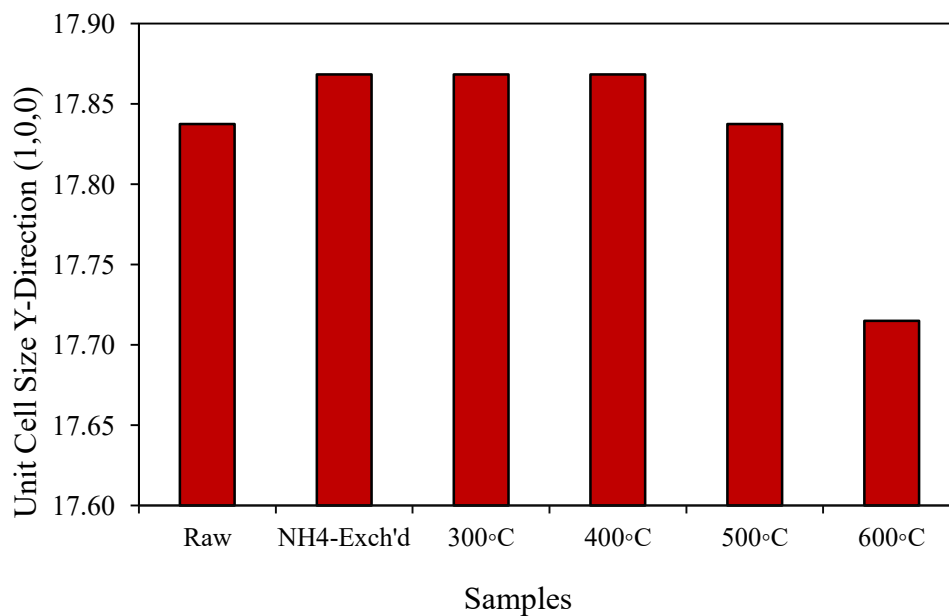


**Figure 3-4.** Variation of  $b$  for as-received,  $\text{NH}_4$ -exchanged /calcined and steamed samples at different temperatures.

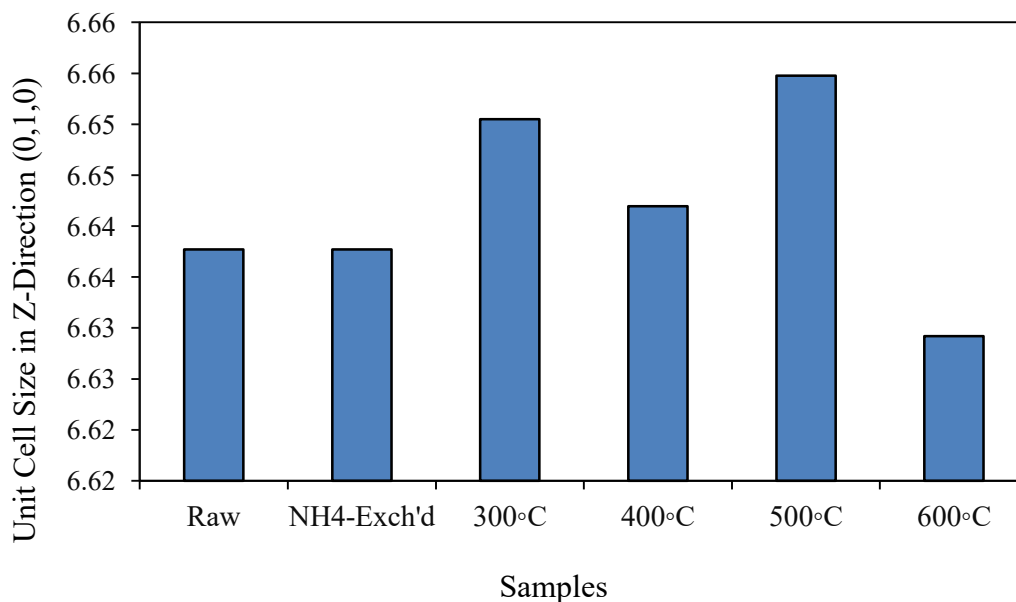


**Figure 3-5.** Variation of *c* for as-received; NH<sub>4</sub>-exchanged /calcined and steamed samples at different temperatures.

Based on the calculated unit cell constants, the unit cell volume of clinoptilolite after each treatment was calculated and showed in Table 3-2. Unit cell volumes also confirmed that the zeolite contraction after heat treatment at 600 °C.

**Table 3-2.** Unit cell volume based on the calculated unit cell constants

Sample	Volume (Angstrom <sup>3</sup> )
Raw CLI (As-Received)	210.5
NH <sub>4</sub> -Exchanged CLI	210.9
CLI steamed at 300 °C	211.6
CLI steamed at 400 °C	211.4
CLI steamed at 500 °C	208.8
CLI steamed at 600 °C	203.1

*CLI: Clinoptilolite*

*IGC.*

IGC elution results expressed in retention time in Table 3-3 showed that, except for the as- received clinoptilolite, adsorption of ethylene was thermodynamically favoured over ethane. Selectivity at 75 °C of ethylene over ethane as a function of steaming temperature is shown in Table 3-3. It indicated the effective pore size of the zeolite underwent a step change. The pore size of the as-received material was too small to admit either of the probe molecules. After ammonium exchange and thermal decomposition of NH<sub>4</sub>-clinoptilolite the major ion inside the pore is H<sup>+</sup> that comparatively is smaller than the alkali cations in as-received zeolite or NH<sub>4</sub>-CLI. Therefore, the pore is large enough to accommodate both gases and adsorption affinity, as expected, is higher for ethylene than ethane.

**Table 3-3.** IGC retention times for the adsorption of ethylene and ethane on raw, cation-exchanged and steamed clinoptilolite (Temperature =75 °C)

Sample	C <sub>2</sub> H <sub>6</sub> (min)	C <sub>2</sub> H <sub>4</sub> (min)	Selectivity
Raw CLI (As-Received)	0.08	0.09	1.13
NH <sub>4</sub> -Exchanged CLI	12.49	63.65	5.13
CLI steamed at 300 °C	1.75	19.87	11.98
CLI steamed at 400 °C	2.52	15.73	6.46
CLI steamed at 500 °C	1.68	17.31	10.89
CLI steamed at 600 °C	0.11	16.64	151.27

Steam treatment at 600 °C caused a significant change in behaviour evidenced by the increase in selectivity measured for this sample. The dealumination resulted in a framework contraction, which had a direct influence on the effective pore size of the framework. The effective pore size of the sample steamed at 600 °C under the test conditions effectively excluded ethane from adsorbing and, as a result, the selectivity increased dramatically. Under these conditions, steamed clinoptilolite at 600 °C effectively separated ethane and ethylene with a limiting selectivity ( $\alpha$ ) of 151 for C<sub>2</sub>H<sub>4</sub> over C<sub>2</sub>H<sub>6</sub>.

#### *Single-gas adsorption isotherms*

Single gas adsorption experiments were carried out to determine whether the pore size effect seen in the IGC was the result of rate-based discrimination or results from the complete exclusion of ethane from the framework.

The isotherm data at different temperatures are presented in Figure 3-6 for the as-received, ion exchanged, and steamed treated samples. The as-received clinoptilolite showed low adsorption capacity due to both gases being unable to diffuse into the framework. The minor amount of adsorption observed was likely due to surface adsorption. The rise in the capacity seen in Figure 6(b) suggested that the exchange and decomposition of the ammonium ions opened the pores enough to allow both gases access to the internal volume of the zeolite. As the sample was steam treated starting at 300 °C, no significant change in the adsorption characteristics was noted. It confirmed that the structure and composition of the sieve was not significantly modified at the lower steaming temperatures. The mild drop in the capacity and selectivity seen in Figure 6(d)

suggested that the adsorption strength of zeolite changed with the increase in steaming temperature and that the framework started to get more siliceous. At 500 °C (Figure 6(e)) this trend continues while at 600 °C (Figure 6(f)), the adsorbent showed significant reduction in capacity and a significantly reduced heat of adsorption indicating widespread change in the composition of the molecular sieve.

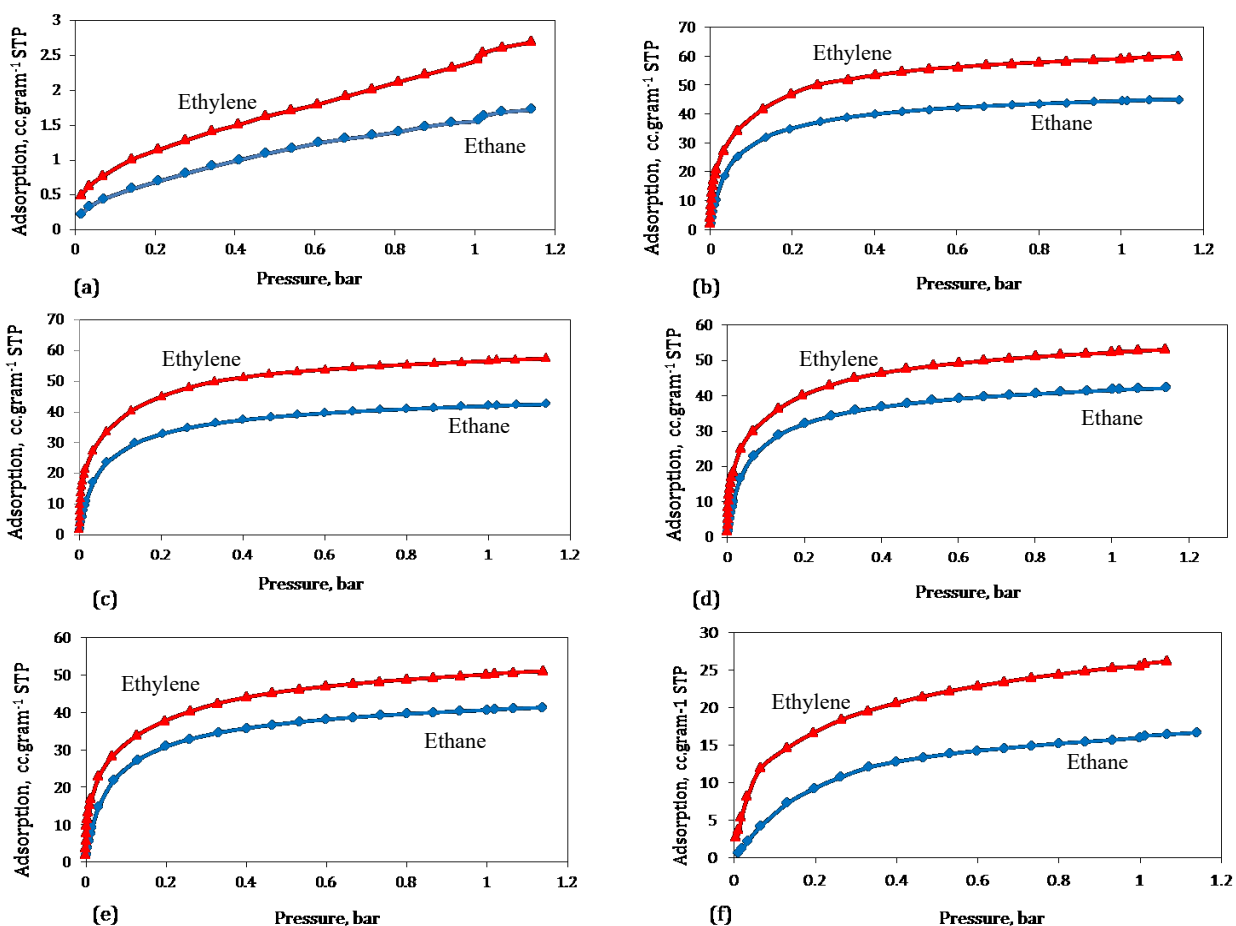


**Figure 3-6.** Adsorption isotherms for ethylene (red) and ethane (blue) on (a) as-received, (b)  $\text{NH}_4$ -exchanged/calcined, (c) steamed at 300 °C, (d) steamed at 400 °C, (e) steamed at 500 °C and (f) steamed at 300 °C clinoptilolite at 25 °C.

Using the isotherm data, the Henry's law selectivity for the various adsorbents was assessed at 30 °C and the results are presented in Table 3-4. The Henry constant for each model was calculated from Equation (1) [50]:

$$A = \lim_{p \rightarrow 0} \frac{q}{p} \quad (1)$$

**Table 3-4.** Henry's Law selectivity for the raw and treated samples

Sample	C <sub>2</sub> H <sub>4</sub> (cc/g.bar)	C <sub>2</sub> H <sub>6</sub> (cc/g.bar)	Selectivity
Raw CLI (As-Received)	5.2	6.4	1.23
NH <sub>4</sub> -Exchanged CLI	955.1	4762	5.00
CLI steamed at 300 °C	921.9	5313	5.76
CLI steamed at 400 °C	908.2	4782	5.26
CLI steamed at 500 °C	798	3878	4.86
CLI steamed at 600 °C	73.5	184.4	2.50

According to the calculated selectivity based on the Henry's law constants, the as-received clinoptilolite had a selectivity approaching unity. This was the expected result for this material because the effective pore size in as-received clinoptilolite, even under equilibrium conditions, excluded both ethane and ethylene. The small selectivity the sample did display toward ethylene might simply be due to the error associated with accurately measuring such low adsorption capacities or it could reflect that the surface of the particles had polarizing elements that could interact more strongly with the large ethylene quadrupole moment.

After the sample was ion exchanged and calcined in air to 500 °C a step change in the ethylene/ethane selectivity was measured. The selectivity for the sample steamed at 300

°C was comparable to the selectivity measured for the same sample under IGC conditions and indicated that the pore size increased to an extent that both gases can diffuse into and adsorb on the interior surface of the solid. Under equilibrium conditions, ethylene is always expected to adsorb more strongly due to having a quadrupole moment twice that as strong as ethane.

The ethylene selectivity increases incrementally as the sample is steamed at 300 °C which was unexpected and indicates that the adsorption sites within the framework display a stronger affinity for ethylene. The trend from 400 °C to 600 °C follows the trend expected for dealumination where there are fewer adsorption sites (as evidenced by the Henry Law values) and the strength of the sites decreases as evidenced by a decrease in the selectivity of the system. None of the isotherms, except for those associated with the as-received clinoptilolite, demonstrate an ability to exclude ethane at equilibrium conditions. This suggests that the difference seen in the calculated selectivity between the IGC and isotherm results for the sample steamed at 600 °C is the result of the difference between the two test methods.

Once the effective pore size for the framework is on the order of the molecular diameter of ethane then the access to the internal surface area will be determined by whether the adsorbate can outdo the diffusion barrier created by the narrow pore mouths and diffuse into the framework to adsorb. Under equilibrium conditions there is sufficient time for the gas molecules to orient themselves and pass through the pore into the framework. Under the dynamic adsorption conditions associated with the IGC experiment, however, there is a fixed period of time that the probe gas is in contact with the solid and if the diffusion barrier cannot be overcome in that period of time then the zeolite will not

adsorb that component. The contrast between the isotherm and IGC results for the sample steamed at 600 °C strongly suggests that this sample could act effectively as a kinetic adsorbent where the separation of ethane and ethylene is accomplished by tuning the gas velocity through the adsorbent bed rather than by manipulating the strength of the adsorbent sites.

### **3.5 Conclusions**

This study demonstrated that by ammonium exchanging and steaming naturally occurring clinoptilolite the effective pore size of the zeolite was reduced to be on the order of the molecular diameter of ethane. The steaming process at 600 °C generated structural changes in the zeolite. The ammonium ions fully decomposed which served to weaken the interaction of ethylene with the surface of the zeolite and resulted in a permanent contraction in the size of the unit cell. These results demonstrated the potential to use steamed clinoptilolite as a rate-based PSA adsorbent, which could offer improved efficiency in the separation of olefin/paraffin.

### 3.6 References

- [1] Z. Bao, L. Yu, I. Vasiliev, Q. Ren, X. Lu and S. Deng, "Adsorption of Ethane , Ethylene , Propane , and Propylene on a Magnesium-Based Metal À Organic Framework", *Langmuir.*, vol. 27, pp. 13554–13562, 2011.
- [2] A. Anson, Y. Wang, C.C.H. Lin, T.M. Kuznicki and S.M. Kuznicki, "Adsorption of ethane and ethylene on modified ETS-10", *Chem. Eng. Sci.*, vol. 63, pp. 4171–4175, 2008.
- [3] D. M. Ruthven, "Principle of adsorption and adsorption processes." John Wiley & Sons, Inc., 1984.
- [4] Y. Wu, H. Chen, D. Liu, Y. Qian, and H. Xi, "Adsorption and separation of ethane /ethylene on ZIFs with various topologies : Combining GCMC simulation with the ideal adsorbed solution theory ( IAST )," *Chem. Eng. Sci.*, vol. 124, pp. 1–10, 2014.
- [5] A. Farjoo, F. Khorasheh, S. Niknaddaf and M. Soltani, "Kinetic modeling of side reactions in propane dehydrogenation over Pt - Sn/ $\gamma$  - Al<sub>2</sub>O<sub>3</sub> catalyst", *Sci. Iran.*, vol. 18, pp. 458–464, 2011.
- [6] E. Finocchio, G. Ramis, G. Busca, V. Lorenzelli and R.J. Willey, "On the mechanisms of light alkane catalytic oxidation and an FT-IR study of the n-butane conversion over MgCr<sub>2</sub>O<sub>4</sub> and a Mg-vanadate catalyst", *Catal. Rev.*, vol 28, pp. 381–389, 1996.

- [7] D. Shee and A. Sayari, "Light alkane dehydrogenation over mesoporous Cr<sub>2</sub>O<sub>3</sub>/Al<sub>2</sub>O<sub>3</sub> catalysts", *Applied Catal. A, Gen.* vol. 389, pp. 155–164, 2010.
- [8] M. Lee, B.M. Nagaraja, K. Young and K. Jung, "Dehydrogenation of alkane to light olefin over PtSn/ $\theta$ -Al<sub>2</sub>O<sub>3</sub> catalyst: Effects of Sn loading", *Catal. Today.*, vol. 232, pp. 53–62, 2011.
- [9] A. Van Miltenburg, W. Zhu, F. Kapteijn and J. A. Moulijn, "Adsorptive Separation of Light Olefin/Paraffin Mixtures", *Chem. Eng. Res. Des.*, vol. 84, pp. 350–354, 2006.
- [10] S. Hosseinpour, S. Fatemi, Y. Mortazavi, M. Gholamhoseini and M.T. Ravanchi, "Performance of CaX Zeolite for Separation of C<sub>2</sub>H<sub>6</sub> , C<sub>2</sub>H<sub>4</sub> , and CH<sub>4</sub> by Adsorption Process; Capacity, Selectivity, and Dynamic Adsorption Measurements', *Sci. Technol.*, vol. 46, pp. 349–355, 2010.
- [11] R.T. Yang and E.S. Kikkinides, "New Sorbents for Olefinparaffin Separations by Adsorption via  $\pi$ -Complexation", *AICHE J.*, vol. 41, pp. 509–517, 1995.
- [12] R. V Jasra and S.G.T. Bhat, "Thermal desorption of normal paraffins from zeolite 5A", *Zeolites.*, vol. 7, pp. 1985–1988, 1987.
- [13] M. Mofarahi and S.M. Salehi, "Pure and binary adsorption isotherms of ethylene and ethane on zeolite 5A", *Adsorption*, vol. 19, pp. 101–110, 2012.

- [14] A. Romero-Perez and G. Aquilar-Armenta, "Adsorption Kinetics and Equilibria of Carbon Dioxide , Ethylene , and Ethane on 4A ( CECA ) Zeolite", *J. Chem. Eng. Data.*, vol. 55, pp. 3625–3630, 2011.
- [15] A. Van Miltenburg, W. Zhu, F. Kapteijn and J. A. Moulijn, "Adsorptive Separation of Light Olefin/Paraffin Mixtures", *Chem. Eng. Res. Des.*, vol. 84, pp. 350–354, 2006.
- [16] D. Hilden and R. F. Stebar, "Evaluation of acetylene as a spark ignition engine fuel", *Energy Res. Soc. Sci.*, vol. 3, pp. 59–71, 1979.
- [17] A. Wehrmeier and B. Dellinger, "Role of Copper Species in Chlorination and Condensation Reactions of Acetylene", *Environ. Sci. Technol.*, vol. 32, pp. 2741–2748, 1998.
- [18] D.W. Breck, "Zeolite Molecular Sieves: Structure, Chemistry, and Use," no. John Wiley & Sons, 1974.
- [19] A. Alberti, "The Crystal Structure of Two Clinoptilolites", *Tschermaks Min. Petr. Mitt.*, vol. 22, pp. 25–37, 1975.
- [20] D. L. Bish and M. D.W., "Natural Zeolites: Occurrence, Properties, Application", *Rev. Miner. Geochemistry*, vol. 45, 2001.
- [21] W. An, P. Swenson, L. Wu, T. Waller, A. Ku and S.M. Kuznicki, "Selective separation of hydrogen from C1/C2 hydrocarbons and CO2 through dense natural zeolite membranes", *J. Memb. Sci.* , vol. 369, pp. 414–419, 2011.

- [22] S. Liu, M. Lim and R. Amal, "TiO<sub>2</sub> -coated natural zeolite : Rapid humic acid adsorption and effective photocatalytic regeneration", *Chem. Eng. Sci.*, vol. 105, pp. 46–52, 2014.
- [23] M. Hasheminejad and A. Nezamzadeh-ejhi, "A novel citrate selective electrode based on surfactant modified nano-clinoptilolite", *Food Chem.*, vol. 172, pp. 794–801, 2015.
- [24] H. Li and R. Dittmeyer, "Inorganic microporous membranes for H<sub>2</sub> and CO<sub>2</sub> separation-Review of experimental and modeling process", *Chem. Eng. Sci.*, vol. 147, pp. 401–417, 2015.
- [25] M. W. Ackley, S.U. Rege, H. Saxena, "Application of natural zeolites in the purification and separation of gases", *Microporous Mesoporous Mater.*, vol. 61, pp. 25–42, 2003.
- [26] T.C. Frankiewicz and R.G. Donnelly, "Methane/ Nitrogen Gas Separation over the Zeolite Clinoptilolite by the Selective Adsorption", *Ind. Gas Sep.*, pp. 213–233, 1983.
- [27] M.W. Ackley, and R.T. Yang, "Adsorption Characteristics of High-Exchange Clinoptilolites", *Ind. Eng. Chem. Res.*, vol 30, pp. 2523–2530, 1991.
- [28] D.O. Connor, P. Barnes, R. Bates and D.F. Lander, "A hydration-controlled nano-valve in a zeolite", *Chem. Commun.*, pp. 2527–2528, 1998.

- [29] G. Engelhardt and U. Lohse, "High resolution Si n.m.r of dealuminated and ultrastable Y-zeolites", *Zeolites.*, vol. 2, pp. 59–62, 1982.
- [30] G. Engelhardt and U. Lohse, "High resolution Si n.m.r of dealuminated Y-Zeolites", *Zeolites.*, vol. 3, pp. 233–238, 1983.
- [31] G. Engelhardt, and V. Patzelova, "Unit Cell Constants of Zeolites Stabilized by Dealumination", *Cryst. Res. Technol.* vol. 19, pp. 6–8, 1983.
- [32] J. Datka, W. Kolidziejski, J. Klinowski, B. Sulikowski, "Dealumination of zeolite Y by H<sub>4</sub>EDTA", *Catal. Letters.*, vol. 19, pp.159–165, 1993.
- [33] A.T. Steel, "Time dependence of the structural changes occurring in NH<sub>4</sub>-Y zeolite on dealumination: A preliminary study using energy-dispersive X-ray diffraction", *Zeolites.*, vol. 13, pp. 336–340, 1993.
- [34] S. Dzwigaj, M.J. Peltre, P. Massiani, A. Davidson, M. Che and T. Sen, "Incorporation of vanadium groups in a dealuminated b zeolite", *Chem. Commun.* pp. 87–88, 1998.
- [35] P. Bartl and W.F. Holderich, "A study of the dealumination methods for zeolite L", *Microporous Mesoporous Mater.*, vol. 38, pp. 279–286, 2000.
- [36] M. Silaghi, C. Chizallet and P. Raybaud, "Challenges on molecular aspects of dealumination and desilication of zeolites", *Microporous and Mesoporous Mater.* vol. 191, pp. 82–96, 2014.

- [37] J.M. Müller, G.C. Mesquita, S.M. Franco, L.D. Borges, J.L. De Macedo and J.A. Dias, , "Solid-state dealumination of zeolites for use as catalysts in alcohol dehydration", *Microporous Mesoporous Mater.*, vol. 204, pp. 50–57, 2015.
- [38] Y. Wang, F. Lin and W. Pang, "Ammonium exchange in aqueous solution using Chinese natural clinoptilolite and modified zeolite", *J. Hazard. Mater.*, vol 142, pp. 160–164, 2007.
- [39] J.B. Lee, H.H. Funke, R.D. Noble, J.L. Falconer, "High selectivities in defective MFI membranes", *J. Memb. Sci.*, vol 321, pp. 309–315, 2008.
- [40] É. Tyrrell, E.F. Hilder, R.A. Shalliker, G.W. Dicoski, R.A. Shellie and M.C. Breadmore, "Packing procedures for high efficiency , short ion-exchange columns for rapid separation of inorganic anions", *J. Chromatogr. A.*, vol. 1208, pp. 95–100, 2008.
- [41] Z. Huang, Q. Subhani, Z. Zhu, W. Guo and Y. Zhu, "A single pump cycling-column-switching technique coupled with homemade high exchange capacity columns for the determination of iodate in iodized edible salt by ion chromatography with UV detection", *Food Chem.*, vol. 139, pp. 144–148, 2013.
- [42] A. Omegna, M. Haouas, A. Kogelbauer, R. Prins, Realumination of dealuminated HZSM-5 zeolites by acid treatment : a reexamination, *Microporous Mesoporous Mater.*, vol 46, pp. 177–184, 2001.

- [43] M. Roži, S. Cerjan-Stefanovic, S. Kurajica, M. Rozmaric Maefat, K. Margeta and A. Farkas, "Decationization and dealumination of clinoptilolite tuff and ammonium exchange on acid-modified tuff", *J. Colloid Interface Sci.*, vol. 284 pp. 48–56, 2005.
- [44] L.Parker and D. Bibby, "Synthesis and some properties of two novel zeolites, KZ-1 and KZ-2", *Zeolites.*, vol. 3, pp. 8–11, 1983.
- [45] D.C. Organique and D. Recherche, "Hydration of n-Butenes Using Zeolite Catalysts influence of the Aluminium Content on Activity", *J. Catal.*, vol. 89 pp. 60–68, 1984.
- [46] I. Halasz, M. Agarwal, B. Marcus and W.E. Cormier, "Molecular spectra and polarity sieving of aluminum deficient hydrophobic H-Y zeolites", *Microporous Mesoporous Mater.*, vol. 84, pp. 318–331, 2005.
- [47] S. Yasyerli, I. Ar, G. Dogu and T. Dogu, "Removal of hydrogen sulfide by clinoptilolite in a fixed bed adsorber", *Chem. Eng. Process.*, vol. 41, pp. 785–792, 2002.
- [48] O. Korkuna, R. Leboda, J. Skubiszewska-Zieab, T. Vrublevs'ka, V.M. Gun'ko and J. Ryczkowski, "Structural and physicochemical properties of natural zeolites : clinoptilolite and mordenite", *Microporous Mesoporous Mater.*, vol. 87, pp. 243–254, 2006.

- [49] J.A. Kaduk and J. Faber, Crystal structure of zeolite Y as a function of ion exchange, *Rigaku J.*, vol. 12, pp. 14–34, 1995.
- [50] A.L. Myers, "Thermodynamics of Adsorption in porous materials", *AICHE J.*, vol. 48, pp. 145-160, 2002.

## **Chapter Four**

---

# **Fundamentals of membranes and membrane gas separation**

## **4.1 Membrane technology**

Membrane technology in the past 30 years has earned vast significance and competes with other established technologies in gas separation, water purification or food processing. Chemical industry is certainly one of the most outstanding areas to employ membrane technology as an essential tool in gas separation through treating streams, recovering valuable materials, and minimizing environmental issues, which are generally believed to be caused by industrial activities and productions. Membranes are also currently playing a special role in the field of alternative energy along with a potential contribution to environmental sustainability and green chemistry. Enhancing processes and designing membranes for chemical and engineering applications is a challenge under study in membrane development area [1].

The essential requirement in membranes and membrane separation processes, is the capacity of a membrane to control the permeation of chemical groups in contact with it. In packaging applications, the intent is to entirely prevent permeation of flow. However, in controlled drug delivery applications, the intent is mainly to reduce the permeation rate of drugs from a reservoir to a body. In separation applications, the intent is to allow permeation of one component of a mixture freely through the membrane while blocking permeation of other components. Since 1960, membrane science has matured from a laboratory curiosity and interest to a widely exercised technology in medicine or in industry and in engineering applications [2]. This growth is likely to continue furthermore particularly in membrane gas separation and pervaporation separation fields.

## 4.2 Membrane and membrane separation

A membrane is defined as a perm-selective barrier or a gate that allows passing of specific molecules while excluding other ones when a driving force is present or applied [3]. The component that passes through the membrane is called permeate, and retentate is identified as the molecules that are stopped on the feed side. In 1748, membrane separation process was observed unexpectedly by Nollet [4]. However in 1873, when Gibbs introduced the theory of Gibbs free energy, what Nollet found in 1748 was further understood [5].

Membrane separations can also be described as a de-mixing process. Because of the natural tendency of molecules to uniformly get mixed and to take up the available spaces, demixing process requires energy to surpass the tendency to equilibrate [4]. The driving force is the source for such energy and in membrane separations, it could be pressure, temperature, concentration or electrical potential [3],[4]. With the special case of membrane distillation, membrane processes are typically at isothermal conditions and in commercial applications, it is not common to find temperature as the driving force [6]. In almost all membrane separation processes, pressure difference is the driving force by either applying pressure on the feed side (e.g. reverse osmosis, micro/micro filtration, etc.) or reducing pressure on the permeate side (e.g. pervaporation, etc.) [6],[7]. Separation processes such as dialysis and membrane extraction employ concentration as the driving force. Electrical potential has also been used as the driving force in electro dialysis process [6].

Membranes performance is evaluated by productivity and selectivity. Separation factor and selectivity are defined as the ratio of molecules that permeate through the membranes

to their retention, and productivity is described by the flux through the membrane [7]. Membranes, based on their materials, are mainly categorized into three classes of polymeric, inorganic, and biological [8]. Polymeric membranes have the most extensive industrial application but they have limited thermal, mechanical and chemical stability. Inorganic membranes such as zeolite membranes provide competitive thermal, chemical or mechanical stability compared to polymeric ones [9]. Despite some shortcomings of polymeric membranes, they are widely used in several industrial processes. This is because synthetic zeolite membranes that are potentially suitable for industrial applications have drawbacks due to their synthesis procedures and support materials. The support materials are thermally treated ceramic or metallic substrates on which the zeolite is developed. Coated zeolite membranes are generally more expensive than polymer membranes [10]. Natural zeolites with pore sizes comparable with kinetic diameters of gas molecules and ion transfer ability through their structure are also popular membranes. Because of the long time and high pressure that natural zeolite deposits have experienced, inter-crystalline grain boundaries (main shortcoming of synthetic zeolite) are combined or eliminated leaving materials with mechanical structural solidness. Natural zeolite membranes are employed mostly with high temperatures feed streams and are effective as membrane reactors in endothermic reactions such as dehydrogenation [11], [12].

### **4.3 Zeolite membrane on support**

Most inorganic membranes are synthesized zeolite materials on porous supports [13]. The mechanical stability of membranes grows by making a thin membrane film on a support structure. As thickness of the membrane is decreased, growth of defects or pinholes may occur which decreases the separation performance [14]. The thin-films that are grown on

the support surface, vary from several microns to about a hundred microns of thickness [9],[15]. To coat or synthesize zeolite crystals on a substrate, compatible physical and chemical properties between the first zeolite layer and the support is required; otherwise the coated layer gets detached from the support as a result of weak adhesion.

Differences in thermal expansion coefficients of the support material and the synthesized layer can also create fractures or cracks in the coated layer. Supported inorganic membranes are usually synthesized by immersing the membrane in a sol gel and taking it out without disturbing the surface layer, this method is referred as slip casting or dip coating [16]. One of the main challenges in coated zeolite membranes is minimizing the potential defects or inter-crystalline pores formed in membranes. Existence of defects in membranes results in weak separation performance. Therefore post-treatment process is often necessary to ensure that no defects exist in the coated film. During synthesis of membranes, factors such as layer thickness, crystal orientation, and quality of crystal boundaries are main players [17–20].

Different techniques are employed to coat zeolite crystals on supports. Typically a post treatment is required to minimize defects or pinholes within the membrane. This additional treatment requires effective process control that may complicate the membrane development process.

#### **4.4 Permeation Mechanisms**

Permeation mechanism is defined as how a molecule passes from the retentate to the permeate side of the membrane. Several factors such as pressure, temperature, molecular weight, kinetic diameter of molecules, zeolite pore size, heat of adsorption, thermal

activation energies and composition of the mixture near the membrane can control the permeation mechanism [16],[17].

Despite different processes and applications in gas and liquid separation, the transport mechanism through porous membranes are comparable on a molecular level for both liquid and gas molecules since the controlling transport mechanisms are not significantly different and in some cases can be quite identical [24],[25].

Gas transport in membranes can be explained by a number of potential mechanisms [22]. These include bulk Poiseuille or viscous flow for large pores, Knudsen diffusion for intermediate size pores, size-restricted diffusion, surface diffusion for small pores, and solid surface diffusion for extremely small pores or no pores [8, 25, 26]. Depending on the properties of the permeating molecules and conditions, a combination of these mechanisms can take place simultaneously. Figure 4-1 demonstrates different gas separation mechanisms in membranes.

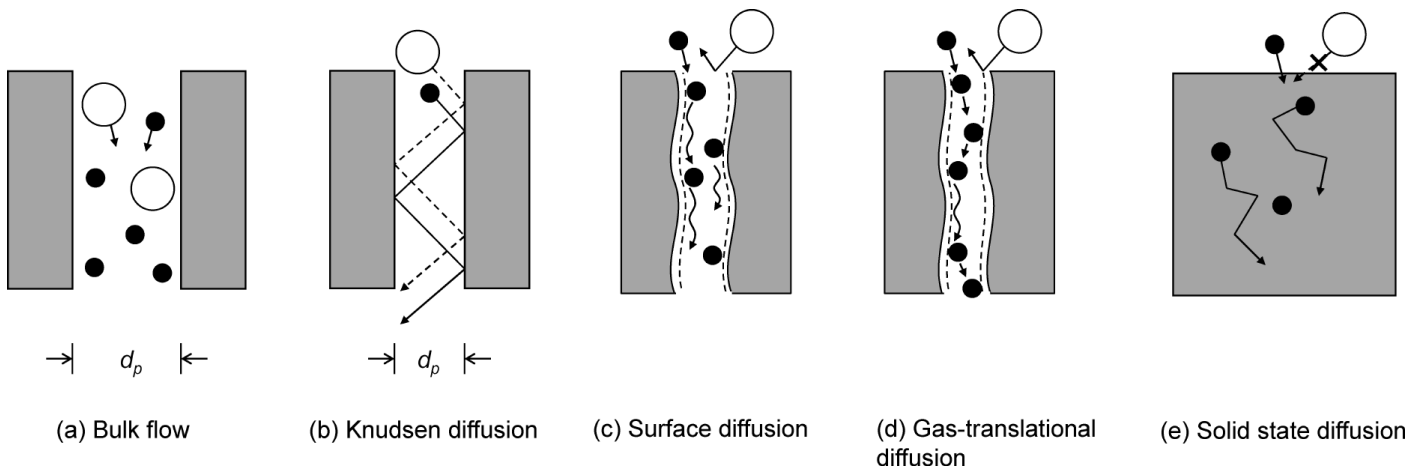


**Figure 4-1.** Different separation mechanisms in membrane [22]

#### 4.4.1. Hagen-Pouisselle Mechanism

The Hagen-Pouisselle mechanism also identified as molecular diffusion takes place when the pore diameter is relatively large compared to the mean free path of the molecules and bulk fluid transport happens through the large pores [21], [22]. In this mechanism, the average velocity  $v$  ( $\text{m/ s}^{-1}$ ) is defined with the following equation:

$$v = \frac{d_p^2}{32\mu l} (p_o - p_L) \quad (1)$$

where  $d_p$  is the diameter of the pore,  $\mu$  ( $\text{kg.m.s}^{-1}$ ) is the viscosity,  $l$  is the length of the pore,  $p_o$  is the inlet pressure, and  $p_L$  is the pressure at a distance  $L$ . The flux is derived through the following formula:

$$N = \frac{P_M}{L} (p_o - p_L) \quad (2)$$

Considering the porosity  $\epsilon$ , tortuosity  $\tau$  of the membrane, and the pore area per total volume,  $a$ , which is related to the pore area per membrane volume  $a_v$ ,  $P_M$  is defined as follows:

$$P_M = \frac{\rho\epsilon^3}{2(1-\epsilon)\mu\tau a_v^2} \quad (3)$$

$$a_v = \frac{a}{(1-\epsilon)} \quad (4)$$

#### 4.4.2 Knudsen Diffusion Mechanism

Knudsen diffusion happens when the pore diameter  $d_p$  is smaller than the mean free path  $\lambda$  of the gas molecules [29]. In this mechanism, elastic collisions happen between gas molecules and the pore wall instead of the gas molecules themselves. The Knudsen diffusivity is resulted from the gas kinetic velocity and the membrane geometric parameters:

$$D_k = \frac{\varepsilon d_p}{\tau} \left( \frac{8RT}{9\mu M} \right)^{0,5} \quad (5)$$

where  $\varepsilon$  is the porosity of the membrane,  $\tau$  the tortuosity,  $R$  the gas constant,  $T$  the absolute Kelvin temperature and  $M$  is the molecular weight of the diffusing gas molecule [30], [31].

Gas transport by Knudsen diffusion occurs in the gaseous state without any adsorption contribution, as the interaction between diffusing molecules and pore wall is not significant [32], [33]. The Knudsen permeance is as follows:

$$P_k = \frac{\varepsilon d_p}{\tau L} \left( \frac{8}{9\pi MRT} \right)^{1/2} \quad (6)$$

where  $L$  is the thickness of the membrane.

#### 4.4.3 Surface Diffusion Mechanism

Surface diffusion occurs at low temperatures that gas molecules cannot escape from the surface potential field because of the strong interaction between the gas molecules and membrane inner surface compared to their kinetic energy. This mechanism is more dominant with relatively smaller pores because of the high proportion of surface area compared to the pore volume.

In the surface diffusion mechanism, gas molecules adsorb onto the surface of the membrane at the pore opening, diffuse through the membrane, and desorb at the pore exit. In membrane applications for gas separation, adsorption is often below a monolayer, and is defined by the Langmuir adsorption model [22]. Surface diffusion processes are described often using a Fickian hopping model:

$$D_{SD} = \frac{\epsilon}{\tau} g_d \lambda^2 \nu \exp\left(\frac{\Delta E_{SD}}{RT}\right) = D_0 \exp\left(\frac{\Delta E_{SD}}{RT}\right) \quad (7)$$

In this mechanism, a molecule with a velocity of  $\lambda$  (m.s<sup>-1</sup>), makes a jump of length  $\lambda$  (m), in the right direction which is estimated by the probability  $g_d$ , with  $\nu$  as the jump frequency (s<sup>-1</sup>) of the molecule between adsorption sites and  $\Delta E_{SD}$  is the energy wall for moving to the other adsorption site [22].

#### 4.4.4 Gas-translational Mechanism

Gas translational mechanism takes place with small pore sizes and sufficient kinetic energy, for the diffusing gas molecules, to escape the surface potential but cannot voluntarily do that because of the presence of a pore wall on the other side. Therefore, activated Knudsen diffusion model or gas-translational model (GT model) is proposed as a mechanism that is the combination of the Knudsen diffusion model and the surface diffusion model [34],[35]. Both of the surface diffusion and gas-translation have

contributions from the surface and are regarded as surface flow mechanisms. By presenting a probability for diffusion through the micropore,  $\rho$ , to the Knudsen diffusion model, the following equation is derived:

$$P_{GT} = \frac{\epsilon d_p \rho}{\tau L} \left( \frac{8}{\pi MRT} \right)^{1/2} \quad (8)$$

The probability,  $\rho$ , consists of a pre-exponential,  $\rho_g$  and the kinetic energy  $\Delta E$  to surpass the diffusion:

$$\rho = \rho_g \exp \left( -\frac{\Delta E}{RT} \right) \quad (9)$$

Therefore, the permeance for single gases is described as:

$$P_{GT} = \frac{\epsilon d_p \rho_g}{\tau L} \left( \frac{8}{\pi MRT} \right)^{1/2} \exp \left( -\frac{\Delta E}{RT} \right) \quad (10)$$

The above equation assumes that the gas diameter is significantly smaller than the pore diameter with no other physical blockage effects.

#### 4.4.5 Solid-State Diffusion Mechanisms

Solid state diffusion happens when the gas molecule interacts strongly with the membrane material with more decrease in the pore size. The solubility is another consideration in this mechanism and is described as:

$$P = S \cdot D \quad (11)$$

Where D and S are solubility and diffusivity respectively. Permeation through glassy membranes ( e.g. silica ), metallic membranes or polymeric membranes are in this class

of transport mechanism.

## 4.5 Transport mechanism in zeolite membranes

Different transport mechanisms such as surface diffusion also known as intracrystalline, microporous, configurational or activated diffusion through zeolite crystals can potentially contribute to the overall flux through zeolite membranes [18]. Mass transport through a zeolite layer is illustrated in Figure 4-2 through a five-step model [19], [20].

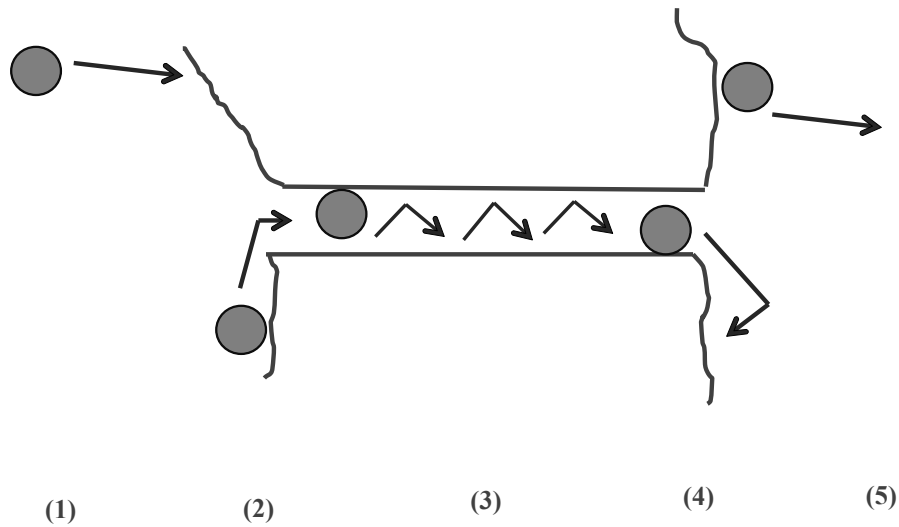


**Figure 4-2.** Mass transfer model for the permeation process through a zeolite in a zeolite pore.

1. Adsorption from the gas phase to the external surface.
2. Diffusion from the external surface to the zeolite pores.
3. Diffusion through the zeolite channel.
4. Diffusion to the external surface of the zeolite pores
5. Desorption from the external surface to the gas phase.

Steps 1 and 5 depend on the conditions on side of the membrane. At high temperatures, for weakly adsorbing groups (adsorption on the external surface, including the pore entrance) will hardly take place. Steps 1 + 2 and 4 + 5 may be considered as combined processes. If entering occurs directly from the gas phase, molecules would have to move under the right angle, otherwise they will get dispersed back. Overall, larger molecules have more difficulty entering into the pores compared to smaller molecules.

Intra-crystalline zeolite diffusion (step 3) is mostly described as configurational diffusion. Steps 1 and 5 are typically assumed to be quick processes particularly at higher temperatures while steps 2, 3, and 4 are usually activated processes [20]. Depending on the activation energy, each step or combination of these steps could determine the rate.

#### 4.6 Membrane evaluation and analytical methods

Membrane performance in a gas membrane system is defined by key parameters such as permeance (or permeation) and permeability. Selectivity and separation factor are used to describe membrane separation efficiency in single and multi-component gas systems respectively.

Permeance is defined as the volume of the feed passing through a unit area of membrane at unit time and under unit pressure gradient and is formulated as [36]:

$$\pi = \frac{V}{A.t.\Delta P} \quad (12)$$

Where  $\pi$  is permeance,  $V$  is the volume of gas,  $A$  is membrane area,  $t$  is time, and  $\Delta P$  is pressure difference. Permeance values are typically reported in  $\text{mol. m}^{-2}.\text{s}^{-1}.\text{Pa}^{-1}$ .

Therefore, for a component crossing the membrane, permeance is calculated as follow:

$$\pi_i \pi_i = \frac{N_i}{\Delta P_i} \quad (13)$$

where  $\pi_i$  is the permeance ( $\text{mol} \cdot \text{m}^{-2} \cdot \text{s}^{-1} \cdot \text{Pa}^{-1}$ ),  $N_i$  is the molar flux ( $\text{mol} \cdot \text{s}^{-1} \cdot \text{m}^{-2}$ ),  $\Delta P_i$  is the partial pressure difference (Pa) of component i across the membrane.

In single gas permeations, ideal selectivity is calculated based on the following definition:

$$S_{ij} = \frac{\pi_i}{\pi_j} \quad (14)$$

where,  $S_{ij}$  is the ideal selectivity of groups i over j.

In mixed gas separations, it is more common to describe the permeation driving force in terms of a fugacity difference rather than a partial pressure difference, due to the non-ideal gas behavior for gas mixtures. The separation factor is given by [21]:

$$\alpha_{AB} = \frac{y_A/y_B}{x_A/x_B} \quad (15)$$

where  $x_i$  is the mole fraction of component i on the feed side and  $y_i$  the mole fraction of component i on the permeate side measured by gas chromatography.

In the following chapters natural clinoptilolite membranes in different configurations such as disk or tubular are developed and tested for hydrogen separation using various flexible fabrication processes, binders or post-treatment methods. Different separation mechanisms, mixtures and parameters are also employed to evaluate membrane performance and productivity.

## 4.7 References

- [1] S. Nunes and K. Peinemann, “*Membrane Technology in the Chemical Industry*”, John Wiley & Sons., 2006.
- [2] R. W. Baker, “Membrane technology,” in “*Encyclopedia Of Polymer Science and Technology*”, John Wiley & Sons, pp. 184–249, 2001.
- [3] K. W. Böddeker, “Liquid Separations with Membranes,” in “*Liquid Separations with Membranes: An Introduction to Barrier Interference*”, Springer, pp. 1–146, 2008
- [4] K. W. Boddeker, “Commentary : Tracing membrane science,” *J. Memb. Sci.*, vol. 100, pp. 65–68, 1995.
- [5] D. L. Bish and J. W. Carey, “Thermal Behavior of Natural Zeolites,” The Mineralogical Society Of America, pp. 403-452, 2001.
- [6] T. Matsuura, “Synthetic Membranes and membrane separation processes”, CRC Press. 1993.
- [7] R. Abedini and A. Nezhadmoghadam, “Application of membranes in gas separation processes: Its suitability and mechanism,” *Pet. Coal*, vol. 52, no. 2, pp. 69–80, 2010.
- [8] S. T. Hwang and K. Kammermeyer, “Membranes in separations,” in “*Techniques of chemistry*”, New York: John Wiley and Sons, p. 442, 1975.

- [9] Y. S. Lin, I. Kumakiri, B. N. Nair, and H. Alsyouri, "Microporous Inorganic Membranes" *Separation & Purif. Rev.*, vol. 31, no. 2., pp. 229–379, 2002.
- [10] S. L. Matson, J. Lopez, and A. Quinn, "Separation of gases with synthetic membranes-Review Article," *Chem. Eng. Sci.*, vol. 38, no. 4, pp. 503–524, 1983.
- [11] S. Sahebdehfar, M. T. Ravanchi, F. Tahriri Zangeneh, S. Mehrazma, and S. Rajabi, "Kinetic study of propane dehydrogenation and side reactions over Pt–Sn/Al<sub>2</sub>O<sub>3</sub> catalyst," *Chem. Eng. Res. Des.*, vol. 90, no. 8, pp. 1090–1097, 2012.
- [12] E. Gobina, K. Hou, and R. Hughes, "Ethane dehydrogenation in a catalytic membrane reactor coupled with a reactive sweep gas," *Chem. Eng. Sci.*, vol. 50, no. 14, pp. 2311–2319, 1995.
- [13] P. Kölsch, D. Venzke, M. Noack, P. Toussaint, and J. Caro, "Zeolite-in-metal membranes: preparation and testing," *J. Chem. Soc., Chem. Commun*, vol. 2, no. 21, p. 2491, 1994.
- [14] L. Cot, J. Durand, C. Guizard, N. Hovnanian, and A. Julbe, "Inorganic membranes and solid state sciences," vol. 2, pp. 313–334, 2000.
- [15] J. Caro and M. Noack, "Zeolite membranes – Recent developments and progress," *Microporous Mesoporous Mater.*, vol. 115, no. 3, pp. 215–233, 2008.
- [16] Y. Gu and G. Meng, "A model for ceramic membrane formation by dip coating," *J. Eur. Ceram. Soc.*, vol. 19, pp. 1961–1966, 1999.

- [17] H. Maghsoudi, "Defects of Zeolite Membranes: Characterization, Modification and Post-treatment Techniques," *Sep. Purif. Rev.*, vol. 45, no. 3, pp. 169–192, 2016.
- [18] J. Caro, M. Noack, P. Kolsch, and R. Schafer, "Zeolite membranes  $\pm$  state of their development and perspective," *Microporous Mesoporous Mater.*, vol. 38, pp. 3–24, 2000.
- [19] E. E. Mcleary, J. C. Jansen, and F. Kapteijn, "Zeolite based films , membranes and membrane reactors: Progress and prospects," *Microporous Mesoporous Mater.*, vol. 90, pp. 198–220, 2006.
- [20] J. Caro and M. Noack, "Zeolite Membranes – Status and Prospective," in "*Advances in Nanoporous Materials*", Elsevier B.V, vol. 1, pp. 1–96. 2009.
- [21] W. An, P. Swenson, L. Wu, T. Waller, A. Ku, and S. M. Kuznicki, "Selective separation of hydrogen from C1/C2 hydrocarbons and CO2 through dense natural zeolite membranes," *J. Memb. Sci.*, vol. 369, pp. 414–419, 2011.
- [22] S. T. O. Yama, "Review on Mechanisms of Gas Permeation through Inorganic Membranes," vol. 54, pp. 298–309, 2011.
- [23] A. Julbe, "Zeolite membranes-synthesis, charactersitic and application," in "*Intorduction to zeolite science and practices*", Elsevier B.V., 2007.

- [24] J. Romero, C. Gijiu, J. Sanchez, and G. M. Rios, "A unified approach of gas, liquid and supercritical solvent transport through microporous membranes," *Chem. Eng. Sci.*, vol. 59, no. 7, pp. 1569–1576, 2004.
- [25] R.W. Rousseau, "Handbook of Separation Process Technology", John Wiley & Sons, 1987.
- [26] J. D. Seader, E. J. Henley, and D. K. Roper, "*Separation process principles: Chemical and biochemical operations*", 3rd ed., John Wiley & Sons, 2011.
- [27] J. Xiao and J. We, "Diffusion mechanism of hydrocarbons in zeolites-Analysis of experimental observations," *Chem. Eng. Sci.*, 1992.
- [28] J. Xiao and J. Wei, "Diffusion mechanism of hydrocarbons in zeolites-Theory," *Chem. Eng. Sci.*, vol. 47, pp. 1123-1141, 1992.
- [29] S. A. H. Hejazi, A. M. Avila, T. M. Kuznicki, A. Weizhu, and S. M. Kuznicki, "Characterization of natural zeolite membranes for H<sub>2</sub>/CO<sub>2</sub> separations by single gas permeation," *Ind. Eng. Chem. Res.*, vol. 50, pp. 12717–12726, 2011.
- [30] R. Krishna and R. Baur, "Modelling issues in zeolite based separation processes," *Sep. Purif. Technol.*, vol. 33, pp. 213–254, 2003.
- [31] S. Thomas, R. Schäfer, J. Caro, and A. Seidel-morgenstern, "Investigation of mass transfer through inorganic membranes with several layers", *Catal. Today*, vol. 67, pp. 205–216, 2001.

- [32] E. A. Mason and A. P. Malinauskas, “*Gas Transport in Porous Media: The Dusty-Gas Model*”, Elsevier: Amsterdam, 1983.
- [33] Y. S. Lin and M. C. Duke, “Recent progress in polycrystalline zeolite membrane research,” *Curr. Opin. Chem. Eng.*, vol. 2, no. 2, pp. 209–216, 2013.
- [34] P. F. Lito, C. F. Zhou, A. S. Santiago, A. E. Rodrigues, J. Rocha, Z. Lin, and C. M. Silva, “Modelling gas permeation through new microporous titanosilicate AM-3 membranes”, *Chemical Engineering J.*, vol. 165, pp. 395–404, 2010.
- [35] P. Bernardo, E. Drioli, and G. Golemme, “Membrane Gas Separation: A Review/State of the Art,” *Ind. Eng. Chem. Res.*, vol. 48, no. 10, pp. 4638–4663, 2009.

## **Chapter Five**

---

### **Pressed clinoptilolite and copper-clinoptilolite disk membranes for hydrogen separation**

This Chapter is submitted for publication (under review) in The "Canadian Journal of Chemical Engineering", April 2016

## **5.1 Summary**

Disk membranes fabricated from high-purity natural clinoptilolite rock demonstrated high efficiency in hydrogen separation; however, these membranes cannot be easily scaled up. To overcome this and create process flexibility, mixed matrix membranes are required combining small particles of natural zeolite with a binder system. A novel method was determined to use metals as binders and was tested by comparing natural clinoptilolite compact disk membranes with and without powdered copper metal. The phase structure and structure of the disks were characterized and gas separation performance was evaluated using single gas permeation tests. Membrane performance was improved by applying metallic copper and copper oxide filling a portion of the inter-particle spaces and creating adhesion with the zeolite particles.

## **5.2 Introduction**

Hydrogen separation by selective transport through membranes is one of the highly utilized methods in commercial gas separation because of its simple process. Membrane technology is becoming widely important in several separation processes in industrial application [1],[2]. Comparing separations using membranes, with other separation methods such as distillation or adsorption, membranes offer a single-pass process with low capital and operating costs, lower energy requirements and overall ease of operation [3],[4]. Membrane technology also has encouraging aspects to be integrated within sustainable energy processes [5],[6].

As the process intensification concept becomes more popular, new cost effective inorganic materials capable of being integrated into compact membrane modules are

attracting both academic and industrial attention [7],[8]. Compared to polymer membrane, the high thermal stability and chemical inertness of the inorganic membranes have made them popular for many commercial applications [9],[10]. Inorganic zeolite membranes are interesting because of their perm selectivity properties and relatively higher stability at elevated temperatures [11].

Synthetic molecular sieve membranes for hydrogen separation have been vastly studied. However, their applications have been limited by high production costs and technical challenges including cracks or defects in the membranes and weak physical and chemical compatibility between thin synthetic membranes and the required porous supports [12], [13]. Natural zeolites in particular clinoptilolite and chabazite, have higher thermal stability and resistance to acidic positions than most industrially used synthetic zeolites [14–17]. Since they are formed under geological conditions of high temperature and pressure, the crystals have larger grain boundaries and experienced severe conditions [18–20]. The small pore size combined with the ability of the zeolite to adsorb more strongly at low partial pressures provides unique separation potential features (kinetic, equilibrium and steric) that only partially exists in type A and other commercially available synthetic zeolites [16],[21–23]. The typical formula of clinoptilolite is  $(\text{Na}^+, \text{K}^+)_6 [\text{Al}_6 \text{Si}_{30} \text{O}_{72}] \cdot 20 \text{H}_2\text{O}$  and its framework structure contains three sets of intersecting channels of eight and ten member rings. The size of the largest channel of clinoptilolite framework is  $5.5 \times 4.0 \text{ \AA}$  [16,18,24]. Therefore, It has the potential to allow smaller molecules such as  $\text{H}_2$  to diffuse quickly while stopping the diffusion of relatively larger molecules such as  $\text{CH}_4$ ,  $\text{C}_2\text{H}_4$  or  $\text{C}_2\text{H}_6$  [18],[ 19]. Selective natural zeolite-based

membranes have the potential to become an economical technique for applications in hydrogen separation [25-27].

Different inorganic composite membranes have been reported for separation of hydrogen fabricated from ceramics, silica, metal alloys or zeolites widely used in gas separation because of their thermal or chemical stability [10],[28,29]. Previously, we reported that natural clinoptilolite membranes directly cut from mineral deposits can be used for H<sub>2</sub> selective separation processes [30]. In order to improve the selectivity of H<sub>2</sub> separation, An et al. [31] used cation exchange modification method to study the effect of the type and size of the extra framework cations on removal of hydrogen. Dehydrogenation of light hydrocarbons is industrially important for production of chemical products [32],[33]. The production yield in this reaction can be improved by using inorganic membranes as selective channels of the products. Avila et al. [34] used natural mordenite in a membrane reactor to remove hydrogen selectively and observed an equilibrium shift in ethane dehydrogenation reaction. Shafie et al. (2012) [35] used inexpensive and selective natural zeolite based cement composite membranes for H<sub>2</sub>/CO<sub>2</sub> separations.

Although effective removal of hydrogen from carbon dioxide and other hydrocarbons has been occurred with these mineral membranes scaling up to an industrial membrane technology for gas separation treatment is still a challenge. The preparation of cost-effective natural zeolite based composite membranes with acceptable permselectivity properties would be valuable in terms of scaling up.

The use of mixed matrix membranes has been extensively studied in the last decades, particularly by using inorganic fillers such as zeolites and carbon particles in a continuous polymer matrix. The challenge in this research area is still associated with the

not enough adhesion between the polymer phase and the inorganic particles which reduce the separation selectivity [36]. To the best of the authors' knowledge metals used as binders have not been widely studied. The robust structure of metals along with their malleability properties can offer features as binder materials in the preparation of inorganic mixed matrix membranes.

In this study, pressed natural clinoptilolite and copper-clinoptilolite composite disk membranes were prepared and tested for hydrogen separation. The focus in this work is a novel approach to use natural zeolites in gas separation by applying copper metal powder as a binder. Membranes were characterized using X-Ray powder Diffraction (XRD), Scanning Electron Microscopy (SEM) and Energy Dispersive X-ray (EDX) analysis. Their permselectivity properties were evaluated using hydrogen, carbon dioxide and ethane permeation tests. Permeances and hydrogen selectivities were quantified and compared between the two types of membrane disks. The effectiveness of metallic copper as a binder material and sealant agent in the copper-clinoptilolite composite membranes was evaluated. A comparative parameter defined in terms of hydrogen single permeability was used, which could be associated with the relative average defect size of each membrane.

### **5.3 Material and methods**

Substantial differences exist in the phase purity of natural zeolite samples from different natural deposits. A mostly pure sample of clinoptilolite, Ash-Meadows were provided by St. Cloud Mining Company (New Mexico, USA), with particle size corresponding to the 325 mesh ( $<44 \mu\text{m}$ ), which represents an optimum sample for modification and

development. The nominal mineralogical composition of the sample is listed in Table 5-1 and the calculated Si/Al molar ratio is equal to 4.13. The zeolite material has a bulk density of ~1.28g. Based on the supplier's product sheet, the clinoptilolite is at least 99% pure.

**Table 5-1.** Energy-dispersive X-ray (EDX) data for the natural clinoptilolite sample (norm wt %).

	Na	K	Ca	Mg	Fe	Al	Ti	Si	Cl	S	O
Clinoptilolite	3.37	3.73	0.5	0.4	0.88	7.14	0.046	30.57	0.07	0.08	53.23

### 5.3.1 Preparation and characterization of membranes

Natural zeolite disk membranes were prepared by dry pressing method. 3 g of zeolite powder was dry-pressed into a disk shape with a manual hydraulic press using 19.0 mm diameter die under a pressure of 210 MPa. Prior to gas permeation tests, the pressed clinoptilolite disk was cured overnight, using a temperature programmable muffle furnace at atmospheric pressure up to 650 °C for 4 hours.

To study the thermal stability of the membrane material, powder samples receiving thermal treatments with increasing increments were analyzed by XRD. XRD patterns were collected by Rigaku Geigerflex Model 2173 diffractometer with a Co tube and a graphite monochromator.

Figure 5-1 shows the XRD patterns for clinoptilolite heat treated at temperatures ranging from 200 °C to 900 °C. The heat treated samples showed that increasing the temperature up to 800 °C had no significant impact on clinoptilolite crystal structure since the peak widths and locations did not change up to 800 °C .

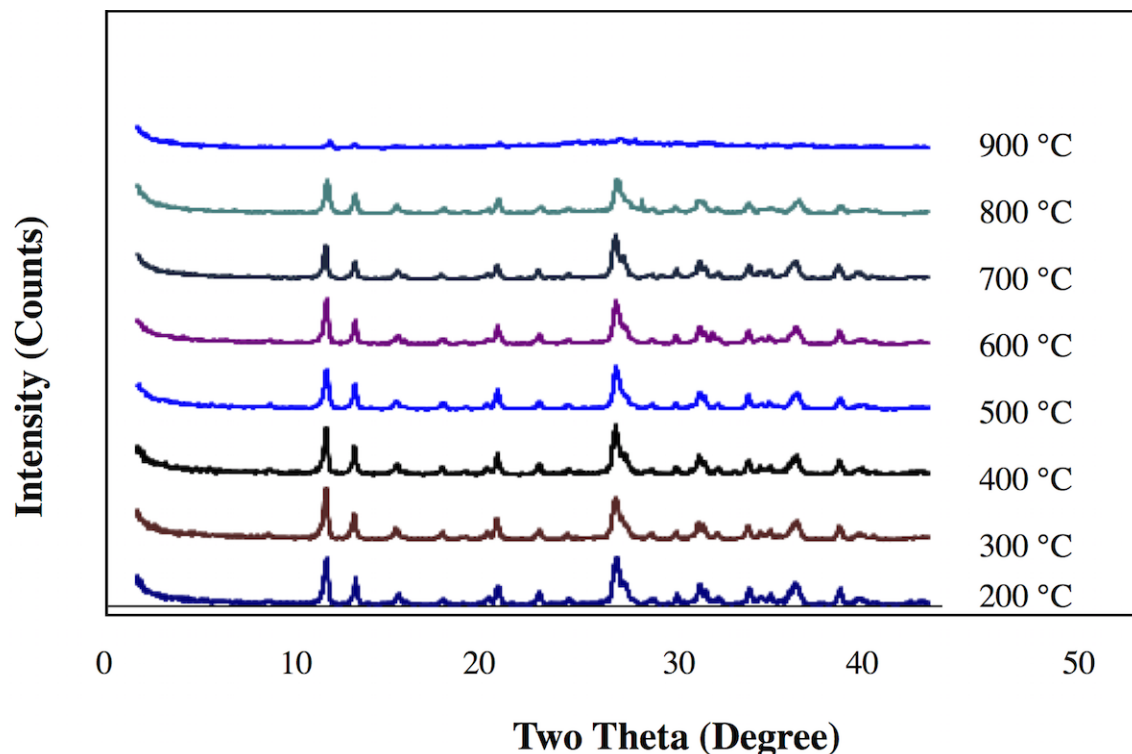


**Figure 5-1.** XRD patterns for natural clinoptilolite samples heat treated at 200 °C, 300 °C, 400 °C, 500 °C, 600 °C, 700 °C, 800 °C and 900 °C for 1 hour.

To characterize and observe surface morphologies of the pressed membranes, SEM (Hitachi S-4800 FESEM) was also used.

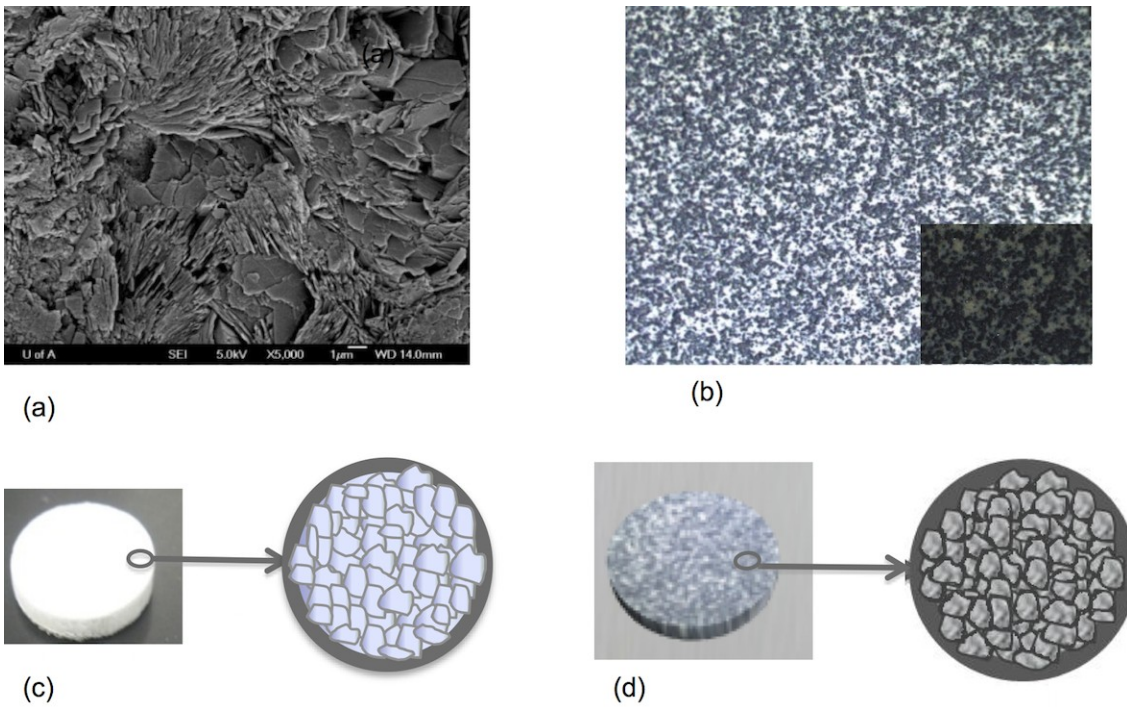
### **5.3.2 Mixed clinoptilolite-copper composite membranes**

Metallic copper powder was added as a binding material to natural clinoptilolite powder to form a natural zeolite-based composite membrane. Copper is a malleable metal with high heat stability and thermal conductivity (melting point: 1085 °C) and is extensively used in powder metallurgical methods as a binder [37],[38]. At 650 °C the temperature at which the composite membrane disks were treated, sintering of the copper powder particles occurred. In these conditions, it was expected that metallic copper would start to

diffuse across the boundaries of particles creating a complete adhesion with the clinoptilolite particles and, thus, decreasing the effective size of inter particle channels.

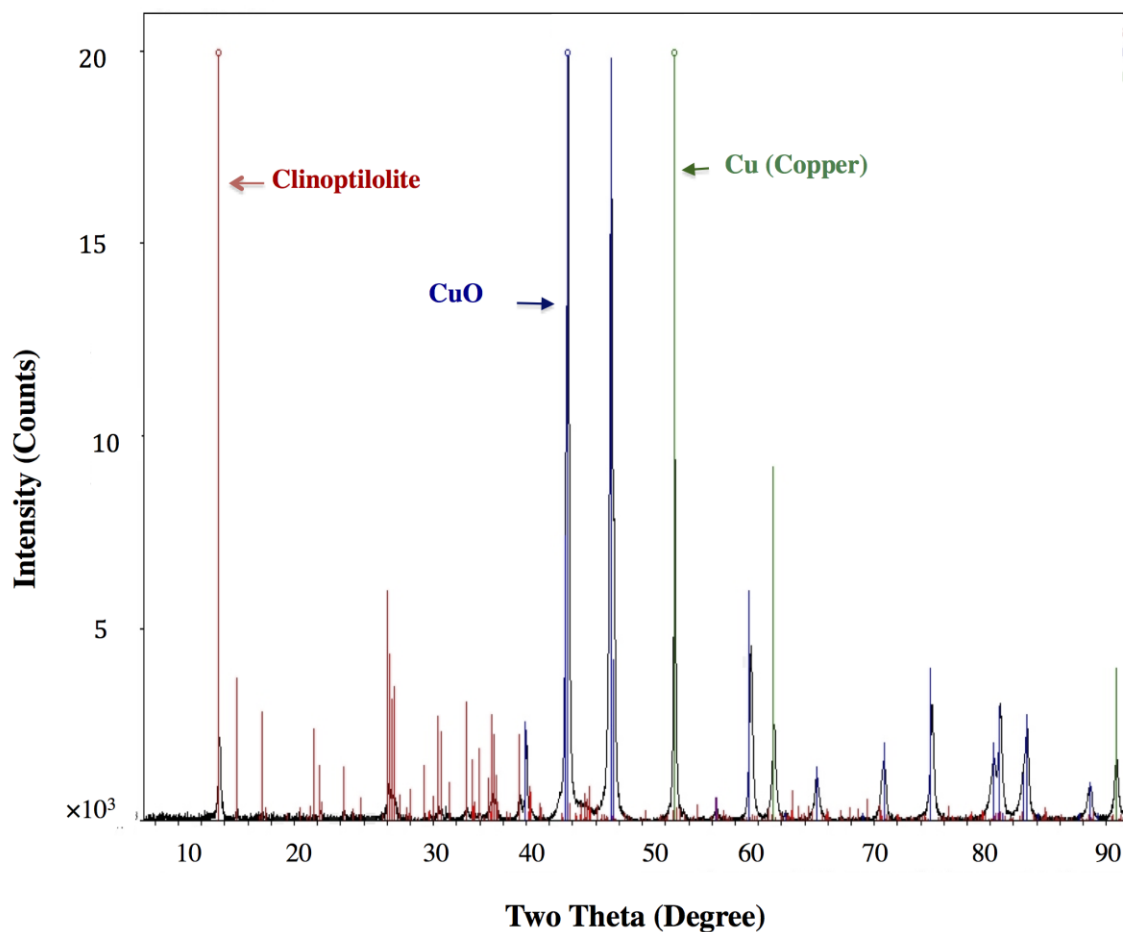
Clinoptilolite and copper powders, supplied by Fisher Scientific Co. (Ontario, Canada) were mixed together in the weight ratio of 1:2 (volume ratio of 2:1). Being completely mixed, the paste was dry-pressed up to 210 MPa. The resulting copper-clinoptilolite (Cu-CLI) and pressed clinoptilolite (CLI) disks had a diameter of 19 mm and thickness of 1.3 mm and 2 mm, respectively. They were further treated in ambient atmosphere at 650 °C for 4 h. Heat treatment in presence of air, formed CuO particles on the surface of the membranes as confirmed by XRD measurements. Optical microscopy examination of these composite membranes showed a dense, crack-free surface morphology and relatively uniform dispersion of CuO particles on the clinoptilolite composite membrane. Scanning electron and optical microscopy images of the membrane disks treated in ambient atmosphere are presented in Figure 5-2 a) and b) respectively. The lighter regions on the membrane surface in Figure 5-2 b) indicate clinoptilolite material while the darker zones contain Cu<sup>0</sup> and CuO particles.

Figure 5-2 c) and d) show the schematic picture of pressed CLI and Cu-CLI composite membranes, respectively. After applying copper, a more compact matrix with a complete adhesion between particles and metal phase was obtained.



**Figure 5-2.** a) SEM image of clinoptilolite powders, b) optical microscopy image of Cu-CLI (16x-64X), c) schematic of CLI membrane disks, and d) schematic of Cu-CLI membrane disks.

XRD patterns of the Cu-CLI membrane heat-treated to 650 °C for 4 hours are shown in Figure 5-3. Sharp and high intensity peaks of the patterns are indicative of crystalline structure after copper was applied as a binder. (XRD) patterns also indicated that the samples were partially composed of a single phase CuO due to heat treatment while the composite membrane still maintained the crystalline structure for gas separation.



**Figure 5-3.** XRD patterns of clinoptilolite, copper and copper oxides in Cu-CLI membrane after heat treatment up to 650 °C for 4 hours.

### 5.3.3 Gas Separation Tests

Single gas permeation of  $H_2$ ,  $C_2H_6$  and  $CO_2$  gases supplied by Praxair Canada was used for evaluating membrane performance in feed pressure range of 110-160 kPa and temperature range of 25 °C -200 °C. The gas permeation was performed using a stainless steel cross flow membrane testing system shown in Figure 5-4. Membranes were sealed in a stainless steel flanged cell with graphite gaskets.

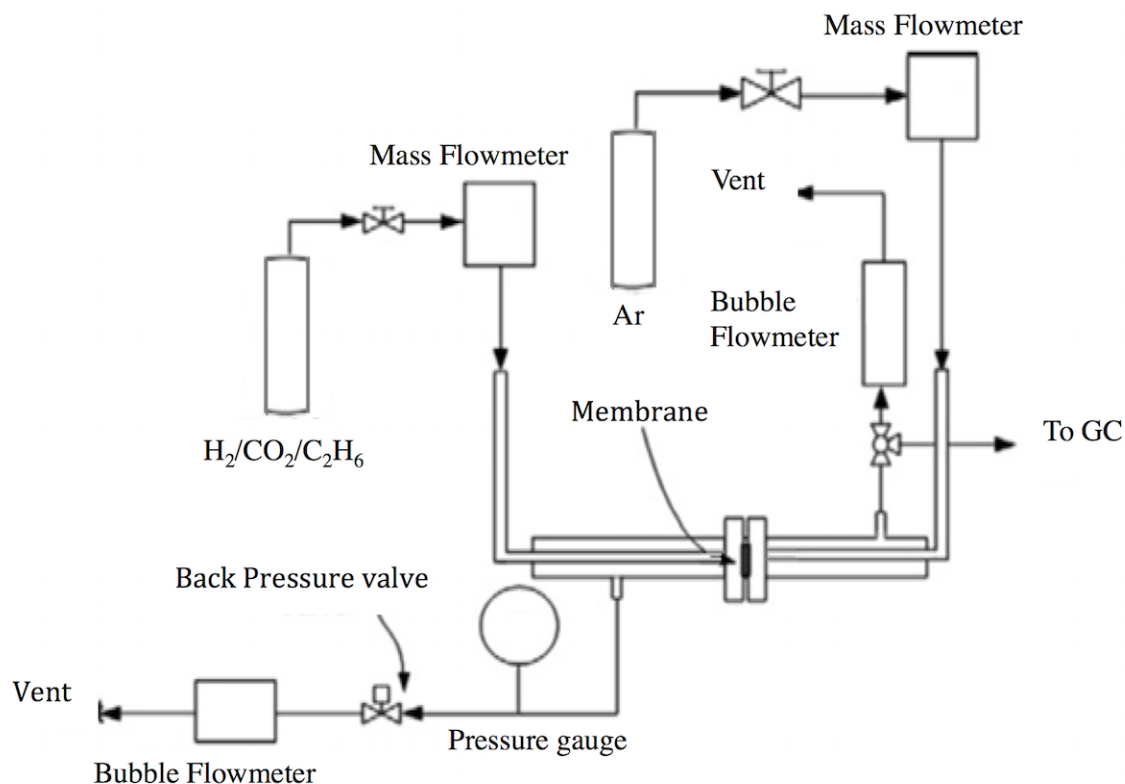


**Figure 5-4.** Schematics of the set up for single gas permeation measurements.

To evaluate membranes at higher temperatures, the flanged membrane cell was placed into a tubing furnace with a multipoint programmable temperature controller. A heating rate of 5 °C/min was set for each temperature interval.

Pressure was controlled by a back pressure regulator located at the outlet of feed side. The feed and sweep gas flow rates were controlled by two mass flow controllers (Sierra Instrument Inc., Ontario, Canada). For all gas permeation tests, feed and sweeping gas flow rates were set constant at 100 mL/min (STP). The retentate and permeate flowrate were measured by bubble flow meters. An on-line Shimadzu Gas Chromatograph GC-14B (GC) equipped with TCD and packed column (HayeSep Q, 80–100 mesh) was used to analyze the outlet gas concentrations. To achieve the maximum thermal conductivity

difference between the carrier gas and the analyte, helium was used as GC carrier gas for CO<sub>2</sub> and C<sub>2</sub>H<sub>6</sub> while argon was used for H<sub>2</sub> analysis.

H<sub>2</sub>, CO<sub>2</sub> and C<sub>2</sub>H<sub>6</sub> permeances and H<sub>2</sub>/CO<sub>2</sub> and H<sub>2</sub>/C<sub>2</sub>H<sub>6</sub> selectivities were calculated based on the following definitions:

$$\pi_i = \frac{N_i}{\Delta P_i} \quad (1)$$

where  $\pi_i$  is the permeance (mol.m<sup>-2</sup> s<sup>-1</sup> Pa<sup>-1</sup>),  $N_i$  is the molar flux (mol s<sup>-1</sup> m<sup>-2</sup>), Pa is the partial pressure difference of component i across the membrane; and

$$S_{ij} = \frac{\pi_i}{\pi_j} \quad (2)$$

where,  $S_{ij}$  is the ideal selectivity of species i over j. In all the reported permeation results, there is an uncertainty estimated by a standard propagation of error analysis [39]. Absolute error propagation was the product of the uncertainties associates with different variables including pressure, temperature, flow rate and gas chromatography measurements.

### 5.3.4 Membrane Screening based on the Relative Averaged Defect Size

It was previously shown in our research team that natural zeolite membranes can be screened based on the relative average defect size using a comparative coefficient obtained when H<sub>2</sub> single permeability is plotted as a function of pressure [40]. The H<sub>2</sub> permeance across the membrane can be considered as a combination of two permeance fractions. One fraction is associated with Poiseuille or viscous flow depends on pressure while the other fraction is not correlated with pressure change and includes Knudsen and zeolitic flux contributions. The permeability calculated for H<sub>2</sub> is calculated as follows:

$$\text{Permeability } (\pi_i \delta) = \alpha_v [P^*] + \beta_{kz} \quad (3)$$

$$P^* = P_m \frac{\Delta P}{\Delta P_i} \quad (4)$$

The first term on the right hand side of Eq. 3 is pressure dependent while the second term is invariable with pressure.  $P_m$  is the mean pressure between the feed and the permeate side. The coefficients  $\alpha_v$  and  $\beta_{kz}$  are the slope and intercept of a linear fitting of the permeability data as a function of  $P^*$ .  $\alpha_v$  is a coefficient associated with viscous flow and  $\beta_{kz}$  is attributed to Knudsen and zeolite fluxes. As it was discussed in [40], the ratio  $\lambda = \alpha_v / \beta_{kz}$  is a comparative parameter which is associated with the averaged defect size of each membranes. The membrane having the smallest averaged non-zeolite pore size corresponds to the lowest value of the  $\lambda = \alpha_v / \beta_{kz}$  ratio. The values for the coefficient  $\lambda$  were estimated and compared for the CLI and the Cu-CLI membrane disks to evaluate the effectiveness of copper as a binder for clinoptilolite particles.

## 5.4 Results and Discussion

### 5.4.1 Gas permeation through pressed clinoptilolite disks

#### *Effect of temperature*

Figure 5-5 shows  $H_2$ ,  $CO_2$  and  $C_2H_6$  permeances through CLI as a function of temperature. The permeances of all gases, hydrogen in particular, increased slightly with the operating temperature. Since the permeance contributions associated with Knudsen and viscous flux decreases with temperature, the increasing permeation trend for all the gases with temperature reflect the prevailing contribution of zeolite flux at these experimental conditions [40–45]. At higher temperatures, a larger fraction of  $H_2$  flux

diffuses through the zeolite crystals. The  $H_2/CO_2$  and  $H_2/C_2H_6$  ideal selectivities were 6.5 and 5 respectively at 25 °C when the feed pressure was 111.2 kPa and the permeate pressures was 108.2 kPa.

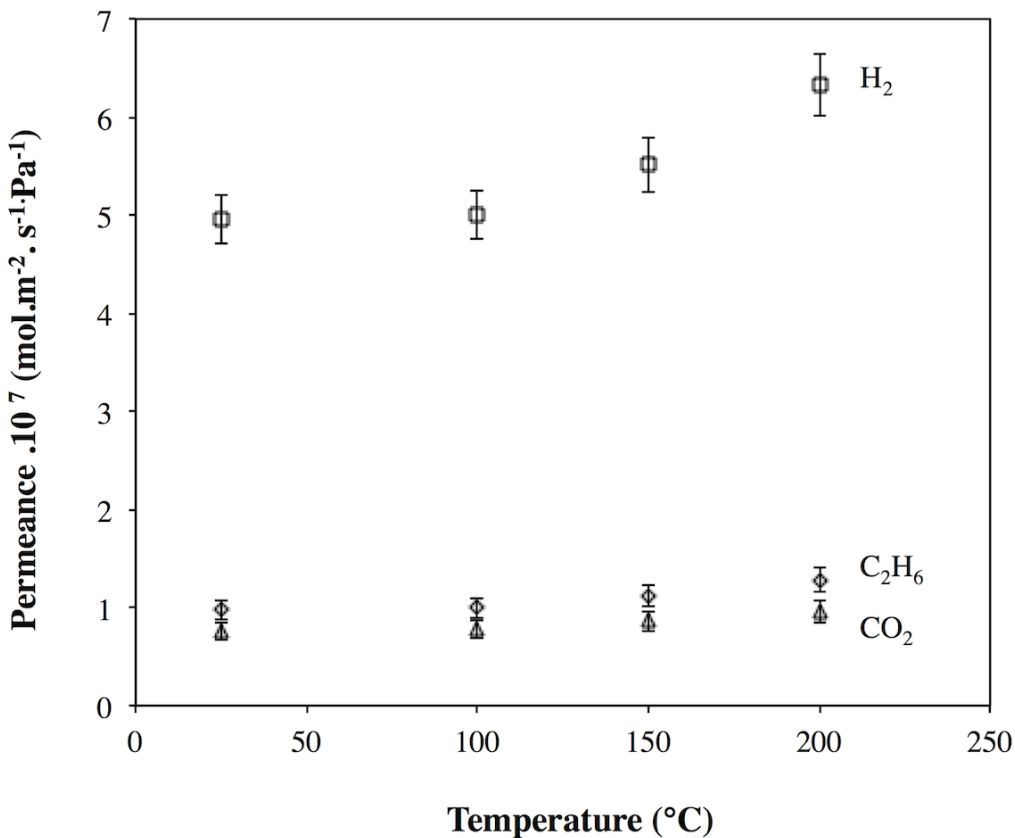


**Figure 5-5.** Single permeance of  $H_2$ ,  $C_2H_6$  and  $CO_2$  through CLI membrane disks as a function of temperature, feed pressure: 111.2 kPa, permeate pressure: 108.0 kPa.

#### *Effect of pressure*

Figure 5-6 shows the permeances of  $H_2$ ,  $CO_2$  and  $C_2H_6$  at different feed pressures. Accordingly, the  $H_2$ ,  $CO_2$  and  $C_2H_6$  permeances through the membrane disks increased, as the feed pressure was higher. However, the permeance fraction associated with the Knudsen flux contribution remains constant as pressure increases [40],[44–46] while permeance related to the zeolitic flux is either constant for weak or non-adsorbing

components ( $H_2$ ) or slightly decreases with pressure for adsorbing groups like  $CO_2$  and  $C_2H_6$ . The increasing trend of permeance with pressure is due to the growing viscous flux contribution through the relatively large non-zeolite pores as feed pressure increased and consequently  $H_2$  selectivity decreased [40,45,47,48].

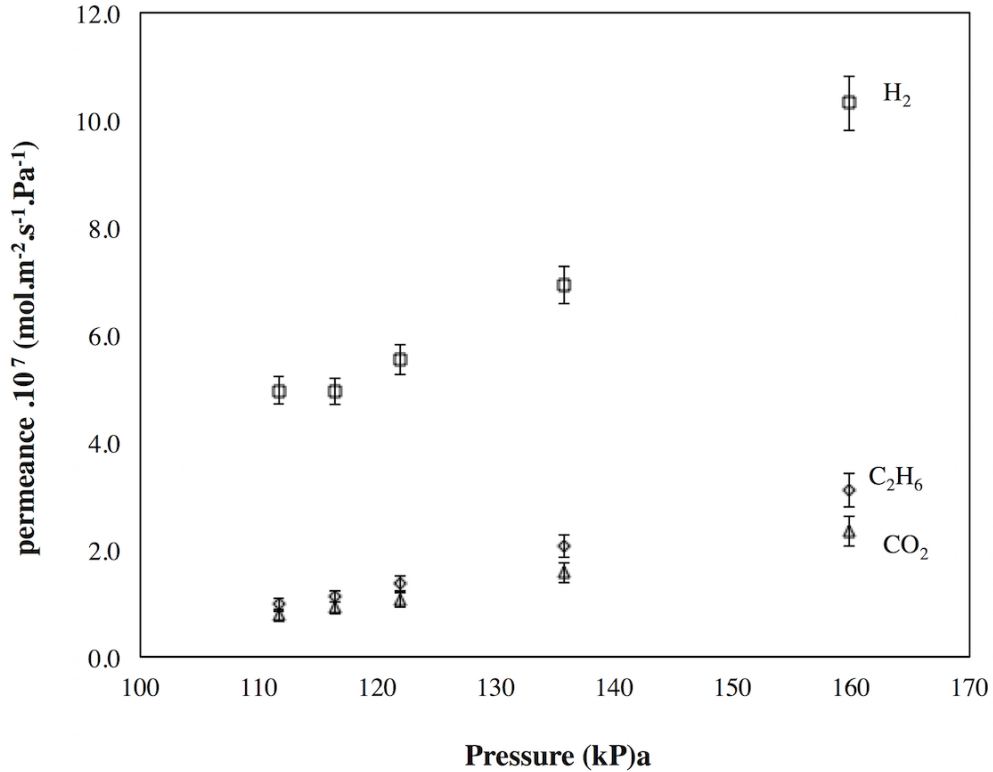
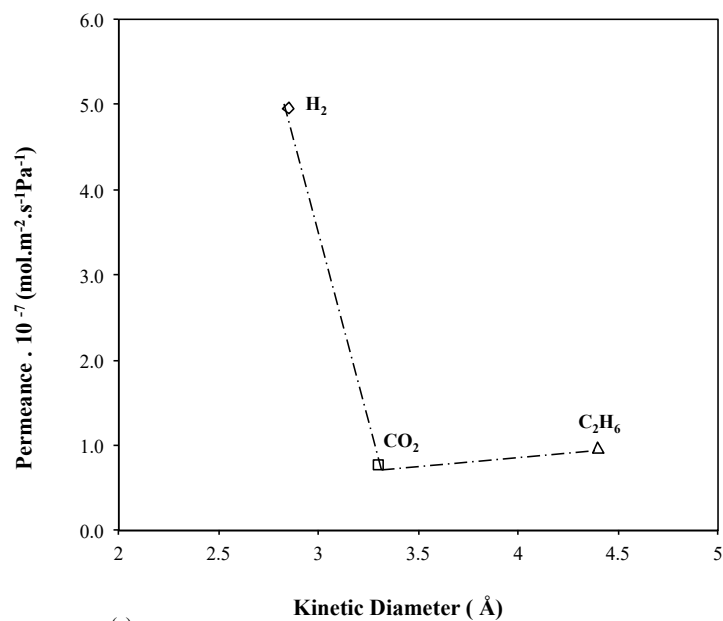


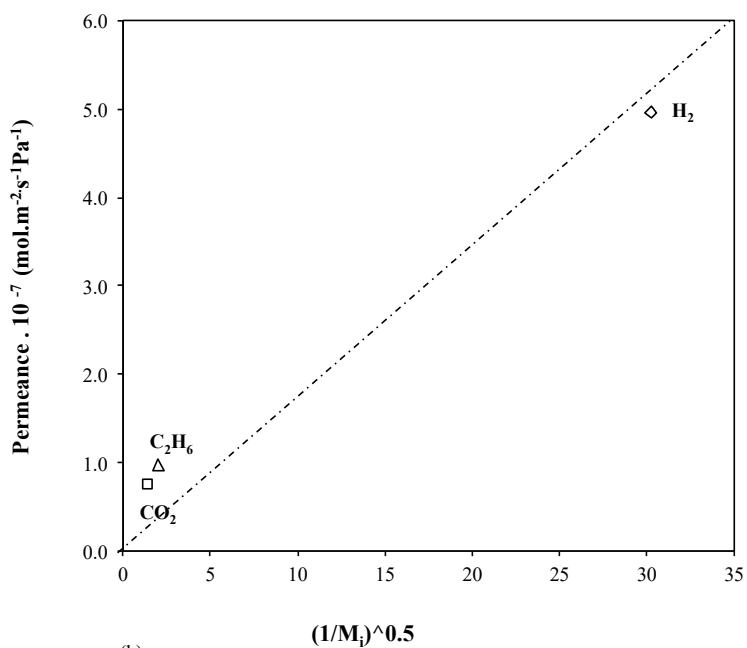
**Figure 5-6.** Single permeance of  $H_2$ ,  $C_2H_6$  and  $CO_2$  through CLI membrane disks at different feed pressures, temperature: 25 °C, permeate pressure: 108.0 kPa.

$H_2$  permeance across pressed clinoptilolite disk ranges between  $\sim 5 \times 10^{-7}$  and  $\sim 1 \times 10^{-6}$  for temperatures increasing from 25 °C to 200 °C and feed pressure values up to 160 kPa. The selectivity values for  $H_2$  over  $CO_2$  and  $C_2H_6$  were higher than those predicted by Knudsen selectivities  $S_{H_2,CO_2}^K = 4.6$ ,  $S_{H_2,C_2H_6}^K = 3.9$ .

Figure 5-7 a) shows that CO<sub>2</sub> permeance through CLI membrane disks does not correlate with the H<sub>2</sub> and C<sub>2</sub>H<sub>6</sub> values in terms of their molecular sizes, which suggest that transport mechanisms other than molecular sieving, are also contributing to the flux permeation. Similarly, gas permeation across CLI disks cannot be described by a pure Knudsen transport mechanism either (Figure 5-7b). Analogous to the permeation behaviour observed previously in natural zeolite rocks disks [30], the gas permeation across the pressed disks relies on the contribution of different transport mechanisms associated with both zeolite and non-zeolite pores.



(a)



(b)

**Figure 5-7.** Permeance of H<sub>2</sub>, CO<sub>2</sub> and C<sub>2</sub>H<sub>6</sub> through CLI disk membrane disks as a function of a) kinetic diameter and b) molecular weight. Temperature: 25 °C, feed pressure: 111.2 kPa, permeate pressure 108.2 kPa.

#### 5.4.2 Mixed clinoptilolite-copper composite membrane

In order to minimize the non-zeolite pores in the pressed clinoptilolite material, copper metal was mixed with clinoptilolite particles to make Cu-CLI composite membranes.

#### 5.4.3 Comparison of permeation results between both types of membrane disks

Figures 5-8 and 5-9 show the comparison for CO<sub>2</sub> and C<sub>2</sub>H<sub>6</sub> permeances as a function of feed pressure for both types of membrane disks respectively. While the CO<sub>2</sub> and C<sub>2</sub>H<sub>6</sub> permeances for the CLI membranes changed from  $\sim 0.8 \times 10^{-7} \text{ mol m}^{-2} \text{ s}^{-1} \text{ Pa}^{-1}$  to  $\sim 2 \times 10^{-7} \text{ mol m}^{-2} \text{ s}^{-1} \text{ Pa}^{-1}$  and  $\sim 1 \times 10^{-7} \text{ mol m}^{-2} \text{ s}^{-1} \text{ Pa}^{-1}$  to  $\sim 3 \times 10^{-7} \text{ mol m}^{-2} \text{ s}^{-1} \text{ Pa}^{-1}$  respectively over the pressure range of range of  $P_{\text{feed}} = 111\text{-}160 \text{ kPa}$ , in the Cu-CLI composite membrane the permeance changed in the ranges of  $\sim 1 \times 10^{-8} \text{ mol m}^{-2} \text{ s}^{-1} \text{ Pa}^{-1}$  to  $\sim 3 \times 10^{-8} \text{ mol m}^{-2} \text{ s}^{-1} \text{ Pa}^{-1}$  and  $2 \times 10^{-8} \text{ mol m}^{-2} \text{ s}^{-1} \text{ Pa}^{-1}$  to  $\sim 5 \times 10^{-8} \text{ mol m}^{-2} \text{ s}^{-1} \text{ Pa}^{-1}$ .

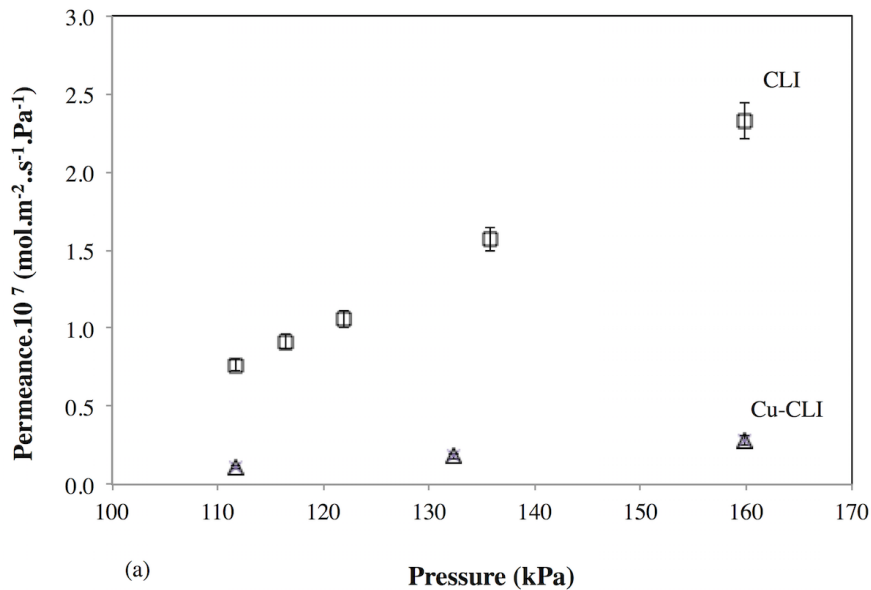


**Figure 5-8.** CO<sub>2</sub> permeance through CLI and Cu-CLI membranes at different feed pressures, permeate pressure: 108.2 kPa, temperature: 25 °C.

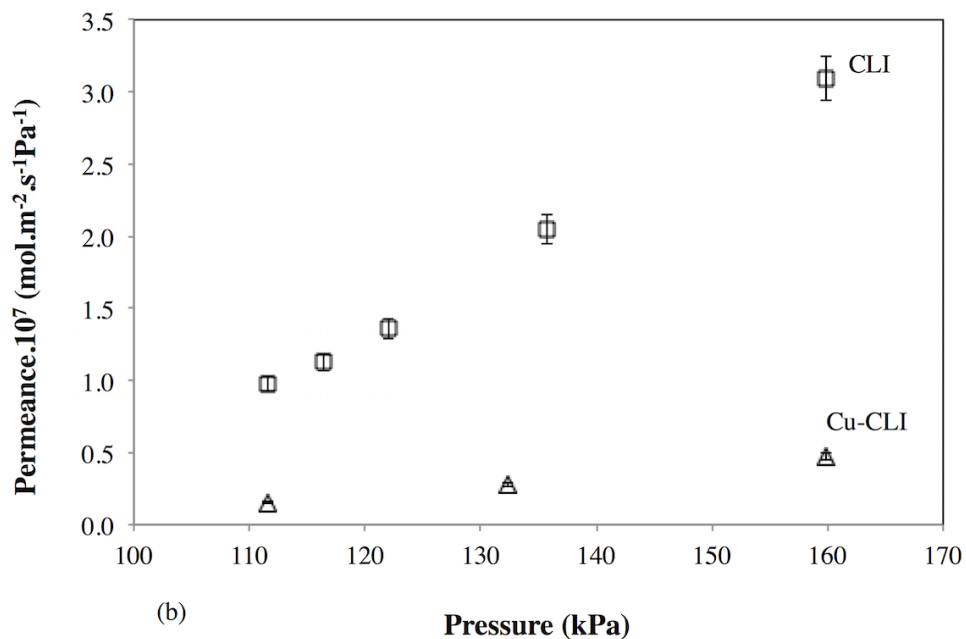


**Figure 5-9.** C<sub>2</sub>H<sub>6</sub> permeance through CLI and Cu-CLI membranes at different feed pressures, permeate pressure: 108.2 kPa, temperature: 25 °C.

The CO<sub>2</sub> and C<sub>2</sub>H<sub>6</sub> gas permeance values through Cu-CLI disks decreased significantly compared to those values obtained in the samples containing only clinoptilolite particles. CO<sub>2</sub> permeance across the composite membrane was only 18% of the corresponding permeance values through the CLI disks. A similar permeance drop was obtained for C<sub>2</sub>H<sub>6</sub>. Besides reducing the non-zeolite pores, a fraction of the permeance drop is associated with the reduction of zeolite content in the Cu-CLI composite material in comparison to the CLI disks. The volume fraction for the clinoptilolite content reduced in the ratio 3:2 when the clinoptilolite particles were mixed with copper powder. Copper and copper oxide may be also covering active zeolite pores for permeation and thus representing an additional contribution to the flux reduction. However, CO<sub>2</sub> and C<sub>2</sub>H<sub>6</sub> gas

permeance also decreased due to the non-zeolite flux reduction occurring in the Cu-CLI membranes.

The CLI and Cu-CLI disks with 2 mm and 1.3 mm thickness respectively provided H<sub>2</sub> permeance values which are comparable to those reported in the literature for micro zeolite films supported membranes [49–53]. H<sub>2</sub> permeability ( $\pi \times \delta$ ) where  $\delta$  is the membrane thickness, was two orders of magnitude higher than other H<sub>2</sub> selective materials (Table 5-2).

**Table 5-2.** Comparison of H<sub>2</sub> permeability of different inorganic membranes.

Membrane	Temperature (°C)	Permeability (mol.m <sup>-1</sup> .s <sup>-1</sup> .pa <sup>-1</sup> )	Thickness ( $\mu$ m)	Ref.
Molecular Sieve Silica	200	$6 \times 10^{-14}$	0.03	[54]
MFI	450	$1.3 \times 10^{-12}$	2	[11]
MOF (ZIF-8)	25	$1.18 \times 10^{-11}$	38	[55]
Cu-CLI	200	$1.11 \times 10^{-10}$	1300	This Work

Figure 5-10 shows the H<sub>2</sub> permeability of each membrane as a function of P\* as defined in Eq. 3. Pressed zeolite (CLI) membrane shows higher permeability, as the intersection at y-axis is larger. The corresponding values of the ratio  $\lambda = \alpha_v / \beta_{kz}$  ratio for each membrane are listed in Table 5-3. CLI membrane shows a higher value of  $\lambda$  than Cu-CLI membrane. This is indicating that the average defect size is smaller for the Cu-CLI composite membrane than for the CLI membrane disks. A smaller value of the average

defect size represents a reduced fraction of non-zeolite fluxes for CO<sub>2</sub> and C<sub>2</sub>H<sub>6</sub> as feed pressure increased. Therefore, the extent of the “non-selective” viscous flux passing through the relatively larger non-zeolite pores was reduced. This is consistent with a smaller defect size for Cu-CLI composite as compared to the pressed CLI disks:

$$([\alpha_v/\beta_{kz}]_{Cu-CLI} < [\alpha_v/\beta_{kz}]_{CLI}).$$

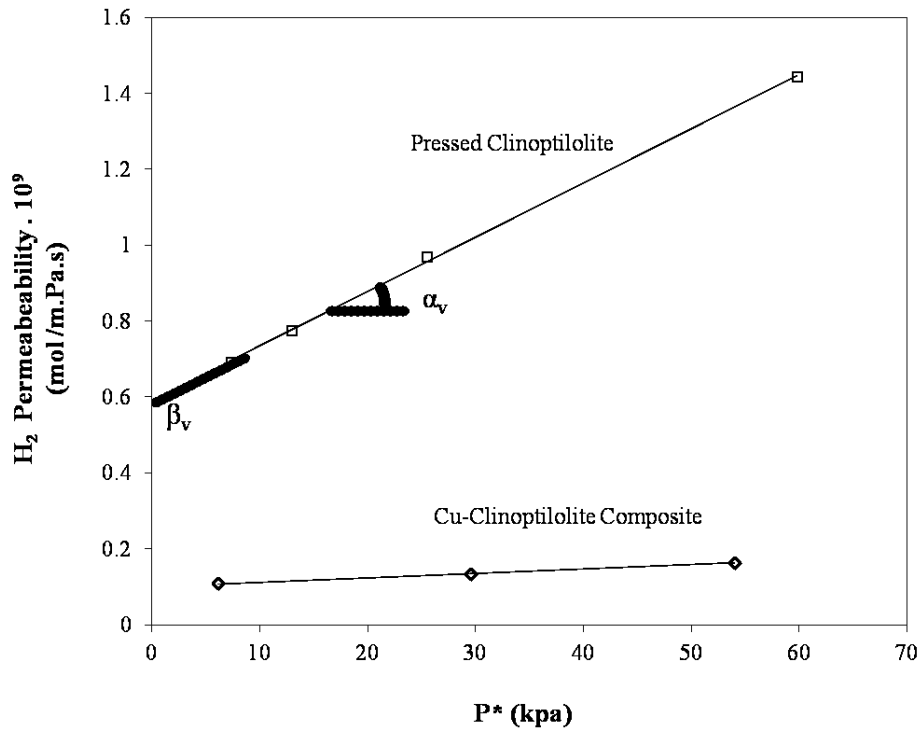


**Figure 5-10.** Comparative parameters ( $\alpha_v$ ,  $\beta_{kz}$ ) for CLI and Cu-CLI membranes, permeate pressure: 108.2 kPa, temperature: 25 °C.

**Table 5-3.** Comparative Parameter ( $\lambda = \alpha_v / \beta_{kz}$ ) for CLI and Cu-CLI disk membranes.

Membrane	$\lambda \times 10^3$ (kpa <sup>-1</sup> )
Pressed CLI	3.44
Composite Cu-CLI	1.09

### 5.5 H<sub>2</sub> selectivity enhancement

The selectivity values of H<sub>2</sub>/CO<sub>2</sub> and H<sub>2</sub>/C<sub>2</sub>H<sub>6</sub> on CLI and Cu-CLI membranes are presented in Figure 5-11. In the temperature range of 25 to 200 °C, the H<sub>2</sub>/CO<sub>2</sub> the averaged selectivity for the Cu-CLI increased ~18 % regarding the original value of the CLI disks while H<sub>2</sub>/C<sub>2</sub>H<sub>6</sub> selectivity increased ~15%.

The increase of H<sub>2</sub> selectivity on Cu-CLI in comparison to the CLI is a clear indication that copper metal was effective as a binder for zeolite particles. H<sub>2</sub> selectivity increased because copper binder decreased the size of inter crystalline or non-zeolite channels across the membrane disk as demonstrated with the estimation of the coefficient  $\lambda = \alpha_v / \beta_{kz}$  shown in Table 5-3. Since the size of relative larger defects in the membrane decreased, the contribution of non-selective flux (viscous or Poiseuille flux) was reduced and thus H<sub>2</sub>/CO<sub>2</sub> and H<sub>2</sub>/C<sub>2</sub>H<sub>6</sub> selectivities increased.

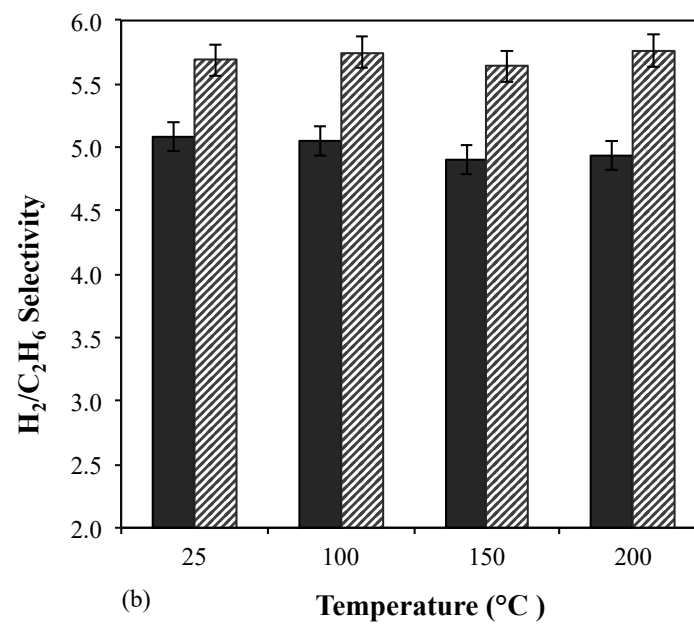
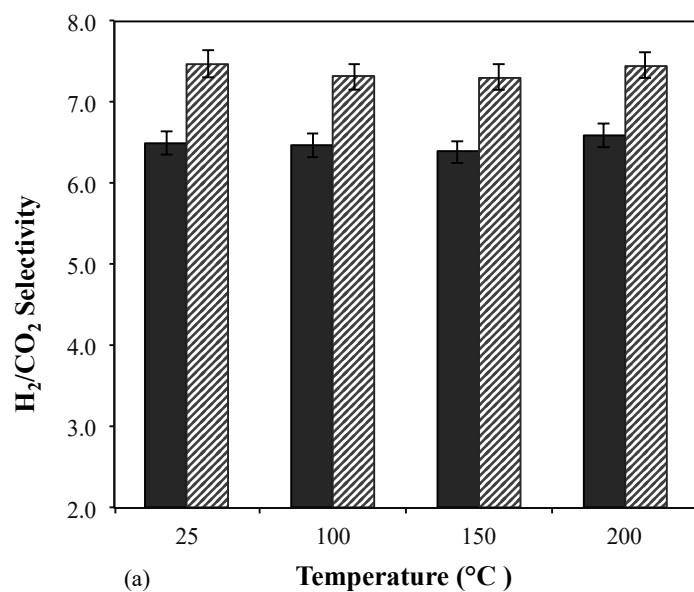


**Figure 5-11.** a) H<sub>2</sub>/CO<sub>2</sub> and b) H<sub>2</sub>/C<sub>2</sub>H<sub>6</sub> separation selectivities through CLI (solid bars) and Cu-CLI (shaded bars) membranes at different temperatures, feed pressure: 111.2 kPa and permeate pressure: 108.2 kPa.

## 5.6 Conclusions

Zeolite molecular sieve membranes for hydrogen separation can be achieved by high purity and inexpensive natural zeolites combined with copper with bonding ability and thermal stability. In this work, copper powders were added as binder and sealant to fill out the non-zeolite region in pressed clinoptilolite membrane. Gas permeance in copper-clinoptilolite membranes decreased due to reduction of the zeolite volume fraction and the reduction of non-selective flux through inter particle channels. The increase of  $H_2/CO_2$  and  $H_2/C_2H_6$  selectivities for the copper clinoptilolite composite membranes is attributed to the metallic copper and copper oxide effectively filling a portion of the inter-particle spaces and creating a complete adhesion with the zeolite particles. It is expected that the membrane permeance can be improved by reducing the membrane thickness through further optimization of the preparation method. The natural zeolite membrane has the additional advantage of high thermal and chemical stability, which provides the possibility of increasing the permeance at higher temperature.

## 5.7 References

- [1] J. Caro, M. Noack, P. Kolsch, and R. Schafer, "Zeolite membranes  $\pm$  state of their development and perspective," *Microporous Mesoporous Mater.*, vol. 38, pp. 3–24, 2000.
- [2] B. Zornoza, C. Casado, A. Navajas," Renewable hydrogen technologies: production, purification, storage, applications and safety"; Elsevier B.V: Amsterdam,Netherland, 2013.
- [3] R. Abedini and A. Nezhadmoghadam, "Application of membranes in gas separation processes: Its suitability and mechanism," *Pet. Coal*, vol. 52, no. 2, pp. 69–80, 2010.
- [4] R. W. Baker, "Membrane technology," in *Encyclopedia Of Polymer Science and Technology*, vol. 3, Menlo Park; California, pp. 184–249, 2001.
- [5] T. Tomita, K. Nakayama, H. Sakai, "Gas separation characteristics of DDR type zeolite membrane", *Microporous Mesoporous Mater.*, vol. 68, pp. 71-75, 2004.
- [6] C. Hon, P. Li, F. Li, T. Chung and D.R. Paul, "Reverse-selective polymeric membranes for gas separations", *Prog. Polym. Sci.* vol. 38, pp. 740–766, 2013.
- [7] R.T. Yang, "Adsorbents:Fundamentals and Applications",John Wiley and Sons, 2003.

- [8] E. Environ, A.W. Thornton, D. Dubbeldam, M.S. Liu, B.P. Ladewig and J. Hill, "Energy & Environmental Science Feasibility of zeolitic imidazolate framework membranes for clean energy", *R. Soc. Chem.*, vol. 5, pp. 7637–7646, 2012
- [9] N.W. Ockwig, T.M. Nenoff, "Membranes for hydrogen separation", *Chem. Rev.*, vol. 107, pp. 4078–110, 2007.
- [10] M.S. Li, Z.P. Zhao and M.X. Wang, "Controllable modification of polymer membranes by LDDLT plasma flow: membrane module scale-up and hydrophilic stability", *Chem. Eng. Sci.*, vol. 122, pp. 53–63, 2015.
- [11] X. Gu, Z. Tang and J. Dong, "On-stream modification of MFI zeolite membranes for enhancing hydrogen separation at high temperature", *Microporous Mesoporous Mater.*, vol. 111, pp. 441–448, 2008.
- [12] J. Caro and M. Noack, "Zeolite membranes – Recent developments and progress", *Microporous Mesoporous Mater.*, vol. 115, pp. 215–233, 2008.
- [13] Y.S. Lin and M.C. Duke, "Recent progress in polycrystalline zeolite membrane research", *Curr. Opin. Chem. Eng.*, vol. 2, pp. 209–216, 2013.
- [14] M.W. Ackley, R.F. Giese and R.T. Yang, "Clinoptilolite: Untapped potential for kinetic gas separations", *Zeolites*, vol. 12, pp. 780–788, 1992.
- [15] D.L. Bish and J.M. Boak, "Clinoptilolite-Heulandite Nomenclature", Los Alamos National Laboratory, Los Alamos, New Mexico, USA, 2001.

- [16] W. Ackley, Mark, S.U. Rege and H. Saxena, "Application of natural zeolites in the purification and separation of gases", *Microporous Mesoporous Mater.* vol. 61, pp. 25–42, 2003.
- [17] W. An, X. Zhou, X. Liu, P.W. Chai, T. Kuznicki and S.M. Kuznicki, "Natural zeolite clinoptilolite-phosphate composite Membranes for water desalination by pervaporation", *J. Memb. Sci.*, vol. 470, pp. 431–438, 2014.
- [18] D.W. Breck, "Zeolite Molecular Sieves: Structure, Chemistry, and Use," no. John Wiley & Sons, 1974.
- [19] M. Nasrollahzadeh, D. Habibi, Z. Shahkarami and Y. Bayat, "A general synthetic method for the formation of arylaminotetrazoles using natural natrolite zeolite as a new and reusable heterogeneous catalyst", *Tetrahedron.*, vol. 65, pp. 10715–10719, 2009.
- [20] S. Wang and Y. Peng, "Natural zeolites as effective adsorbents in water and wastewater treatment", *Chem. Eng. J.*, 156, pp. 11–24, 2010.
- [21] L.B. Mccusker and D.H. Olson, "Atlas of Zeolite Framework Types", Elsevier, 2007.
- [22] Y. S. Lin, I. Kumakiri, B. N. Nair, and H. Alsyouri, "Microporous Inorganic Membranes," in "*Separation and Purification Methods*", vol. 31, no. 2, pp. 229–379, 2002.

- [23] R. Szostak, "Handbook of Molecular Sieves", New York: Van Nostrand Reinhold, 1992.
- [24] <http://www.iza-structure.org>.
- [25] A.W. Thornton, T. Hilder, A.J. Hill and J.M. Hill, "Predicting gas diffusion regime within pores of different size, shape and composition", *J. Memb. Sci.*, vol. 336, pp. 101–108, 2009.
- [26] J. Dong, Y.S. Lin, M. Kanezashi and Z. Tang, "Microporous inorganic membranes for high temperature hydrogen purification", *J Applied Physcis*, vol. 104, pp. 1-17, 2013.
- [27] F. Gallucci, E. Fernandez, P. Corengia and M. van Sint Annaland, "Recent advances on membranes and membrane reactors for hydrogen production", *Chem. Eng. Sci.*, vol. 92, pp. 40–66, 2013.
- [28] N. Nishiyama, M. Yamaguchi, T. Katayama, Y. Hirota, M. Miyamoto and Y. Egashira, "Hydrogen-permeable membranes composed of zeolite nano-blocks", *J. Memb. Sci.*, vol. 306, pp. 349–354, 2007.
- [29] S. Battersby, T. Tasaki, S. Smart, B. Ladewig, S. Liu and M.C. Duke, "Performance of cobalt silica membranes in gas mixture separation", *J. Memb. Sci.*, vol. 329, pp. 91–98, 2009

- [30] W. An, P. Swenson, L. Wu, T. Waller, A. Ku and S.M. Kuznicki, "Selective separation of hydrogen from C1/C2 hydrocarbons and CO<sub>2</sub> through dense natural zeolite membranes", *J. Memb. Sci.*, vol. 369, pp. 414–419, 2011.
- [31] W. An, P. Swenson, A. Gupta, L. Wu, T.M. Kuznicki and S.M. Kuznicki, "Improvement of H<sub>2</sub>/CO<sub>2</sub> selectivity of the natural clinoptilolite membranes by cation exchange modification", *J. Memb. Sci.*, vol. 433, pp. 25–31, 2013.
- [32] T.F. Narbeshuber, H. Vinek and J.A. Lercher, "Monomolecular conversion of light alkanes over H-ZSM-5", *J. Catal.*, vol. 157, pp. 388-395, 1995.
- [33] A. Farjoo, F. Khorasheh, S. Niknaddaf and M. Soltani, "Kinetic modeling of side reactions in propane dehydrogenation over Pt - Sn/ $\gamma$  - Al<sub>2</sub>O<sub>3</sub> catalyst", *Sci. Iran.*, vol. 18, pp. 458-464, 2011
- [34] A.M. Avila, Z. Yu, S. Fazli, J.A. Sawada, S.M. Kuznicki, "Hydrogen-selective natural mordenite in a membrane reactor for ethane dehydrogenation", *Microporous Mesoporous Mater.*, vol. 190, pp. 301–308, 2014.
- [35] A.H. Shafie, W. An, S.A. Hosseinzadeh Hejazi, J. a. Sawada, S.M. Kuznicki, "Natural zeolite-based cement composite membranes for H<sub>2</sub>/CO<sub>2</sub> separation", *Sep. Purif. Technol.* 88 (2012) 24–28. doi:10.1016/j.seppur.2011.11.020.
- [36] R.D. Noble, "Perspectives on mixed matrix membranes", *J. Memb. Sci.*, vol. 378 pp. 393–397, 2011.

- [37] A.M. Abyzov, S. V. Kidalov and F.M. Shakhov, "High thermal conductivity composites consisting of diamond filler with tungsten coating and copper (silver) matrix", *J. Mater. Sci.*, vol. 46, pp. 1424–1438, 2011.
- [38] C. Joyce, L. Trahey, S.A. Bauer, F. Dogan and J.T. Vaughey, "Metallic copper binders for lithium-ion battery silicon electrodes", *J. Electrochem. Soc.* vol. 159, pp. 909–914, 2012.
- [39] D.K.R. Bevington and Philip R., "Data reduction and error analysis for the physical sciences", 3rd ed., Mc Graw-Hill Companies, 2003.
- [40] S.A.H. Hejazi, A.M. Avila, T.M. Kuznicki, A. Weizhu and S.M. Kuznicki, "Characterization of natural zeolite membranes for H<sub>2</sub>/CO<sub>2</sub> separations by single gas permeation", *Ind. Eng. Chem. Res.*, vol. 50, pp. 12717–12726, 2011.
- [41] J. A. Ritter and A.D. Ebner, "State of the Art Adsorption and Membrane Separation Processes for Hydrogen Production in the Chemical and Petrochemical Industries", *Sep. Sci. Technol.*, vol. 42, pp. 1123–1193, 2007.
- [42] A.M. Tarditi, E.A. Lombardo and A.M. Avila, "Xylene permeation transport through composite Ba-ZSM-5/SS tubular membranes : modeling the steady-state permeation", *Ind. Eng. Chem. Res.*, vol. 47, pp. 2377–2385, 2008.
- [43] R.M. Barrer, "Porous Crystal Membranes", *J. Chem. Soc.*, vol. 86, pp. 1123–1130, 1990.

- [44] S. W. Webb, "Gas Phase Diffusion in Porous Media: Comparison of Models", Sandia National Laboratories, New Mexico, 1998.
- [45] E. A. Mason and A. P. Malinauskas, "*Gas Transport in Porous Media: The Dusty-Gas Model*", Elsevier: Amsterdam, 1983.
- [46] H. Li and R. Dittmeyer, "Inorganic microporous membranes for H<sub>2</sub> and CO<sub>2</sub> separation-Review of experimental and modeling process", Chem. Eng. Sci., vol. 127, pp. 401-417, 2015.
- [47] S. Colin, "Rarefaction and compressibility effects on steady and transient gas flows in microchannels", Microfluid Nanofluid., vol. 1, pp. 268–279, 2005.
- [48] S. Thomas, R. Schäfer, J. Caro and A. Seidel-Morgenstern, "Investigation of mass transfer through inorganic membranes with several layers", Catal. Today, vol. 67, pp. 205–216, 2001.
- [49] V.A. Alekseevich, V.V. Kurbatkina, A.A. Zaitsev, D. Andreevna, Sidorenko and S.I. Rupasov, "Copper based binder for the fabrication of diamond tools", US0325049, 2012.
- [50] K.S. Rothenberger, A. V Cugini, B.H. Howard, R.P. Killmeyer, M. V Ciocco and B.D. Morreale, "High pressure hydrogen permeance of porous stainless steel coated with a thin palladium film via electroless plating", J. Memb. Sci. vol. 244, pp. 55–68, 2004.

- [51] B. Sea and K. Lee, "Molecular sieve silica membrane synthesized in mesoporous  $\gamma$ -alumina layer", *Bull. Korean Chem. Soc.*, vol. 22, pp. 1400–1402, 2001.
- [52] S. Yan, H. Maeda, K. Kusakabe and S. Morooka, "Thin palladium membrane formed in support pores by metal-organic chemical vapor deposition method and application to hydrogen separation", *Ind. Eng. Chem. Res.*, vol. 33, pp. 616–622, 1994.
- [53] A. Huang, Y. Chen, Q. Liu, N. Wang, J. Jiang and J. Caro, "Synthesis of highly hydrophobic and permselective metal organic framework Zn(BDC)(TED)<sub>0.5</sub> membranes for H<sub>2</sub>/CO<sub>2</sub> separation", *J. Memb. Sci.*, vol. 454, pp. 126–132, 2014.
- [54] R.M. De Vos and H. Verweij, "Improved performance of silica membranes for gas separation", *J. Memb. Sci.*, vol. 143, pp. 37–51, 1998.
- [55] H. Bux, F. Liang, Y. Li, J. Cravillon and M. Wiebcke, "Zeolitic imidazolate Framework molecular sieving membrane titania support", *J. Am. Chem. Soc.*, vol. 131, pp. 16000–16001, 2009.

## **Chapter Six**

---

# **Composite Coated Stainless Steel Tubular Membranes for Gas Separation**

This Chapter is accepted for publication in The "Canadian Journal of Chemical Engineering", February 2016

## 6.1 Summary

Inorganic mixed matrix zeolite membranes from clinoptilolite particles in an aluminosilicate binder were coated on tubular stainless steel supports. The phase composition, structure and homogeneity of the membrane slurry were characterized by X-ray powder diffraction, scanning electron microscopy and particle size distribution. Membrane performance was evaluated using H<sub>2</sub>, C<sub>2</sub>H<sub>6</sub> and CO<sub>2</sub> single gas permeations and showed potential in H<sub>2</sub> separation from CO<sub>2</sub> and C<sub>2</sub>H<sub>6</sub> at different temperatures and pressures. Up to two layers of coatings were coated on the inner surface of the porous stainless steel support and the separation performance was evaluated after applying each layer. Introduction of the second layer significantly improved the performance of the membrane system. The experiments on the double-layered membranes measured a hydrogen permeance of  $1.65 \times 10^{-7}$  mol. m<sup>-2</sup>.s<sup>-1</sup>.Pa<sup>-1</sup> at 300 °C, H<sub>2</sub>/CO<sub>2</sub> and H<sub>2</sub>/C<sub>2</sub>H<sub>6</sub> single gas selectivity were 10.2 and 8.45 respectively at 25 °C and feed pressure of 110 kPa.

**Keywords:** Clinoptilolite; mixed matrix membranes; hydrogen separation; stainless steel support

## 6.2 Introduction

Hydrogen is considered an industrially popular source of energy for clean power production and high in energy content as it burns leaving a clean by-product. Hydrogen is currently produced from fossil or biomass fuels by steam reforming of natural gas and utilizing water gas shift reactions that require further separation.

Hydrogen separation by selective transport through membranes is one of the widely utilized areas of gas separation because of its simple process. Comparing separations using membranes with other separation methods such as distillation or adsorption, membranes provide a single-pass process with low capital and operational expenditures, and typically ease of operation [1], [2]. Currently, there are four types of membrane materials used for hydrogen separation: Palladium (Pd), polymer (organic), inorganic silica and zeolites.

Dense metallic membranes made of Pd and its alloys are used for several applications to produce hydrogen but their cost is the major concern for the preparation [3–5]. Recent studies were focused on thin metallic membranes to reduce using of precious metals and to increase the hydrogen flux. Yet, they are not stable especially in acidic environments causing damage to membrane. Polymeric membranes also experience relatively low thermal stability for applications at higher temperature [6-9]. Microporous silica membranes should be produced as thin as possible (about thirty nanometers) to get high permeance. This introduces two challenges, one is the control of the thickness of the coating and minimization of the mesoporous and macroporous defects and pinholes [10].

Therefore, using zeolites, micro-porous poly-crystalline aluminosilicates, as membranes, due to their thermal, chemical and acidic stability [11-13] are sought for.

First studies to use zeolites in the form of a membrane were pure polycrystalline zeolite membranes without any supports. These zeolite membranes showed lower mechanical strength to experience higher pressures and most of the recent zeolite membranes reported are fabricated within porous substrates [14 –20].

Because of the long time and high pressure that natural zeolite deposits have experienced, inter-crystalline grain boundaries, the main shortcomings of synthetic zeolite membranes, have been linked or eliminated leaving materials with mechanical robustness unavailable in synthetic analogues [15, 21-24]. This structural solidness in natural zeolites also reduces technical and material challenges including requirements for support properties and several synthesis processes for synthetic zeolites [25-27].

Clinoptilolite is one of the most common natural zeolites and was reported in 1923 [26]. The formula of clinoptilolite is typically referred as  $(\text{Na}^+, \text{K}^+)_6[\text{Al}_6 \text{Si}_{30} \text{O}_{72}] \cdot 20 \text{H}_2\text{O}$  and its framework structure has three sets of intersecting channels of eight and ten member rings. The dimension of the largest channel of clinoptilolite framework is  $5.5 \times 4.0 \text{ \AA}$  [15] however, due to the positions of the framework cations the effective pore size is smaller than most hydrocarbons and comparable with the kinetic diameter of hydrogen. This feature defines natural clinoptilolite as a candidate for hydrogen separation, since hydrogen goes through the pores while the retentate gets rejected based on size.

Several natural zeolite membranes have been reported for separation of hydrogen from hydrocarbons mixtures or a mixture of  $\text{H}_2/\text{CO}_2$  [30],[31] or as membrane reactors to improve the production yield in dehydrogenation [32],[33]. We previously reported that

natural clinoptilolite membranes cut from mineral deposits for selective H<sub>2</sub> separation processes [30]. To scale up production of such membranes regardless of their shape, geometry or aspect ratios using a mixed matrix membrane (MMM) could be a solution. The use of two or more materials with unique selectivities and fluxes to produce membranes provides the possibility of preparation of one type of membrane technology identified as MMMs [34].

The dip coating (slip-casting) process is a technique to make ceramic mixed-matrix membrane (MMM) in which the ceramic slurry is introduced onto or into a porous substrate of the specific shape. When a dry porous substrate is dipped into the slurry and removed from the slurry's main mix, a dense, wet coating is formed on the substrate surface which is later on air dried and heat-treated [35- 37].

In this study, membranes out of natural zeolites are shown to effectively separate hydrogen from CO<sub>2</sub> and C<sub>2</sub>H<sub>6</sub>. The focus in this work is coating the tubular membranes; they were characterized using Scanning Electron Microscopy (SEM), X-Ray Diffraction (XRD), Energy-Dispersive X-ray (EDX) and Particle Size Distribution (PDS) analysis. The separation performance was evaluated by single gas permeation using hydrogen, carbon dioxide and ethane. To study the uniformity of the membrane, a comparative parameter associated with the relative average defect size of the MMM was defined. To the best of our knowledge this is the first report that a natural zeolite membrane integrated onto commercial porous stainless steel tubes for hydrogen separation applications.

## 6.3 Experimental

### 6.3.1 Materials

The membrane slurry was a mixture of clinoptilolite powder and a solution binder of aluminosilicate (ALS). ALS is a single component aluminum oxide based ceramic adhesive and has thermal resistance up to 1650 °C [38]. When ALS is heat treated and namely cured, the ALS attaches to ceramics and to low expansion metals. Zeolites with similar chemical properties compared to the aluminosilicate binder with a strong chemical bonding which makes it a suitable binder material for production of natural zeolite mixed matrix membranes [39],[40]. The binder was supplied by Accumet Materials (Ossining, NY, USA). The weight ratio of Si to Al in the binder solution based on the Inductively Coupled Plasma (ICP) analysis was calculated to the value of 1675.

Clinoptilolite powders were supplied by St. Cloud Mining Company (Winston, NM, USA) with particle size corresponding to mesh size of 325 ( $< 44 \mu\text{m}$ ). The molecular composition of St. Cloud's deposit is shown in Table 6-1. Based on the composition data the Si/Al molar ratio is 4.13. According to the Accumet's product sheet, clinoptilolite has the purity of at least 99%.

**Table 6-1.** Energy-dispersive X-ray (EDX) data for the natural zeolite samples.

	EDX Data (Atomic mole ratio)							
	Na	K	Ca	Mg	Fe	Al	Ti	Si
Clinoptilolite (Ash-Meadows)	0.553	0.361	0.047	0.063	0.0601	1	0.0036	4.125

The porosity and pore diameter of substrates control the membrane formation process.

Substrates with a more of smaller pores offer higher capillary suction and are preferred for the membrane formation [35], [41–43]. Tubular, porous 316 L stainless steel substrate was supplied by Graver Technologies (Glasgow, DE, USA) and has a pore size of 0.02  $\mu\text{m}$  which was used as the membrane support. Tubes were pre-coated with a porous  $\text{TiO}_2$  layer of about 10  $\mu\text{m}$  to improve the surface area contact between the metallic support metal and the zeolite layer. As-received porous stainless steel supporting tube is shown schematically in Figure 6-1.

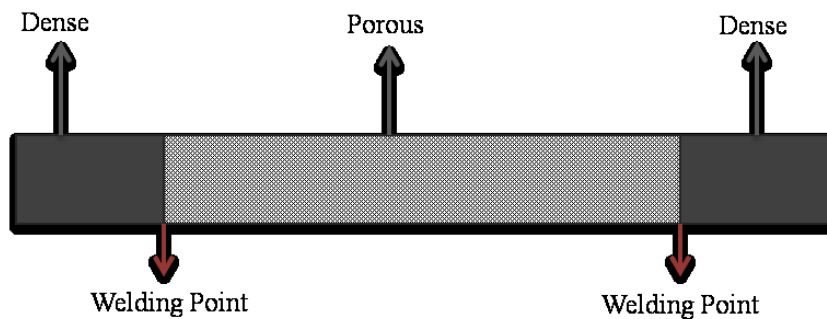


**Figure 6-1.** Schematic picture of stainless steel support for zeolite membranes.

### 6.3.2 Preparation and Characterization of Membranes

The stainless steel tubes were washed with an alkaline solution (Decon Labs, King of Prussia, PA, USA) and cleaned fully with distilled water in an ultrasonic bath for about an hour to remove any potential fabrication residues.

The surface of porous stainless steel tubes were dip coated by introducing the slurry into the tube using a syringe pump. During the dip-coating process, the dry porous substrate contacts the slurry and capillary suction by the porous substrate leads the ceramic particles to cover the substrate and slurry boundary and form a wet membrane [35, 37, 41–43]. The total driving force in membrane formation process ( $\Delta P$ ) is the combination of pressure over the membrane,  $\Delta P_m$ , ( $\text{N}\cdot\text{m}^{-2}$ ) used to drive the liquid pass through the

membrane and the pressure driving the liquid flow in the pores of the support identified as capillary suction ( $\Delta P_S$ ) ( $N.m^{-2}$ ).

$$\Delta P = \Delta P_m + \Delta P_S \quad (1)$$

To minimize the defects or pinholes associated with the substrate surface coarseness, multilayer coating method was applied. At the same time the layer thickness was kept as small as possible to maintain higher permeation.

The slurry was introduced from the bottom with a syringe pump into a porous stainless steel tube as shown schematically in Figure 6-2. The syringe was connected to the tube using a flexible rubber hose. When the tube was filled with coating slurry the pump was stopped immediately. The excess slurry was also let out when the syringe was removed from the bottom of the tube into a separate container.

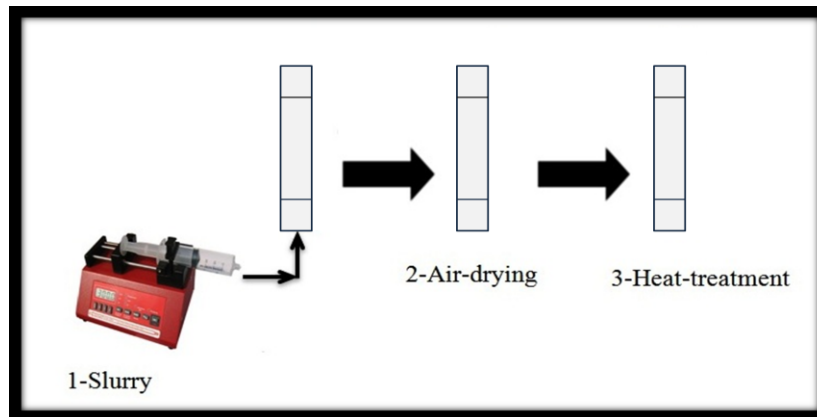


**Figure 6-2.** Dip coating procedure using a syringe pump for slurry injection

The coated tubes were initially air dried at ambient temperature and atmospheric pressure over the night and later on the binder was cured by heating the coated tube in a programmable muffle furnace at 371 °C for 4 hours. The membrane formation by dip coating process is summarized schematically in Figure 6-3.

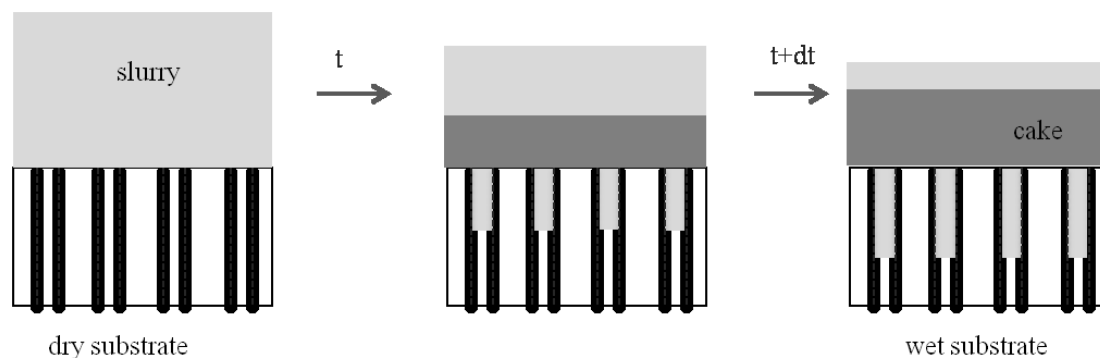


**Figure 6-3.** Membrane formation process on a porous substrate by the capillary suction pressure.

The second coating layer was applied using the similar procedure. The resulting single and double layered tubing membranes had a thickness of  $0.5 \times 10^{-4}$  m and  $0.8 \times 10^{-4}$  m respectively.

#### *PSD*

Solid volume fraction, mixing method and homogeneity of the zeolite slurry can affect the membrane coating process among other factors such as the coating method and substrate porosity.

In this study clinoptilolite powder, distilled water and aluminosilicate were mixed with two different mixing methods. In one mixing method, ALS and distilled water were completely mixed for duration of 30 minutes at the rate of 350 rpm using a magnetic stirrer and clinoptilolite powders were added after and stirred at 700 rpm for 2 hours.

In another mixing method, clinoptilolite powder, ALS and distilled water were mixed first separately using a planetary ball mill machine (Laval Lab, Laval, QC, Canada) at 300 rpm for 20 minutes. Effect of the mixing processes was evaluated by Particle Size Distribution (PSD) analysis. In both methods, the composition of clinoptilolite powder, ALS and distilled water in the slurry was 25 wt%, 50 wt% and 25 wt % respectively.

### *XRD*

The XRD patterns were collected to study the homogeneity and the phase composition of the membrane slurry using a Rigaku Geiger flex 2173 (Rigaku Corporation, Tokyo, Japan). The diffractor was equipped with a vertical goniometer equipped with a D/Tex detector and a Fe filter. To prepare the sample for XRD analysis, the slurry was introduced into a flat plastic container, after drying at room temperature overnight, a flat layer was formed, separated from the container and heat-treated using the same procedure as explained earlier in this chapter. Prior to the XRS analysis, the heat-treated sample was pulverized and ground to a powder using a mortar and pestle.

### *SEM*

SEM analysis (Hitachi S 3000N) was used to characterize the morphological coated regions of the zeolite slurry (clinoptilolite powder: 25 wt%, ALS: 50 wt%, and distilled water: 25 wt % in the slurry) that was prepared for the developed membranes.

## **6.4 Gas Separation Tests**

Single gas permeation of H<sub>2</sub>, C<sub>2</sub>H<sub>6</sub> and CO<sub>2</sub> gases supplied by Praxair Canada (99.9% concentration) was used for evaluating membrane performance at a feed pressure range of 110 to 160 kPa and temperature range of 25 °C to 300 °C. Gas permeation was measured in a stainless steel cross flow membrane testing system shown in Figure 6-4. Membranes were sealed in a stainless steel tubing chamber. Leak tight swagelok compression fittings were used between the tube and the chamber. The two regions (tubing and the chamber sides) were separated by the MMM coating. The feed and

retentate passed through the tube side while argon and permeate flowed through the chamber side. For permeation tests at higher temperatures, the membrane cell was placed into a programmable tube furnace with a multipoint temperature controller. The membrane was heated at 5 ° C/min between set points.

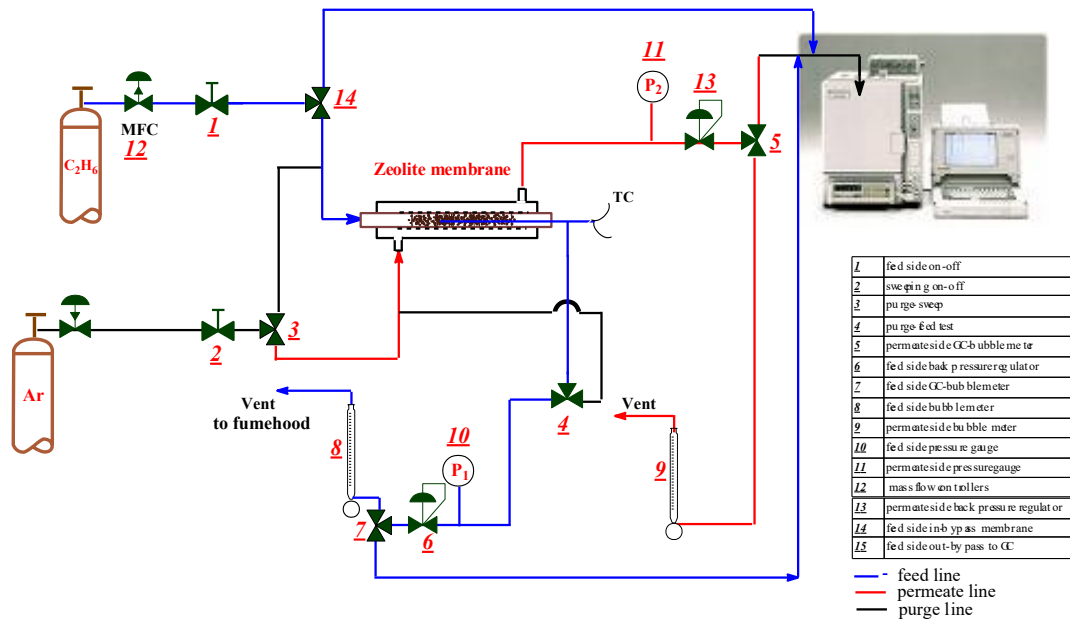


**Figure 6-4.** Schematic of the set-up for single gas permeation measurements.

Trans-membrane pressure was controlled by a back-pressure regulator located at the outlet of the feed side. The feed and sweeping gas flow rates were controlled by two mass flow controllers (Sierra Instrument Inc., CA, USA). For all gas permeation tests, feed and sweeping gas flow rates were constant at 100 mL/min (STP). The flow rate of the outlet streams was measured using a bubble flowmeter. An on-line Shimadzu Gas Chromatograph GC-14B (GC) equipped with a Thermal Conductivity Detector (TCD) and packed column (Haye Sep Q, 80–100 mesh) was used to analyze the outlet gas concentrations. To achieve the maximum thermal conductivity difference between carrier

gas and the analyte, helium was used as a carrier gas for CO<sub>2</sub>, C<sub>2</sub>H<sub>6</sub> while argon was used for H<sub>2</sub> analysis.

H<sub>2</sub>, CO<sub>2</sub> and C<sub>2</sub>H<sub>6</sub> permeances and H<sub>2</sub>/CO<sub>2</sub> and H<sub>2</sub>/C<sub>2</sub>H<sub>6</sub> selectivity were calculated based on the following definitions [44] , [45]:

$$\pi_i = \frac{N_i}{\Delta P_i} \quad (2)$$

where  $\pi_i$  is the permeance (mol.m<sup>-2</sup>. s<sup>-1</sup>. Pa<sup>-1</sup>),  $N_i$  is the molar flux (mol . s<sup>-1</sup>. m<sup>-2</sup>),  $\Delta P_i$  is the partial pressure difference (Pa) of component i across the membrane; and

$$S_{ij} = \frac{\pi_i}{\pi_j} \quad (3)$$

where,  $S_{ij}$  is the ideal selectivity of species i over j.

## 6.5 Relative Average Defect Size

Gas transport through a zeolite membrane is due to contributions from both zeolite and non zeolite fluxes [46], [47–50]. Potential transport passages through a zeolite membrane are illustrated in Figure 6-5.

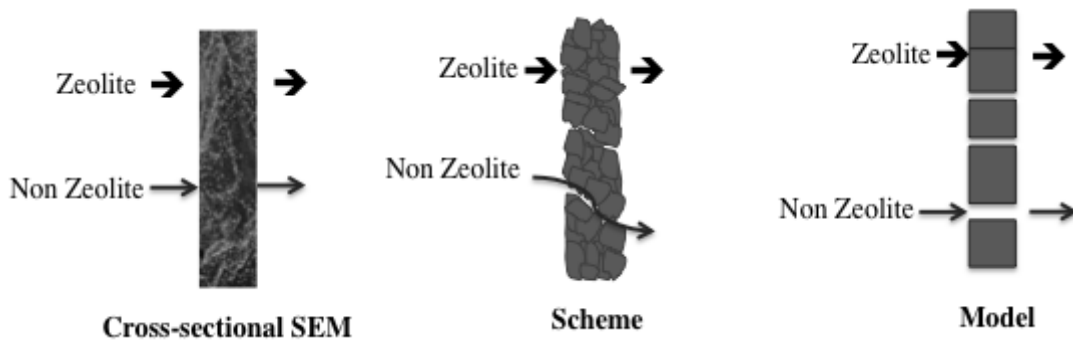


**Figure 6-5.** Gas transport passages through the membrane.

To measure how much non-zeolite contribution was reduced after applying the second layer, a comparative parameter associated with the relative average defect size was calculated. It was previously shown that natural zeolite membranes can be screened based

on the relative average defect size using a comparative coefficient obtained when H<sub>2</sub> permeability is plotted as a function of pressure [46]. The H<sub>2</sub> permeance across the membrane can be considered as a combination of two permeance fractions. One fraction, associated with Poiseuille or viscous flow depending on pressure. The other fraction is essentially not correlated with pressure variation and includes Knudsen and zeolitic flux contributions. The permeability calculated for H<sub>2</sub> is expressed as follows:

$$\text{Permeability} = \alpha_v [P^*] + \beta_{kz} \quad (4)$$

$$P^* = P_m \frac{\Delta P}{\Delta P_i} \quad (5)$$

The first term in the above equation is pressure dependent while the second term is invariable with pressure.  $P_m$  is the mean pressure between the feed and the permeate side. The coefficients  $\alpha_v$  and  $\beta_{kz}$  are the slope and intercept of a linear fitting of the permeability data as a function of  $P^*$ .  $\alpha_v$  is a coefficient associated with viscous flow (non-selective flux fraction) and  $\beta_{kz}$  is attributed to Knudsen and zeolite fluxes (selective flux fractions). As it was discussed in [46], the ratio  $\lambda = \alpha_v / \beta_{kz}$  is a comparative parameter which is associated with the average defect size of each membrane. The membrane having the smallest average non-zeolite pore size corresponds to the lowest value of the  $\lambda = \alpha_v / \beta_{kz}$  ratio. The values for the coefficient  $\lambda$  were estimated and compared after the first and the second layer of the coating was applied on the stainless steel support to evaluate the effectiveness of the each layer.

## 6.6 Results and Discussions

### *XRD*

Powder XRD patterns of the raw clinoptilolite powder and the mixture of clinoptilolite

and aluminosilicate binder are shown in Figure 6-6. The XRD pattern for membrane slurry is similar to the standard clinoptilolite confirming the crystalline framework structure in members slurry. The patterns also shows that the crystalline zeolite structure was not damaged or influenced drastically by mixing or the heat treatment process

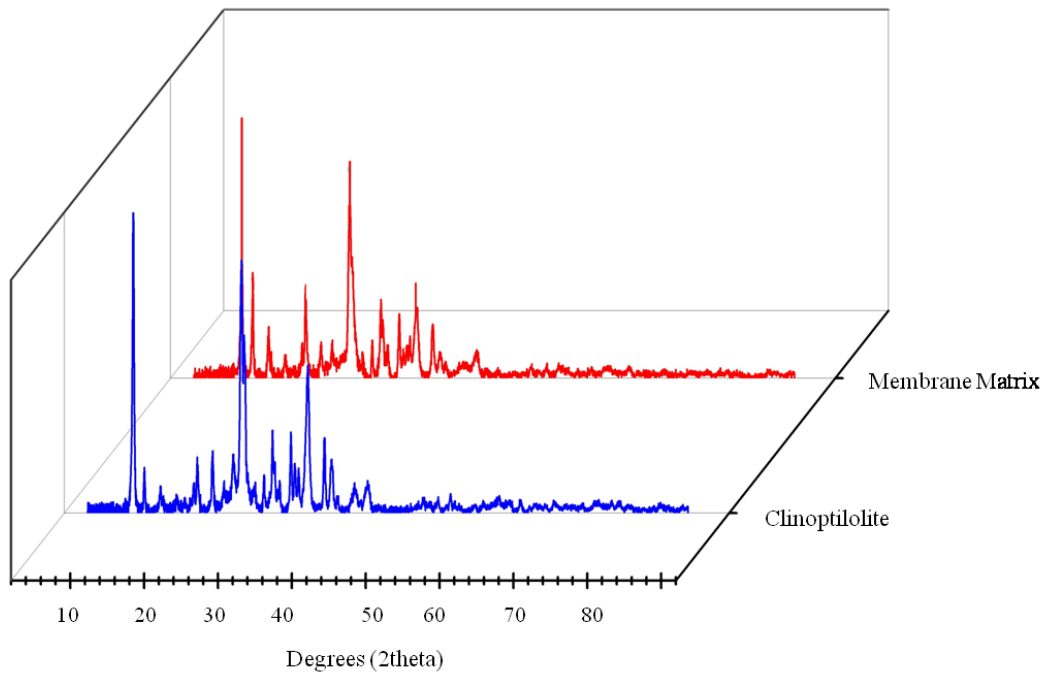


**Figure 6-6.** XRD patterns of the natural zeolite clinoptilolite powders and the natural zeolite clinoptilolite membrane slurry.

#### *Particle size distribution (PDS)*

The particle size distribution analysis for the as-received clinoptilolite powder and the membrane slurries prepared by two mixing methods (e.g. magnetic stirring versus ball mill mixing) are shown in Table 6-2. Sample 1 was homogenized using a magnetic stirrer while sample 2 was prepared using a ball mill. The analysis software assumed spherical shape for the particles with the diameter of D10, D50 and D90 that respectively refers to

10%, 50% and 90 % of the particle sizes. The D50 for the clinoptilolite was identified as 12.30  $\mu\text{m}$ , in sample 1 as 5.64 and in sample 2 as 5.16. While mixing the slurry by ball mill method resulted in a slightly more homogenized mixture, the two mixing methods did not show any significant differences in terms of particle size reduction or homogeneity.

**Table 6-2.** Particle size distribution analysis of the zeolite powder and coating slurry

<b>Sample</b>	<b>D10, (<math>\mu\text{m}</math>)</b>	<b>D50, (<math>\mu\text{m}</math>)</b>	<b>D90, (<math>\mu\text{m}</math>)</b>
Natural clinoptilolite zeolite	2.8	12.3	38.1
Sample 1(magnetic stirrer)	1.6	5.6	14
Sample 2 (ball mill)	1.6	5.2	12.6

### *SEM*

Figure 6-7 shows the SEM images of air dried and heat-treated coating slurry. SEM image showed a consistent mixture at the solid ratio that was selected for the membrane slurry. Characterization of membrane using optical microscopy and SEM after heat-treatment was employed to find the appropriate ratios of zeolite and binder in the mixed matrix slurry. Figure 6-8 shows the cross-section of a porous tubular membrane coated, air dried and heat treated with natural clinoptilolite zeolite slurry. The inside of the as-received porous stainless steel tube was already pre-coated by the manufacturer with a layer of  $\text{TiO}_2$  to adjust the substrate porosity.

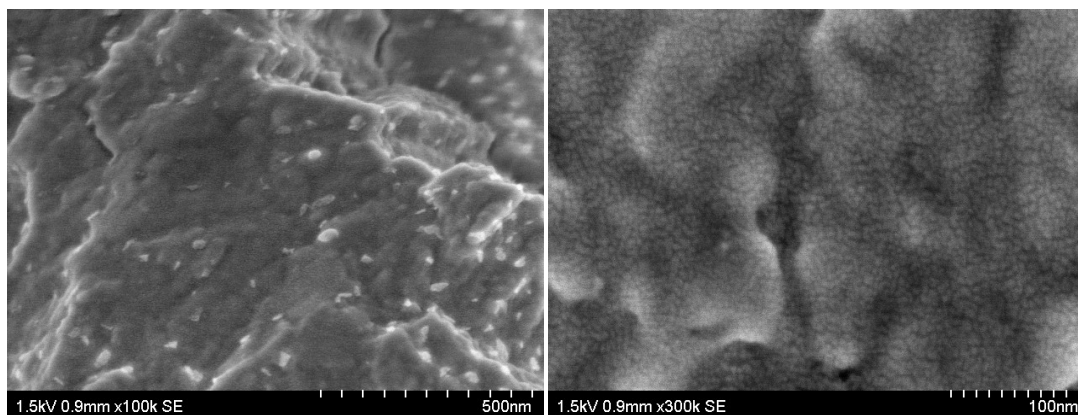


**Figure 6-7.** Surface structure of the air-dried and heat-treated zeolite slurry by SEM

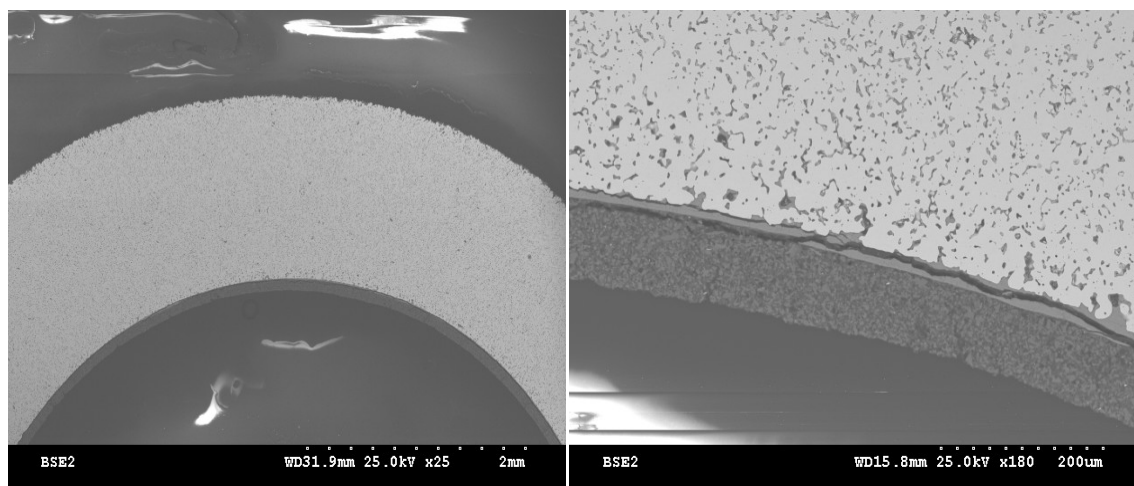


**Figure 6-8.** Cross-section of a stainless steel tube, coated with TiO<sub>2</sub> layer and natural clinoptilolite slurry

### *Single gas permeations*

#### **6.6.1 Single Layered Membranes**

Single-gas permeation was measured after applying the first layer of the membrane. Since normally water vapour molecules take up zeolite pores, prior to the gas permeation experiments, membranes were activated *in-situ* to ensure zeolite flow.

### Effect of Pressure

The coated tubular membranes were tested at different feed pressures using H<sub>2</sub>, CO<sub>2</sub> and C<sub>2</sub>H<sub>6</sub> permeation. The permeance as a function of feed pressure is shown in Figure 6-9.

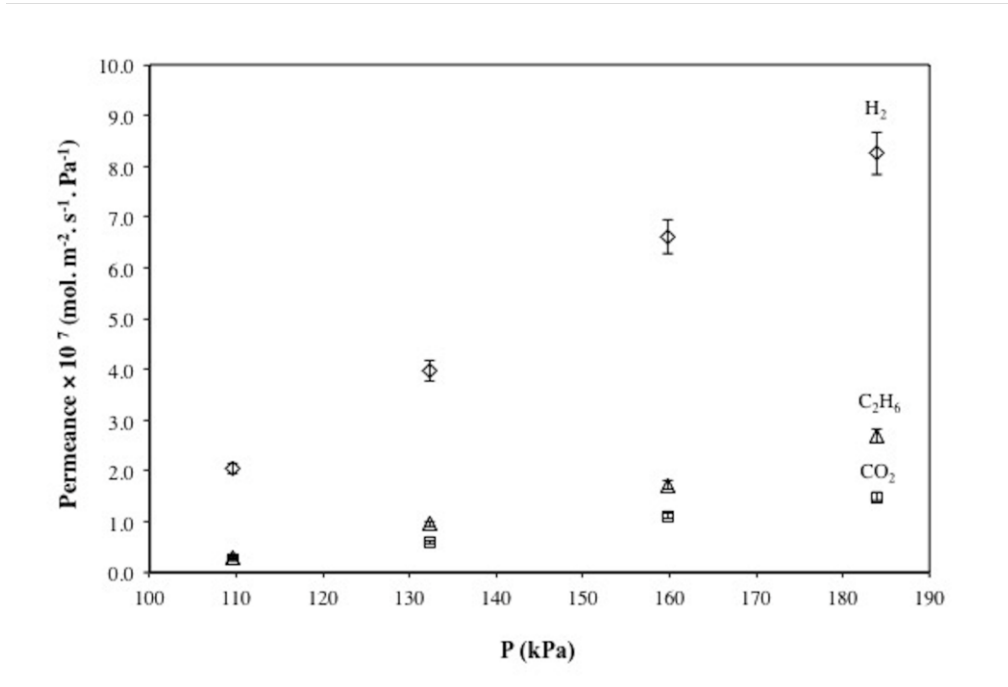


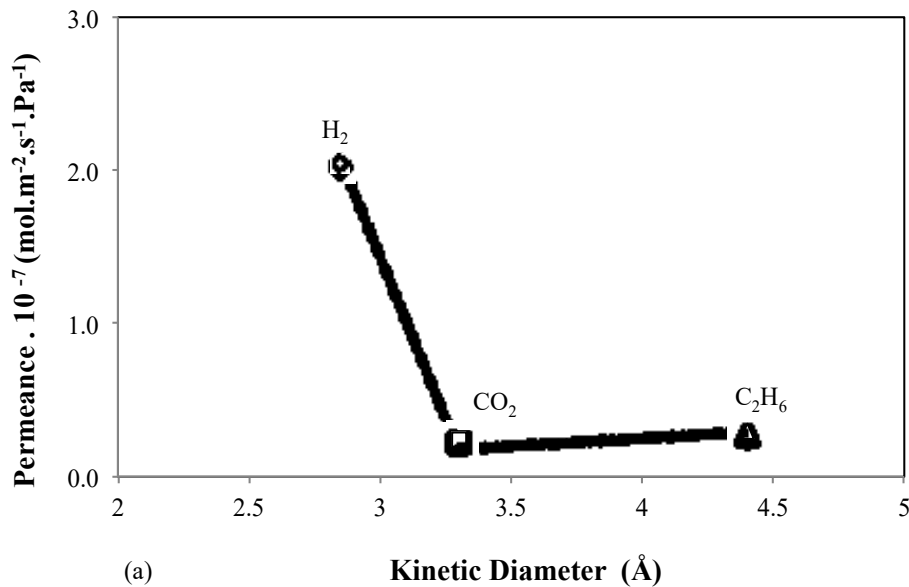
**Figure 6-9.** Permeance of individual gases through the single-layered membrane at different feed pressures, permeate pressure: 108 kPa, temperature = 25 °C.

H<sub>2</sub>, CO<sub>2</sub> and C<sub>2</sub>H<sub>6</sub> permeance through the membranes increased as feed pressure rose. This is due to the higher viscous flux contribution through the relatively large non-zeolite pores. The permeance associated with the Knudsen flux, as a zone between selective and non selective flux fractions, remains constant as pressure increases while the permeance related to the zeolitic flux is either constant or decreases slightly with pressure [51-52, 46]. The trends in Figure 6-9 confirms that the zeolite flux contribution was not the dominant transport mechanism for the single-layer membrane [46].

H<sub>2</sub>/CO<sub>2</sub> and H<sub>2</sub>/C<sub>2</sub>H<sub>6</sub> separation selectivity of membranes was 8.9 and 6.9 respectively. Both H<sub>2</sub>/CO<sub>2</sub> and H<sub>2</sub>/C<sub>2</sub>H<sub>6</sub> selectivities were higher than the corresponding Knudsen

selectivity (  $S_{\text{H}_2, \text{CO}_2}^{\text{K}} = \left(\frac{M_{\text{wCO}_2}}{M_{\text{wH}_2}}\right)^{1/2} = 4.6$  ,  $S_{\text{H}_2, \text{C}_2\text{H}_6}^{\text{K}} = \left(\frac{M_{\text{wC}_2\text{H}_6}}{M_{\text{wH}_2}}\right)^{1/2} = 3.9$  ) suggesting dominant microporous behaviour, while the micropores can be either zeolite or nonzeolite pores such as pinholes or cracks [45-46, 53].

To estimate membrane pore size, permeance is plotted as a function of kinetic diameter and molecular weight. Single gas permeances of H<sub>2</sub>, CO<sub>2</sub> and C<sub>2</sub>H<sub>6</sub> decreased with increasing kinetic diameter. Figure 6-10a shows that CO<sub>2</sub> permeance does not correlate with H<sub>2</sub> and C<sub>2</sub>H<sub>6</sub> in terms of molecular sizes as expected from the micro-porous diffusion mechanism, suggesting that transport mechanisms other than molecular sieving (Knudsen or zeolitic) were also contributing to the flux permeation [46,53-55]. Similarly, gas permeation across single layered membrane cannot be described by a pure Knudsen transport mechanism either (Fig. 6-10b). Since permeance is not linearly proportional to  $1/(M_i)^{0.5}$  as in Knudsen flux mechanism.



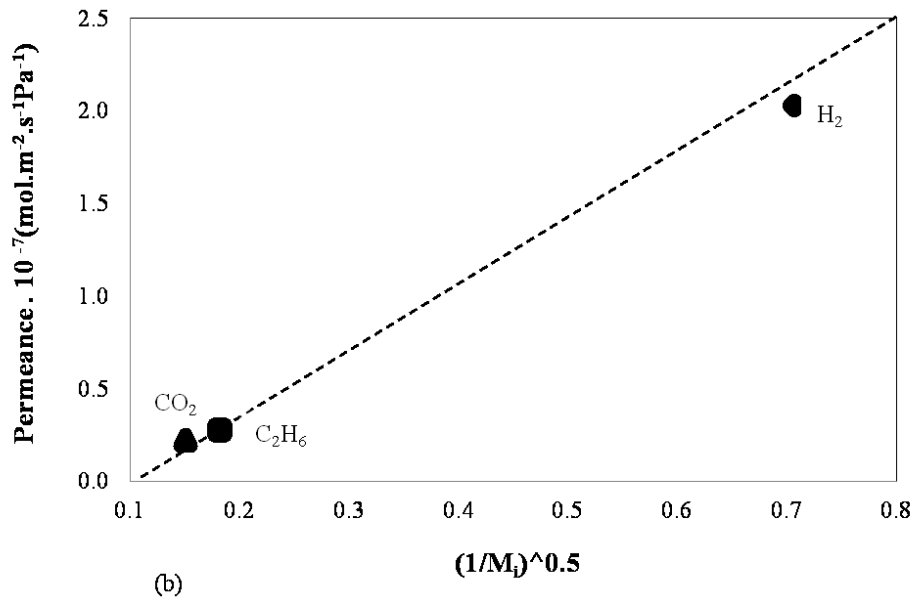


**Figure 6-10.** Permeance of H<sub>2</sub>, CO<sub>2</sub> and C<sub>2</sub>H<sub>6</sub> through single layered tubing membrane as a function of (a) kinetic diameter and (b) molecular weight. Temperature: 25 °C, feed pressure: 111.2 kPa, permeate pressure 108.2 kPa.

### 6.6.2 Double Layered Membranes

The gas permeation through the single layered membranes depends on the contribution of different transport mechanisms associated with both zeolite and non-zeolite pores. While presence of non-zeolite pores decreased hydrogen separation efficiency, subsequent coating layers were applied to reduce the number of nonselective regions in the film, using the same procedure as the first layer.

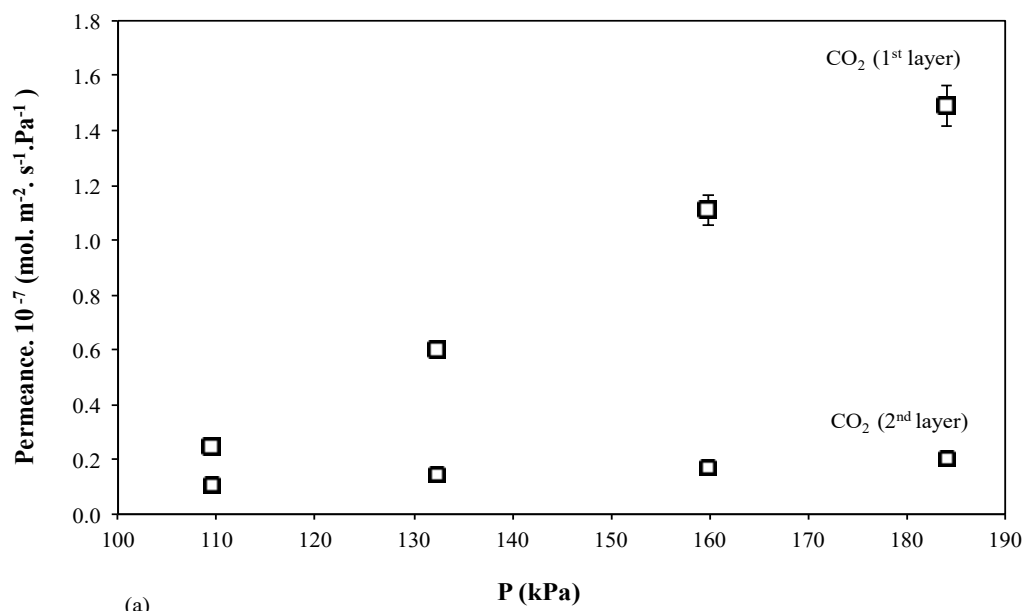
#### *Effect of Pressure*

Figure 6-11 shows the single gas permeation results on the tubular membrane after applying the second layer. Compared to single gas permeation at different pressures, by

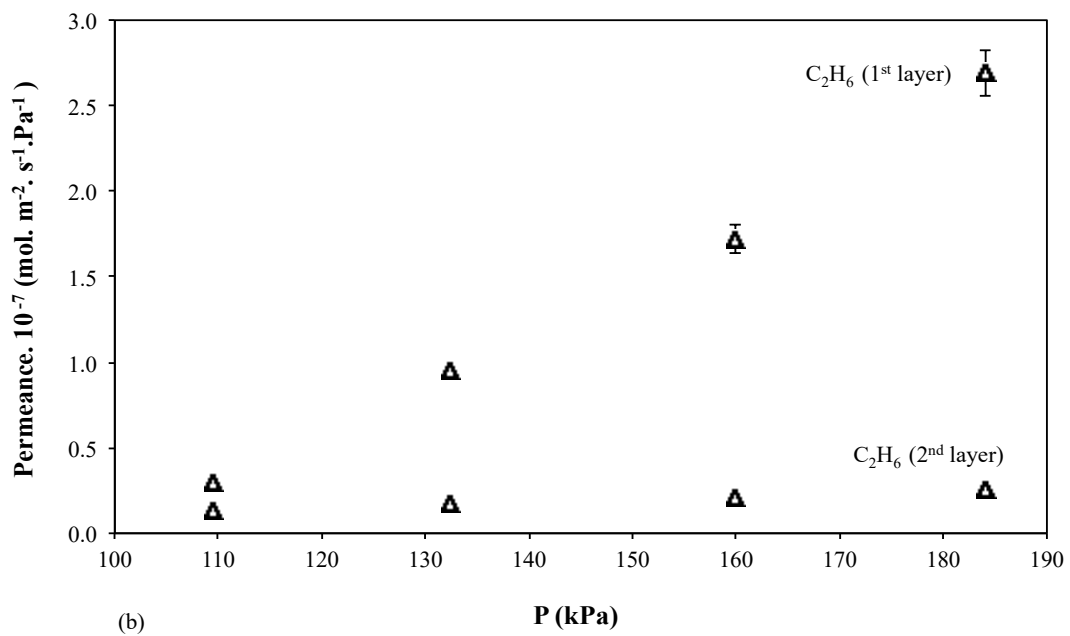
increasing the pressure, the average permeation rates of CO<sub>2</sub> and C<sub>2</sub>H<sub>6</sub> decreased noticeably.

While CO<sub>2</sub> and C<sub>2</sub>H<sub>6</sub> permeance in single-layered membrane increased by factors of 5 and 9 respectively over the feed pressure range of  $\Delta P = 110$  to 185 kPa, in double layered membrane the permeance of CO<sub>2</sub> and C<sub>2</sub>H<sub>6</sub> enhanced by the factor of 2. Since clinoptilolite pores are only comparable with kinetic diameter of hydrogen, the decrease in CO<sub>2</sub> and C<sub>2</sub>H<sub>6</sub> permeation values shows the decrease in non-selective, non-zeolitic pores after application of second layer.

Hydrogen permeance reduction in Figure 6-11c also shows hydrogen transport through non-zeolite pores in the first layer since in the second layer permeance was not affected by pressure as the first layer. However, an additional contribution to hydrogen flux reduction is also associated with the reduction of zeolite content after applying the second layer. The slight increase in permeation with pressure shows the existence of nonzeolite pores in membrane. However larger contribution of flux can be connected to the zeolite flux.



(a)



(b)

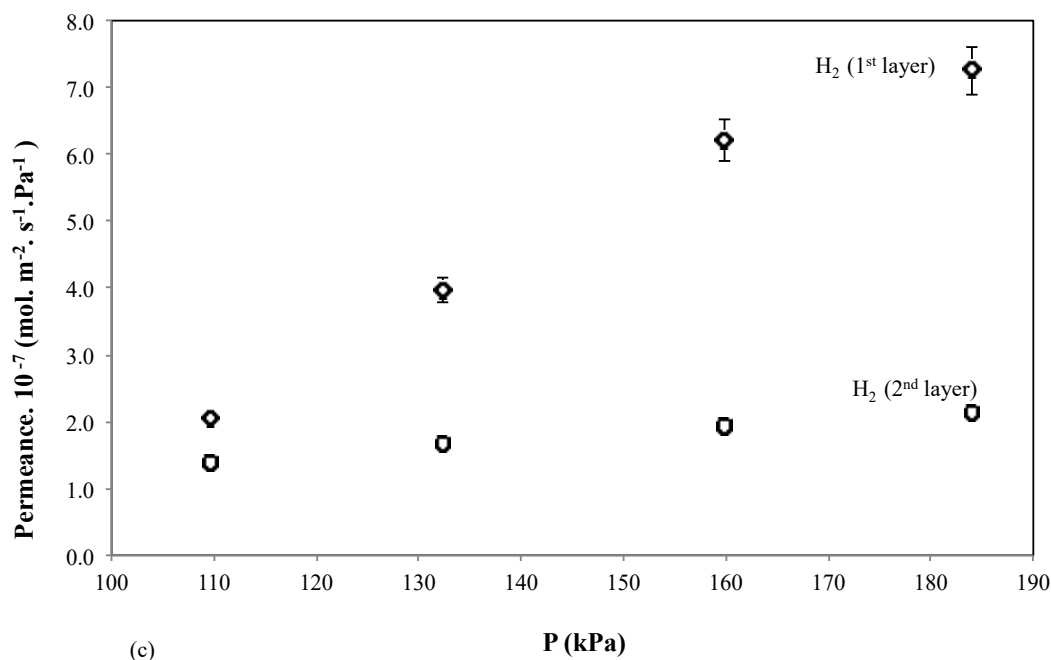


**Figure 6-11.** CO<sub>2</sub> (a), C<sub>2</sub>H<sub>6</sub> (b), H<sub>2</sub> (c) permeance through single and double layered membranes at different feed pressures, permeate pressure: 108.2 kPa, temperature: 25 °C.

Figure 6-12 shows the permeability of membrane after applying each layer as a function of  $P^*$  as defined in Eq. 4. Singled-layered membrane showed higher permeability, as the intersection at y-axis is larger. The corresponding values of  $\lambda = \alpha_v / \beta_{kz}$  for each membrane are listed in Table 6-3. Single layered membrane showed a higher value for  $\lambda$  ratio than the double layered membrane, this is appears to mean that the average defect size is slightly larger for the single layered membrane than for the double layered one. A larger average defect size represents higher non-zeolite fluxes for CO<sub>2</sub> and C<sub>2</sub>H<sub>6</sub> as feed pressure increased. The extent of the “non-selective” viscous flux passing through the relatively larger non-zeolite pores increased as the total pressure difference rises. This is consistent with a larger defect size for single layered tube as compared to double layered one:

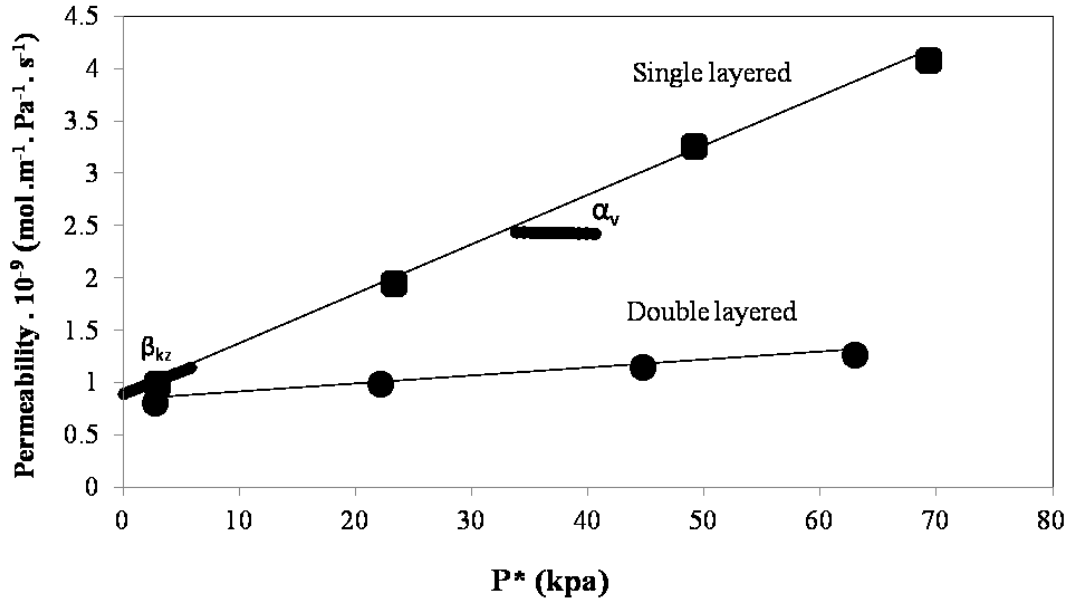


**Figure 6-12.** Comparative parameters ( $\alpha_v/\beta_{kz}$ ) for single and double layered membranes, permeate pressure: 108.2 kPa, temperature: 25 °C.

**Table 6-3.** Comparative parameter ( $\lambda = \alpha_v/\beta_{kz}$ ) for single layered and double layered tubing membranes.

Membrane/Parameter	$\lambda \times 10^2 \text{ (kPa}^{-1}\text{)}$
Single layered	5.2
Double layered	0.9

### *Effect of Temperature*

To study membrane performance and separation mechanism at higher temperatures, gas permeation was conducted in the range of 25 °C to 300 °C. Figure 6-13 shows H<sub>2</sub>, CO<sub>2</sub> and C<sub>2</sub>H<sub>6</sub> permeance after applying the second layer. Hydrogen permeance increased 53% as temperature increased from 25 °C to 300 °C while permeance of C<sub>2</sub>H<sub>6</sub> and CO<sub>2</sub>

was almost constant.

Since the crystalline pores in clinoptilolite is in the order of the kinetic diameter of hydrogen [56] and zeolitic permeance increases as temperature rises [57] higher fraction of H<sub>2</sub> flux passing through the zeolite crystals associated with the larger contribution of zeolite flux to the total flux across the membrane [51], [58].

The permeance associated with viscous flux decreases with increasing temperatures which is similar to the Knudsen permeance mechanism [46, 59-60]. At more elevated temperatures, with a weak adsorption affinity, molecules are expected to permeate according to the activated gaseous diffusion regime [51, 58, 61]. The combined effects of zeolitic diffusion flux as an activated process and non-zeolitic flux resulted in a constant progression of the single CO<sub>2</sub> and C<sub>2</sub>H<sub>6</sub> overall permeation flux through the membranes.

This membrane behaviour can be valuable for potential applications in hydrogen separation industry where the process temperatures can reach to 300 °C or higher.

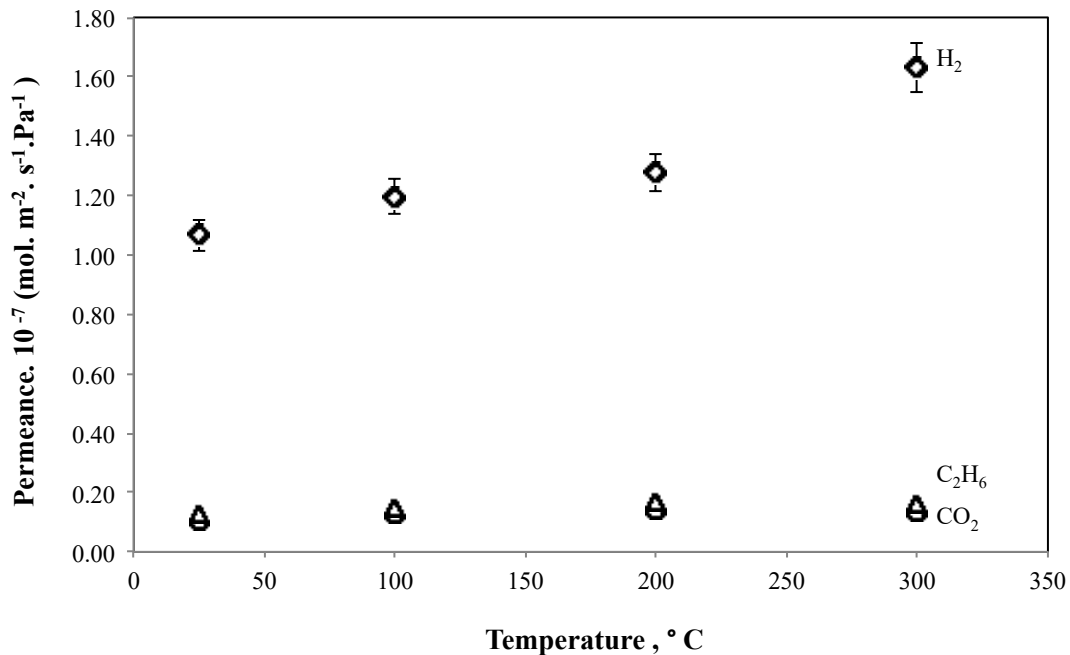


**Figure 6-13.** Permeance of individual gases through double-layered membrane at different temperatures, feed pressure: 111.2 kPa, permeate pressure 108.2 kPa.

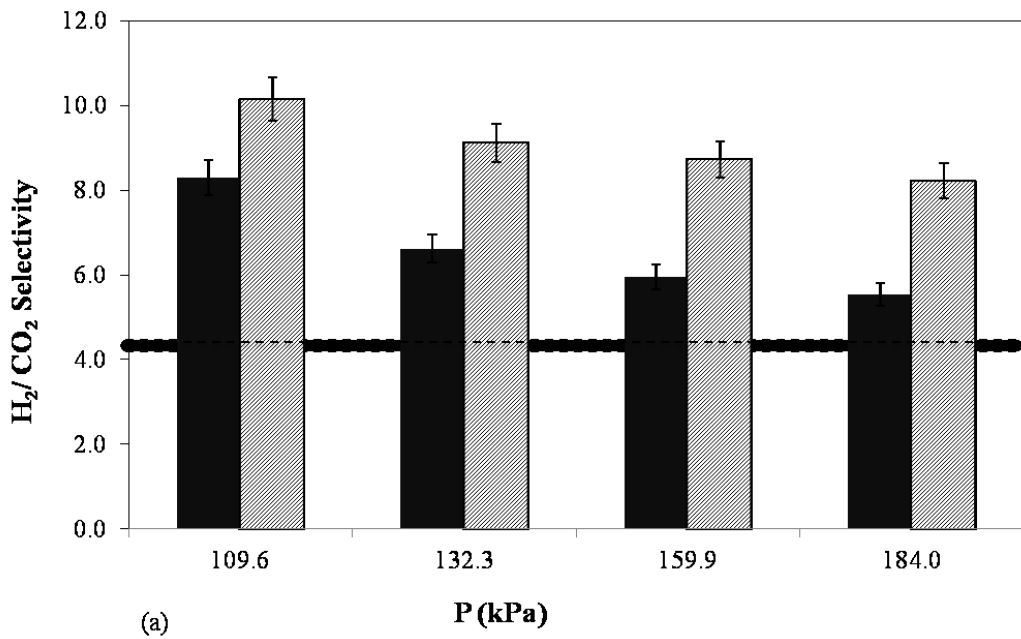
### 6.7 H<sub>2</sub> Selectivity Enhancement

The ideal selectivity of H<sub>2</sub>/C<sub>2</sub>H<sub>6</sub> and H<sub>2</sub>/CO<sub>2</sub> on single and double-layered zeolite membranes is shown in Figure 6-14. Hydrogen selectivity decreased as the feed pressure increased, while the fraction of the non-selective viscous flux passing through the relatively larger nonzeolite pores increased as the total pressure difference rose. For both of the layers, H<sub>2</sub>/CO<sub>2</sub> and H<sub>2</sub>/C<sub>2</sub>H<sub>6</sub> selectivities were higher than the corresponding Knudsen selectivity ( $S_{\text{H}_2/\text{CO}_2}^{\text{Kn}} = 4.7$ ,  $S_{\text{H}_2/\text{C}_2\text{H}_6}^{\text{Kn}} = 3.8$ ). By applying the second layer, separation selectivity for H<sub>2</sub>/C<sub>2</sub>H<sub>6</sub> increased from 6.9 to 8.4 and for H<sub>2</sub>/CO<sub>2</sub> it also increased from 8.3 to 10.2 at room temperature at feed pressure of 110 kPa.

A comparison of relative average defect sizes (coefficient  $\lambda$  in Table 6-3) is consistent with the experimental values of the ideal selectivities as the pressure increased at room

temperature. The average defect size is larger for single layered membrane and as a result the selectivity decreased at a faster rate than double-layered membrane with pressure increase.

Comparing the two membranes, for the double-layered membrane, the separation efficiency increased which suggests the non-selective regions causing viscous flow were reduced. However, non-zeolite regions still exist in the double-layered membranes that are confirmed by the increasing trend in permeance over the pressure range of 110 to 185 kPa and decrease in the selectivity.



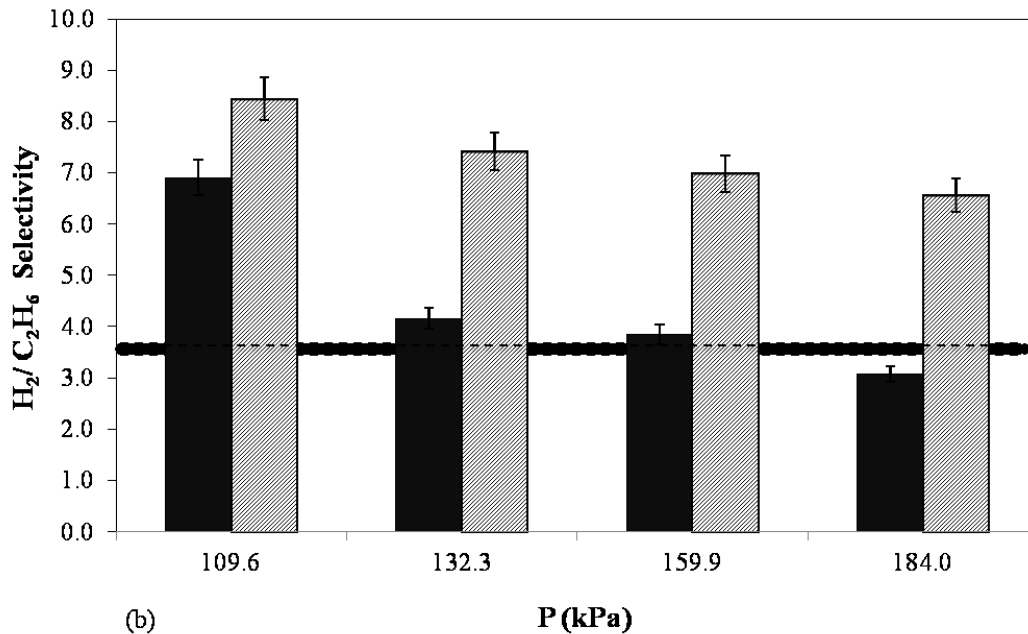


**Figure 6-14.** H<sub>2</sub>/CO<sub>2</sub> (a) H<sub>2</sub>/C<sub>2</sub>H<sub>6</sub> (b) separation selectivity through single layered (solid bars) and double layered (shaded bars) membranes at different pressures, temperature: 25 °C, kPa, permeate pressure: 108.2 kPa, (Dashed line: Knudsen selectivity) .

## 6.8 Conclusion

A natural clinoptilolite composite membrane was developed on a stainless steel tubular support. The clinoptilolite mixed matrix membrane showed potential in H<sub>2</sub> separation from CO<sub>2</sub> and C<sub>2</sub>H<sub>6</sub>. To improve membrane separation performance, second layer of membrane was applied. The improve in selectivity from 8.3 to 10.2 and 6.9 to 8.3 for H<sub>2</sub>/CO<sub>2</sub> and H<sub>2</sub>/C<sub>2</sub>H<sub>6</sub> respectively suggests that the number and size of nonselective, nonzeolite pores reduced after applying the second layer which was also confirmed by the comparative parameter. Total H<sub>2</sub> permeance increased 53% with the increase of temperature due to the larger contribution of the selective compared to the non-selective flux fraction. Further improvement on the membrane quality and performance could be

expected by optimizing the coating composition and thermal treatment conditions. This study shows that natural zeolite coated stainless steel tubular membranes have great potential for large-scale hydrogen purification at high temperature requirements.

## 6.9 References

- [1] Y. Yampolskii, "Polymeric gas separation membranes," *Macromol. (ASC Publ.)*, vol. 45, no. 8, pp. 3298–3311, 2012.
- [2] R. W. Baker, "Membrane technology," in *Encyclopedia Of Polymer Science and Technology*, vol. 3, Menlo Park; California, 2001, pp. 184–249.
- [3] S. Yan, H. Maeda, K. Kusakabe, and S. Morooka, "Thin palladium membrane formed in support pores by metal-organic chemical vapor deposition method and application to hydrogen separation," *Ind. Eng. Chem. Res.*, vol. 33, pp. 616–622, 1994.
- [4] K. S. Rothenberger, A. V Cugini, B. H. Howard, R. P. Killmeyer, M. V Ciocco, B. D. Morreale, R. M. Enick, F. Bustamante, I. P. Mardilovich, and Y. H. Ma, "High pressure hydrogen permeance of porous stainless steel coated with a thin palladium film via electroless plating," *J. Memb. Sci.*, vol. 244, pp. 55–68, 2004.
- [5] Y. Huang and R. Dittmeyer, "Preparation and characterization of composite palladium membranes on sinter-metal supports with a ceramic barrier against intermetallic diffusion," vol. 282, pp. 296–310, 2006.
- [6] D. Q. Vu, W. J. Koros, and S. J. Miller, "Mixed matrix membranes using carbon molecular sieves II. Modeling permeation behavior," *J. Memb. Sci.*, vol. 211, pp. 335–348, 2003.

- [7] S. Rafiq, Z. Man, S. Maitra, N. Muhammad, and F. Ahmad, "Kinetics of Thermal Degradation of Polysulfone/Polyimide Blended Polymeric Membranes," *J. Appl. Polym. Sci.*, 2012.
- [8] B. Zornoza, B. Seoane, J. M. Zamaro, C. Tøllez, and J. Coronas, "Combination of MOFs and Zeolites for Mixed-Matrix Membranes," *ChemphysChem*, vol. 12, pp. 2781–2785, 2011.
- [9] C. Casado-coterillo, J. Soto, M. T. Jimare, S. Valencia, A. Corma, C. Tellez, and J. Coronas, "Preparation and characterization of ITQ-29/polysulfone mixed-matrix membranes for gas separation: Effect of zeolite composition and crystal size," *Chem. Eng. Sci.*, vol. 73, pp. 116–122, 2012.
- [10] L. Cot, J. Durand, C. Guizard, N. Hovnanian, and A. Julbe, "Inorganic membranes and solid state sciences," vol. 2, pp. 313–334, 2000.
- [11] S. Battersby, T. Tasaki, S. Smart, B. Ladewig, S. Liu, M. C. Duke, V. Rudolph, and J. C. Diniz, "Performance of cobalt silica membranes in gas mixture separation," *J. Memb. Sci.*, vol. 329, pp. 91–98, 2009.
- [12] J. B. Miller, B. D. Morreale, M. W. Smith, and W. Virginia, "Pd-Alloy membranes for hydrogen separation," in *The chemistry and physics of separation by dense metal membranes*, Elsevier B.V., 2014, pp. 135–161.
- [13] N. Nishiyama, M. Yamaguchi, T. Katayama, Y. Hirota, M. Miyamoto, Y. Egashira, K. Ueyama, K. Nakanishi, T. Ohta, A. Mizusawa, and T. Satoh,

- “Hydrogen-permeable membranes composed of zeolite nano-blocks,” *J. Memb. Sci.*, vol. 306, pp. 349–354, 2007.
- [14] W. Ackley, Mark, S. U. Rege, and H. Saxena, “Application of natural zeolites in the purification and separation of gases,” *Microporous Mesoporous Mater.*, vol. 61, pp. 25–42, Jul. 2003.
- [15] D.W. Breck, “Zeolite Molecular Sieves: Structure, Chemistry, and Use,” no. John Wiley & Sons, Ltd, 1974.
- [16] R. Szostak, *Handbook of Molecular Sieves*. New York: Van Nostrand Reinhold, 1992.
- [17] R. M. Barrer, “Porous Crystal Membranes,” *J. Chem. Soc.*, vol. 86, no. 7, pp. 1123–1130, 1990.
- [18] E. E. Mcleary, J. C. Jansen, and F. Kapteijn, “Zeolite based films , membranes and membrane reactors: Progress and prospects,” *Microporous Mesoporous Mater.*, vol. 90, pp. 198–220, 2006.
- [19] K. Kusakabe, S. Yoneshige, A. Murata, and S. Morooka, “Morphology and gas permeance of ZSM-5-type zeolite membrane formed on a porous  $\alpha$ -alumina support tube,” *J. Memb. Sci.*, vol. 116, pp. 39–46, 1996.
- [20] J. Dong, Y. S. Lin, M. Z. Hu, R. A. Peascoe, and E. A. Payzant, “Template-removal-associated microstructural development of porous-ceramic-supported

- MFI zeolite membranes,” *Microporous mesoporous Mater.*, vol. 34, pp. 241–253, 2000.
- [21] G.V.Tsitsishvili, N.S.Skhirtladze, T.G.Andronikashvili, V.G.Tsitsishvili, and A.V.Dolidze, “Natural zeolites of Georgia: occurrences, properties, and application,” in *Porous Materials in Environmentally Friendly Processes*, vol. 125, Elsevier Science B.V., 1999, pp. 715–722.
- [22] A. S. Zarchy, Amawalk, R. Correia, Elmsford, C. C. Chao, and Millwood, “Process for the adsorption of hydrogen sulfide with clinoptilolite molecular sieves,” 1992.
- [23] M. Nasrollahzadeh, D. Habibi, Z. Shahkarami, and Y. Bayat, “A general synthetic method for the formation of arylaminotetrazoles using natural natrolite zeolite as a new and reusable heterogeneous catalyst,” *Tetrahedron*, vol. 65, no. 51, pp. 10715–10719, 2009.
- [24] S. Wang and Y. Peng, “Natural zeolites as effective adsorbents in water and wastewater treatment,” *Chem. Eng. J.*, vol. 156, no. 1, pp. 11–24, 2010.
- [25] M. P. Pina, M. Arruebo, M. Felipe, F. Fleta, M. P. Bernal, and J. Santamar, “A semi-continuous method for the synthesis of NaA zeolite membranes on tubular supports,” *J. Memb. Sci.*, vol. 244, pp. 141–150, 2004.

- [26] G. Yang, X. Zhang, S. Liu, K. Lun, and J. Wang, "A novel method for the assembly of nano-zeolite crystals on porous stainless steel microchannel and then zeolite film growth," *J. Phys. Chem. Solids*, vol. 68, pp. 26–31, 2007.
- [27] J. Caro, M. Noack, P. Kolsch, and R. Schafer, "Zeolite membranes  $\pm$  state of their development and perspective," *Microporous Mesoporous Mater.*, vol. 38, pp. 3–24, 2000.
- [28] W. T. Schaller and U. S. Geological, "the Mordenite-Ptilolite Group; Clinoptilolite, a New Species," *Mineral. Soc. Am.*, vol. 8, pp. 128–134, 1923.
- [29] F. A. and Mumpton, "The american mineralogist, vol. 45, march\_april, 1960," *Am. Mineral.*, vol. 45, pp. 351–369, 1960.
- [30] W. An, P. Swenson, L. Wu, T. Waller, A. Ku, and S. M. Kuznicki, "Selective separation of hydrogen from C1/C2 hydrocarbons and CO<sub>2</sub> through dense natural zeolite membranes," *J. Memb. Sci.*, vol. 369, no. 1–2, pp. 414–419, Mar. 2011.
- [31] A. H. Shafie, W. An, S. A. Hosseinzadeh Hejazi, J. a. Sawada, and S. M. Kuznicki, "Natural zeolite-based cement composite membranes for H<sub>2</sub>/CO<sub>2</sub> separation," *Sep. Purif. Technol.*, vol. 88, pp. 24–28, Mar. 2012.
- [32] A. Farjoo, F. Khorasheh, S. Niknaddaf, and M. Soltani, "Kinetic modeling of side reactions in propane dehydrogenation over Pt - Sn/ $\gamma$  - Al<sub>2</sub>O<sub>3</sub> catalyst," *Sci. Iran.*, vol. 18, no. 3, pp. 458–464, Jun. 2011.

- [33] A. M. Avila, Z. Yu, S. Fazli, J. A. Sawada, and S. M. Kuznicki, "Materials Hydrogen-selective natural mordenite in a membrane reactor for ethane dehydrogenation," *Microporous mesoporous Mater.*, vol. 190, pp. 301–308, 2014.
- [34] M. Rajiv, D. Q. Vu, and W. J. Koros, "Mixed Matrix Membranes Materials: An Answer to the Challenges Faced by Membrane Based Gas Separations Today," *J. Chin. Inst. Chem. Engrs.*, 2002.
- [35] Y. Gu and G. Meng, "A model for ceramic membrane formation by dip coating," *J. Eur. Ceram. Soc.*, vol. 19, pp. 1961–1966, 1999.
- [36] M. Norio, Y. Okamoto, J. Tamaki, K. Morinaga, and N. Yamazoe, "Oxygen semipermeability of mixed conductive oxide thick-film prepared by slip casting," *Solid State Ionics*, vol. 79, pp. 195–200, 1995.
- [37] "The preparation and characterization of alumina membranes with ultrafine pores," *J. Colloid Interface Sci.*, vol. 105, no. 1, pp. 27–40, 1985.
- [38] "<http://www.accumetmaterials.com/refractobond.htm>." .
- [39] B. L. Krasnyi, V. P. Tarasovskii, and A. B. Krasnyi, "Study of the effect of Aluminosilicate binder chemical composition on physicochemical properties of porous permeable ceramic," *Refract. Ind. Ceram.*, vol. 52, no. 6, pp. 405–408, 2012.

- [40] A. S. Wagh and S. Y. Jeong, “Chemically Bonded Phosphate Ceramics: III, Reduction Mechanism and Its Application to Iron Phosphate Ceramics,” *J. Am. Ceram. Soc.*, vol. 55, pp. 1850–1855, 2003.
- [41] J. H. . Hampton, S. B. Savage, and D. R.A.L, “Experimental analysis and modeling of slip casting,” *J. Am. Ceram. Soc.*, vol. 71, no. 12, pp. 1040–1045, 1988.
- [42] F. M. Tiller and C. Tsai, “Theory of filtration of ceramics : I , slip casting,” *J. Am. Ceram. Soc.*, vol. 69, no. 12, pp. 882–87, 1986.
- [43] D. S. Adcock and I. . Mcdowall, “The mechanism of filter pressing and slip casting,” *J. Am. Ceram. Soc.*, vol. 40, no. 10, pp. 355–360, 1956.
- [44] W. An, P. Swenson, A. Gupta, L. Wu, T. M. Kuznicki, and S. M. Kuznicki, “Improvement of H<sub>2</sub>/CO<sub>2</sub> selectivity of the natural clinoptilolite membranes by cation exchange modification,” *J. Memb. Sci.*, vol. 433, pp. 25–31, Apr. 2013.
- [45] Y. S. Lin, I. Kumakiri, B. N. Nair, and H. Alsayouri, “Microporous Inorganic Membranes,” in *Separation and Purification Methods*, vol. 31, no. 2, 2002, pp. 229–379.
- [46] S. A. H. Hejazi, A. M. Avila, T. M. Kuznicki, A. Weizhu, and S. M. Kuznicki, “Characterization of natural zeolite membranes for H<sub>2</sub>/CO<sub>2</sub> separations by single gas permeation.,” *Ind. Eng. Chem. Res.*, vol. 50, pp. 12717–12726, 2011.

- [47] E. A. Mason and A. P. Malinauskas, *Gas Transport in Porous Media: The Dusty-Gas Model*. 1983.
- [48] S. W. Webb, “Gas Phase Diffusion in Porous Media: Comparison of Models.”
- [49] S. Colin, “Rarefaction and compressibility effects on steady and transient gas flows in microchannels,” *Microfluid Nanofluid*, vol. 1, pp. 268–279, 2005.
- [50] R. Krishna and R. Baur, “Modelling issues in zeolite based separation processes,” *Sep. Purif. Technol.*, vol. 33, pp. 213–254, 2003.
- [51] J. Xiao and J. Wei, “Diffusion mechanism of hydrocarbons in zeolites-Theory,” *Chem. Eng. Sci.*, 1992.
- [52] M. Kanezashi and Y. S. Lin, “Gas permeation and diffusion characteristics of MFI-type zeolite membranes at high temperatures,” pp. 3767–3774, 2009.
- [53] A. M. Avila, H. H. Funke, Y. Zhang, J. L. Falconer, and R. D. Noble, “Concentration polarization in SAPO-34 membranes at high pressures,” *J. Memb. Sci.*, vol. 335, no. 1–2, pp. 32–36, 2009.
- [54] A.J. Burggraaf, “Important characteristics of inorganic membranes,” in *Fundamentals of Inorganic Membrane Science and Technology*, 1996.
- [55] H. Li, K. Haas-Santo, U. Schygulla, and R. Dittmeyer, “Inorganic microporous membranes for H<sub>2</sub> and CO<sub>2</sub> separation—Review of experimental and modeling progress,” *Chem. Eng. Sci.*, vol. 127, pp. 401–417, 2015.

- [56] O. Korkuna, R. Leboda, J. Skubiszewska-Zieab, T. Vrublevs'ka, V. M. Gun'ko, and J. Ryczkowski, "Structural and physicochemical properties of natural zeolites : clinoptilolite and mordenite," *Microporous Mesoporous Mater.*, vol. 87, pp. 243–254, 2006.
- [57] S. Yasyerli, I. Ar, G. Dogu, and T. Dogu, "Removal of hydrogen sulfide by clinoptilolite in a fixed bed adsorber," *Chem. Eng. Process.*, vol. 41, pp. 785–792, 2002.
- [58] J. Xiao and J. We, "Diffusion mechanism of hydrocarbons in zeolites-Analysis of experimental observations," *Chem. Eng. Sci.*, 1992.
- [59] A. M. Tarditi, E. A. Lombardo, and A. M. Avila, "Xylene permeation transport through composite Ba-ZSM-5/SS tubular membranes : modeling the steady-state permeation," *Ind. Eng. Chem. Res.*, vol. 47, pp. 2377–2385, 2008.
- [60] J. a. Ritter and A. D. Ebner, "State of the Art Adsorption and Membrane Separation Processes for Hydrogen Production in the Chemical and Petrochemical Industries," *Sep. Sci. Technol.*, vol. 42, no. 6, pp. 1123–1193, Apr. 2007.
- [61] M. Kanezashi, J. O. Brien-Abraham, and Y. S. Lin, "Gas Permeation Through DDR-Type Zeolite Membranes at High Temperatures," *AIChE J.*, vol. 54, no. 6, pp. 1478–1486, 2008.

## **Chapter Seven**

---

### **Single and multi-component transport through metal supported clinoptilolite membranes**

## 7.1 Summary

At room temperature and a feed pressure of 110 kPa considerable differences for separation efficiency of hydrogen from lower n-alkanes ( $\text{CH}_4$ ,  $\text{C}_2\text{H}_4$ ,  $\text{C}_2\text{H}_6$ ) was observed. After increasing the temperature up to 600 °C, hydrogen permeance increased considerably while the permrance of hydrocarbons slightly increased. The permeance of the weakly adsorbing molecules such as hydrogen was found to drop at room temperature resulting in lower hydrogen selectivities in the presence of strongly adsorbing molecules. At higher temperatures (higher than 300 °C) molecules with kinetic diameters larger than the zeolite pore were not adsorbed into the micropores, however, some transport was observed. This might be attributed either to some larger pores in clinoptololite structure or the vibration of the zeolite pore as the temperature was increased. Experimental analysis showed that for mixtures of a fast-weakly adsorbing component and a slow-strongly adsorbing component, the average selectivity for hydrogen separation was a factor of 2 lower than the one obtained under ideal single gas permeations.

## 7.2 Introduction

The application of molecular sieve materials, such as zeolites in gas separation and purification processes suggests alternative methods compared to conventional separation technologies. Since zeolite pores are comparable with kinetic diameters of gases such as hydrogen, it allows them for separation of components on the basis of differences in adsorption affinity or differences in shape and geometry. Molecular sieves can be used as adsorbents in pressure-swing adsorption (PSA), temperature-swing adsorption (TSA), or as inorganic membranes. Inorganic membranes with intrinsic thermal, structural and

chemical stability are preferred in particular for applications involving extreme conditions such as high-temperatures with the possibility of regeneration in the process.

Zeolite membranes have been used for separation of different gases depending on the particular application including separation of weakly adsorbing gases such as hydrogen [1]–[4] or strongly adsorbing components such as butane [5]–[7].

Predicting the separation performance of zeolite membranes in microporous materials depends on both multicomponent adsorption and diffusion properties. The adsorption of gases in the crystalline channels of the zeolite has an influence on the diffusivity of the molecules. When studying a gas mixture, depending on its composition, competitive adsorption could have a considerable play on the diffusion of molecules. Although in an ideal view, there is a tendency to predict mixture permeation based on single-component parameters, however, different interpretation from mixed gases showed that the behaviour for gas mixtures is different, according to process operating conditions.

Theoretical modeling of multicomponent permeance and separation through microporous inorganic membranes is multifaceted and a inclusive study has not been reported so far [8], [9]. The studies reported in the past years, have shown that the microstructure of a polycrystalline zeolite membrane and structural change of the zeolite in the membrane can have an effect on gas permeation and separation properties of the zeolites membrane. One may suppose that zeolite crystallite size and shape, crystal direction in the film, intercrystalline pore size and shape should be among the key parameters that describe the microstructure of a zeolite membrane. However, even a pure polycrystalline zeolite membrane often contains both zeolite and micro-porous non-zeolite pores, however, in most cases, gas passes through both types of the micro-pores. The presence of micro-

porous intercrystalline pores (with similar size of the zeolite pore) can affect separation mechanism by a zeolite membrane. Making a distinction between these two types of pores is not simple and therefore, considering the effect of each type of pore, cannot be precisely predicted.

Literature reports on the permeation of gas mixtures in microporous membranes, are limited even though practical applications of the zeolite membranes are likely to involve multicomponent systems. While competitive adsorption may be modeled for zeolite systems, permeance through defects will not be subjected to the same molecular forces, which influences the predictability of the membrane layer. The most precise test for membrane performance is therefore to test them under conditions similar to the end use.

The objective of this study is to predict the separation performance of a natural zeolite mixed matrix membrane at altering operating conditions (e.g. temperature and pressure) in comparison with single-component data. The contribution of adsorbate-adsorbent interaction is evaluated by comparing single gas and multicomponent gas experimental data through the mixed matrix zeolite membranes and measuring the adsorption data.

### **7.2.1 Classification of gas mixtures**

When dealing with a gas mixture, depending on the composition, competitive adsorption may have a major influence on the diffusion of the target permeate. The following circumstances describe the expected molecular behaviour of gas mixtures [10 – 12]:

1- Weakly (W) - weakly (W) adsorbing gases ( $H_2/CH_4$ ):

For combination of W – W adsorbing gases, the separation factor values are close to the ideal selectivity values but are typically somewhat lower.

$$\text{Separation Factor} \approx \text{Ideal Selectivity}$$

2- Weakly (W) - Strongly (S) adsorbing gases ( $H_2/C_2H_4$ ):

For a W–S mixture, the flux of weakly adsorbing component can be considerably reduced by the presence of the strongly adsorbing component. This effect is due to the adsorption among gas molecules mixture, compared to the single gas permeation.

Separation Factor < Ideal Selectivity

3- Strongly (S) - Strongly (S) adsorbing gases ( $CO_2/C_2H_4$ ):

The permeance of both gases decreases considerably. In this scenario, the stronger adsorbing gas of the two has lower permeance values. Separation factor is low at low temperatures.

Separation Factor  $\ll$  *Ideal Selectivity*

### 7.3 Experimental

A gas blend specified by NOVA Chemicals ( $H_2$ : 34%,  $CH_4$ : 6%,  $C_2H_4$ : 33%,  $C_2H_6$ : 27%) was used for evaluating membrane performance in feed pressure range of 110-160 kPa and temperature range of 25 °C – 600 °C.

Gas permeation through the natural zeolite tubing membranes was measured using the test system shown in Figure 7-1. The membrane was sealed in a tube-and-shell chamber made from stainless steel tube. Feed and retentate passed through the tube side while argon and permeate entered and exited through the shell side. For permeation tests at higher temperatures, the membrane cell was placed into a tube furnace with a multipoint programmable temperature controller. A heating rate of 5 °C/min was used to ramp to each specified temperature.

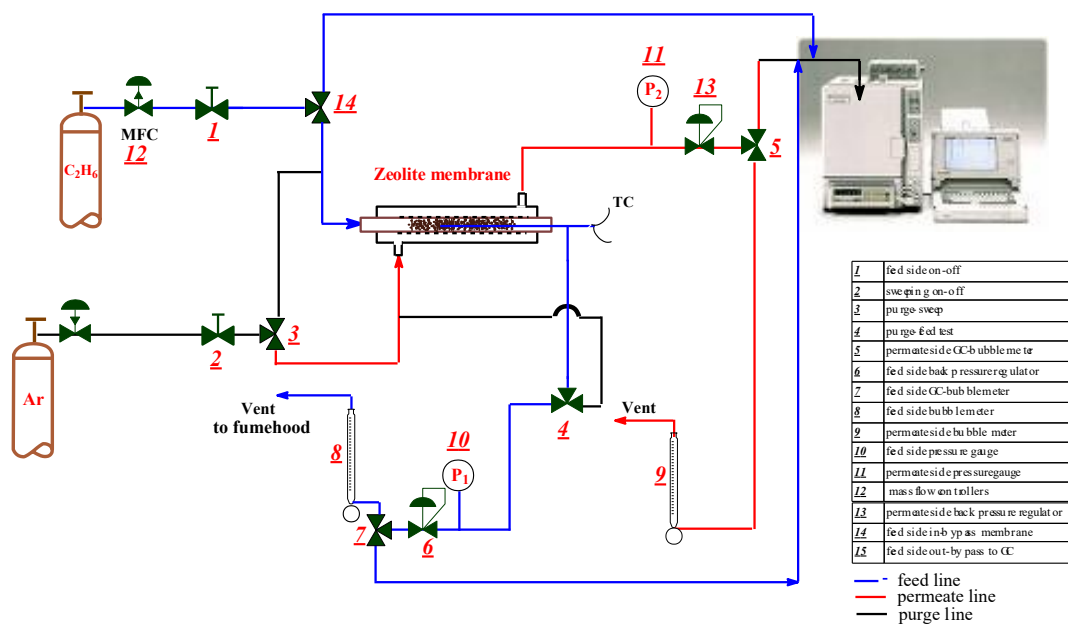


**Figure 7-1.** Schematic of the set-up for gas permeation measurement

The trans-membrane pressure was controlled using a backpressure regulator located at the feed side outlet. The feed and sweeping gas flow rates were controlled by two mass flow controllers (Sierra Instrument Inc.). For all gas permeation tests, flow rates of the feed and sweeping gas were constant at 100 mL/min (STP) and 100 mL/min (STP), respectively. The flow rate of outlet streams was measured using bubble flowmeters. A Shimadzu Gas Chromatograph GC-14B (GC) equipped with TCD and packed column (HaySep Q, 80–100 mesh) was used to analyze both the permeate and retentate concentrations.

To achieve the maximum thermal conductivity difference between the carrier gas and the analyte in single gas experiments, helium was used as GC carrier gas for CO<sub>2</sub> and C<sub>2</sub>H<sub>6</sub> while argon was used for H<sub>2</sub> analysis. For mixed gas permeance tests, however, the GC was re-calibrated to detect all the gases at the same time using argon as the GC carrier gas. Some loss of sensitivity was to be expected when argon was used as the sole sweep

gas but the sensitivity was expected to be adequate for the concentrations that we were measuring here. The thermal conductivity of different gases is brought in Table 7-1.

**Table 7-1.** Thermal conductivity of gases at 25 °C

<b>Gas</b>	<b>Thermal Conductivity (mW/m.K)</b>
N <sub>2</sub>	26
Ar	17.9
H <sub>2</sub>	186.9
He	156.7
CO <sub>2</sub>	16.8
C <sub>2</sub> H <sub>6</sub>	21.3
CH <sub>4</sub>	34.1
C <sub>2</sub> H <sub>4</sub>	20.5

### 7.3.1 Error propagation

In all reported permeation results in this study, there is an uncertainty which is approximated through a standard propagation of errors analysis [13]. Absolute error propagation was the product of the uncertainties associates with different variables including pressure, temperature, flow rate and gas chromatography measurements.

$$\frac{\delta \pi}{\pi} = \sqrt{\left(\frac{\delta T}{T}\right)^2 + \left(\frac{\delta \Delta P_i}{\Delta P_i}\right)^2 + \left(\frac{\delta (X_i)}{(X_i)}\right)^2 + \left(\frac{\delta V_i}{V_i}\right)^2} \quad (1)$$

Where,  $T$ ,  $X_i$ ,  $\Delta P$  and  $V_i$  are operating temperature, GC detection value, trans-membrane pressure and outlet volumetric flow rate respectively:

$$V_i = \frac{Volume}{t} \quad (2)$$

$$\frac{\delta V_i}{V_i} = \sqrt{\left(\frac{\delta \text{Volume}}{\text{Volume}}\right)^2 + \left(\frac{\delta t}{t}\right)^2} \quad (3)$$

Where, volume is the measured amount of gas exiting a column in milliliters (mL) and t is the measured time in seconds. Table 7-2 summarises the uncertainty associated with source of error.

$$\Delta P_i = P_{feed} - P_{Permeate} \quad (4)$$

$$\delta \Delta P_i = \delta P_{feed} + \delta P_{permeance} \quad (5)$$

**Table 7-2.** Uncertainty associated with each source of error

Parameter	Uncertainty ( $\delta$ )
T	1°C
Volume	0.1 mL
t	0.1 S
$\Delta P$	0.2 psi
x	0.1 %

The uncertainty of reported values is shown in each graph by the error bars according to the above equations and the calculated uncertainty.

## 7.4 Results and Discussion

### *Effect of Pressure*

To characterize and compare the membrane performance, single and multicomponent gas separation was conducted by varying the feed side pressure while maintaining atmospheric pressure at the permeate side. The permeation tests, as the first set of

experiments in membrane characterization was conducted at room temperature.

As shown in Figures 7.2, 7.3 and 7.4, the permeation and separation factors for all the gases decreased over the feed pressure range of 110-160 kPa at room temperature. The decreasing trend implies that the gas permeation across the tubing membrane has contributions from different transport mechanisms associated with both zeolite and non-zeolite pores. The decreasing trend of permeance with pressure is expected to be due to the growing contribution from viscous flux through the relatively large non-selective (non-zeolite) pores as feed pressure was increased and consequently  $H_2$  selectivity decreased.

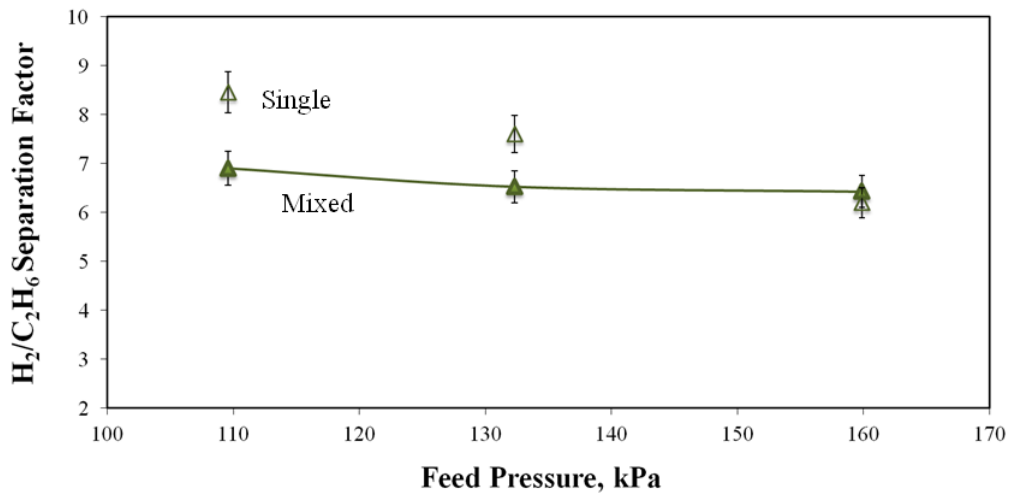


**Figure 7-2.**  $H_2/C_2H_6$  separation factor in multi component and single gas permeation test through tubular mixed matrix membrane at different feed pressures, Temperature: 25 °C, Permeate pressure: 108.0 kPa.

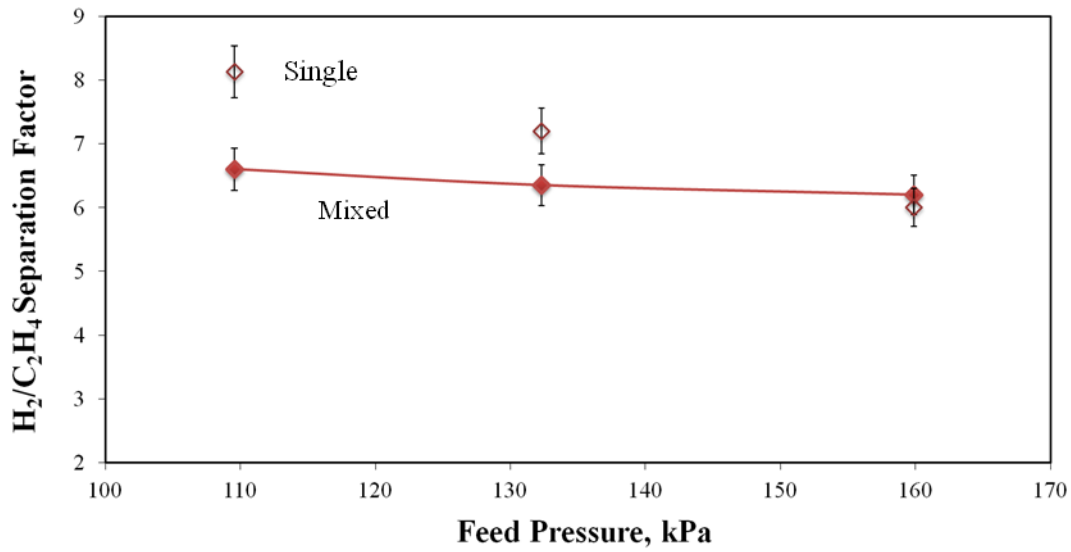


**Figure 7-3.** H<sub>2</sub>/C<sub>2</sub>H<sub>4</sub> separation factor in multi component and single gas permeation test through tubular mixed matrix membrane at different feed pressures, Temperature: 25 °C, Permeate pressure: 108.0 kPa.

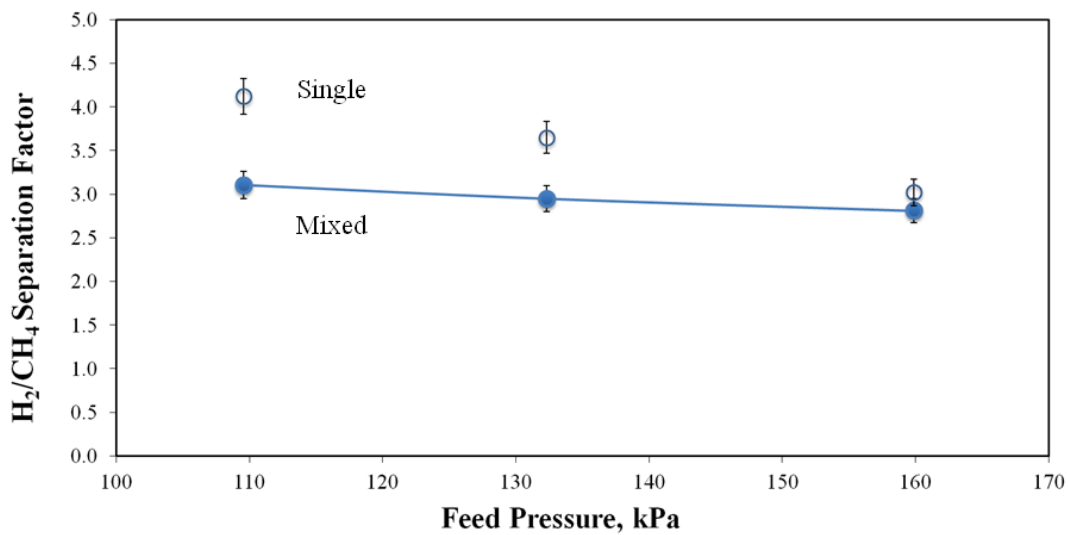


**Figure 7-4.** H<sub>2</sub>/CH<sub>4</sub> separation factor in multi component and single gas permeation test through tubular mixed matrix membrane at different feed pressures, Temperature: 25 °C, Permeate pressure: 108.0 kPa.

Although in the single and mixed gas measurement test, the separation efficiency decreased over the pressure range, however, two major differences in the behavior is noticeable. First the average separation efficiency is higher for the single gas test, while due to the competitive behavior of the gases, difference in sizes/geometries and the non-similarity in adsorptive behavior at room temperature, the average separation factor for the mixture is lower than the single gas selectivity. Secondly, for the single gas test, the decrease in selectivity is sharper than the mixed gas, which is attributed to the competition between the gases.

Increasing trans-membrane pressure had the opposite effect on the permeation of the non-adsorbing hydrogen than the adsorbing hydrocarbon components. On the one hand, an increase in feed pressure provided larger partial pressure differences across the membrane for hydrogen and hydrocarbons that appears to increase their permeation. On the other hand, increasing feed pressure at room temperature raised the partial pressures of the strongly adsorbing hydrocarbons, which enhanced adsorption on the zeolite and further blocked the zeolitic pores, resulting in inhibition of hydrogen and methane permeance. Thus hydrogen separation factor for mixed gas was not affected as much as single gas selectivity in the same pressure range.

The decrease in selectivity for  $H_2/C_2H_6$ ,  $H_2/C_2H_4$ ,  $H_2/CH_4$  in the pressure range of 108 to 165 kPa in single gas permeation was 23.64%, 26.2% and 26.7% while for the mixed gas separation the separation factor reduced 5%, 7.7% and 6% respectively. Therefore, when dealing with a gas mixture, zeolite membrane operates at a slightly higher operating pressure [14–16].

### *Effect of Temperature*

To compare single and mixed component gas selectivity in hydrogen separation, single gas permeation was tested up to 600 °C. Figures 7.5, 7.6 and 7.7 show selectivity of clinoptilolite membrane for H<sub>2</sub>/C<sub>2</sub>H<sub>6</sub>, H<sub>2</sub>/C<sub>2</sub>H<sub>4</sub> and H<sub>2</sub>/CH<sub>4</sub> respectively. Selectivity of single gases is almost constant as the temperature was increased. As the permeance contributions associated with Knudsen flux and viscous flux decreases with temperature, the constant permeation trend for all the gases with temperature reflects that both zeolite and non-zeolite pores and related mechanisms exist in this membrane [17–19]. Therefore, since the zeolite permeance is expected to increase as a function of temperature so that the two effects was seen to be cancelling out.

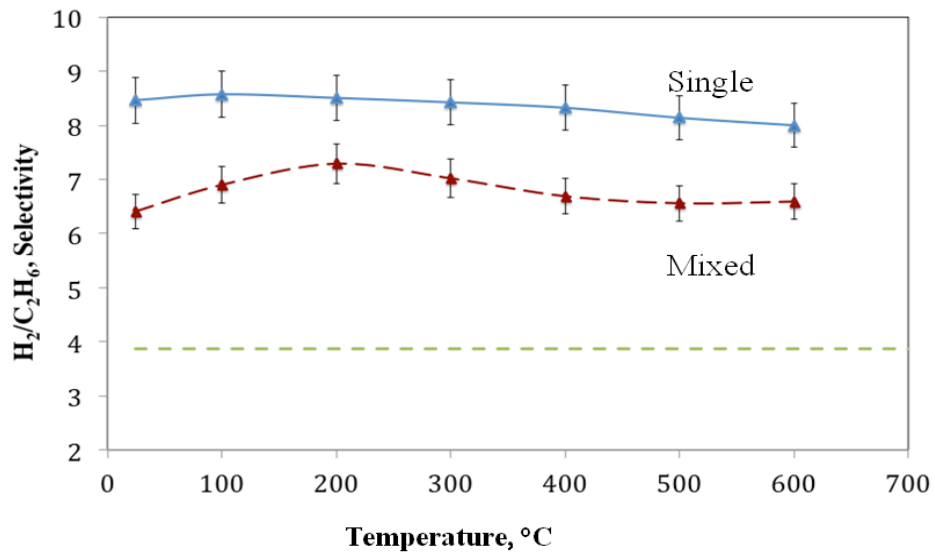


**Figure 7-5.** Mixed (Blue), Ideal (Red), Knudsen (green), H<sub>2</sub>/C<sub>2</sub>H<sub>6</sub> separation selectivity through tubular mixed matrix membrane at different temperatures, Feed pressure: 111.2 kPa, Permeate pressure: 108.2 kPa.

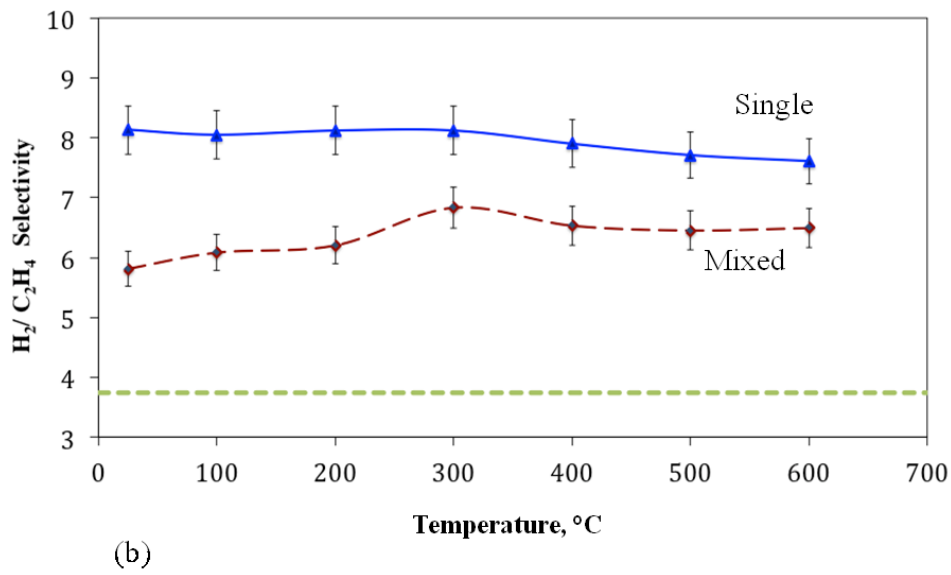


**Figure 7-6.** Mixed (Blue), Ideal (Red), Knudsen (green), H<sub>2</sub>/C<sub>2</sub>H<sub>4</sub> separation selectivity through tubular mixed matrix membrane at different temperatures, Feed pressure: 111.2 kPa, Permeate pressure: 108.2 kPa.

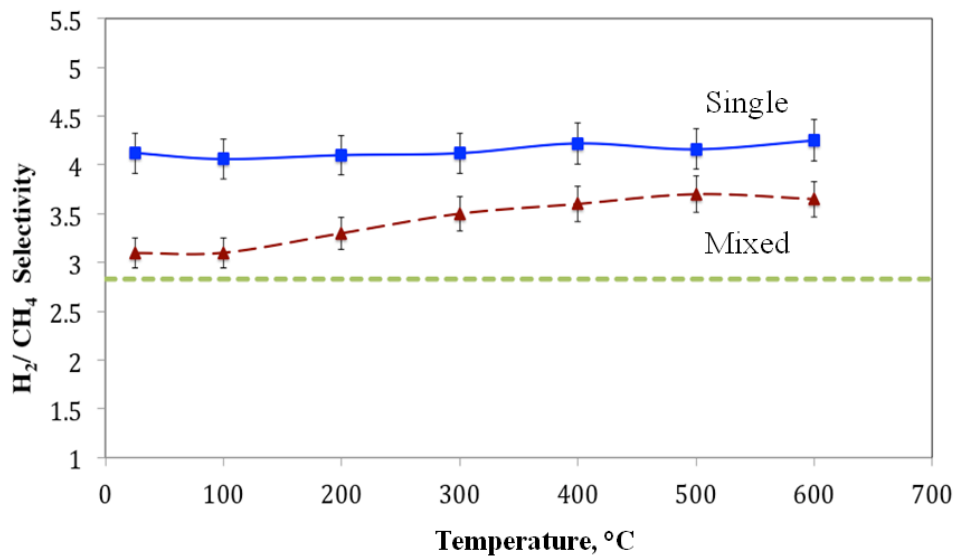


**Figure 7-7.** Mixed (Blue), Ideal (Red), Knudsen (green), H<sub>2</sub>/CH<sub>4</sub> separation selectivity through tubular mixed matrix membrane at different temperatures, Feed pressure: 111.2 kPa, Permeate pressure: 108.2 kPa

At higher temperatures, a larger fraction of H<sub>2</sub> flux diffused through the zeolite crystals, However, because single gas selectivity was constant, at higher temperatures other gases in addition to hydrogen were passing from the feed side to the permeate side. This phenomenon can be because of two reasons. First, all the channels allowing gas transfer to the permeate side were not zeolitic channels that accommodate gases other than hydrogen, such as C<sub>2</sub>H<sub>4</sub>, C<sub>2</sub>H<sub>6</sub> or CH<sub>4</sub> which resulted in constant selectivity trend for the single gas permeation. Furthermore, the thermal vibrations of both the zeolite (framework flexibility) and the probe molecules at higher temperatures had an effect [11].

The difference between single selectivity and mixed gas separation factor was larger up to 300 °C. At lower temperatures competitive adsorption dominated and ethylene, as the stronger adsorbing gas blocked the passages for hydrogen to permeate through the zeolite pores and as a result adsorption took over. With further temperature rise, the zeolite surface possession decreased.

At high temperatures where limited adsorption occurs, mass transport is kinetically verified [11]. At temperatures over 300 °C, adsorption of light hydrocarbons on clinoptilolite zeolite was negligible and the permeation became gaseous diffusion. Permeation of hydrogen was taken over by the adsorbed hydrocarbons in zeolitic pores at low temperatures, and increased with increasing temperature. Since the zeolite adsorption is negligible at 600 °C for all the components, gas permeation is essentially determined by the diffusivity of the gases in the zeolite pores.

For separation of multicomponent mixture, an inversion in separation selectivity could be observed during temperature-programmed permeation, when the separation mechanism shifted from adsorption at lower temperatures towards diffusion at higher temperatures.

## 7.5 Adsorption Parameters

The use of accurate adsorption data is imperative to extract transport properties from the single-component permeation as well as for modeling multi component permeation.

In the region of strong adsorption, molecules will have strong interactions with zeolite membrane dissimilar to the region of weak adsorption (Henry region) that would influence the diffusion behaviour.

The difference between single and multi-component gas behavior was maximized up to 300 °C and adsorption was discussed as one of the possible reasons causing this trend. To check the effect of adsorption for this specific mixture on the zeolite membrane, adsorption isotherms were measured. Ethane, ethylene and methane adsorption isotherms on clinoptilolite (0–120 kPa) were measured at 25, 100, 200, 300, and 400 °C with a Micromeritics ASAP 2020C in its chemisorption configuration. Sample was activated under a flow of 200 ml/min of N<sub>2</sub> to 350 °C and held isothermally for 15 min. The sample was evacuated under vacuum (10<sup>-4</sup> Pa) for 60 min and dosed with fixed quantities of gas until a pressure of 1.14 bars, was reached. Adsorption isotherms of ethylene, ethane and methane at different temperatures are shown in Figure 7.8. As shown in Figure 7-8, adsorption strength decreased in the following order:

ethylene > ethane > methane > hydrogen.

No adsorption was measurable for hydrogen at the experimental conditions. Methane and ethane adsorption isotherms were in essence linear with the partial pressure, while ethylene was adsorbed more strongly and non-linearly.

While the adsorption strength of all hydrocarbons were strongest at 25 °C temperature, further increase in temperature reduced adsorption on zeolites and this difference was

minimized at 300 °C and ignorable at 400 °C. The adsorption results confirmed the permeance behavior on zeolite membrane.

In this work, hydrogen is considered as the non-adsorbing or weakly adsorbing gas, ethane/methane as moderately adsorbing gas and ethylene as the strongly adsorbing gas.

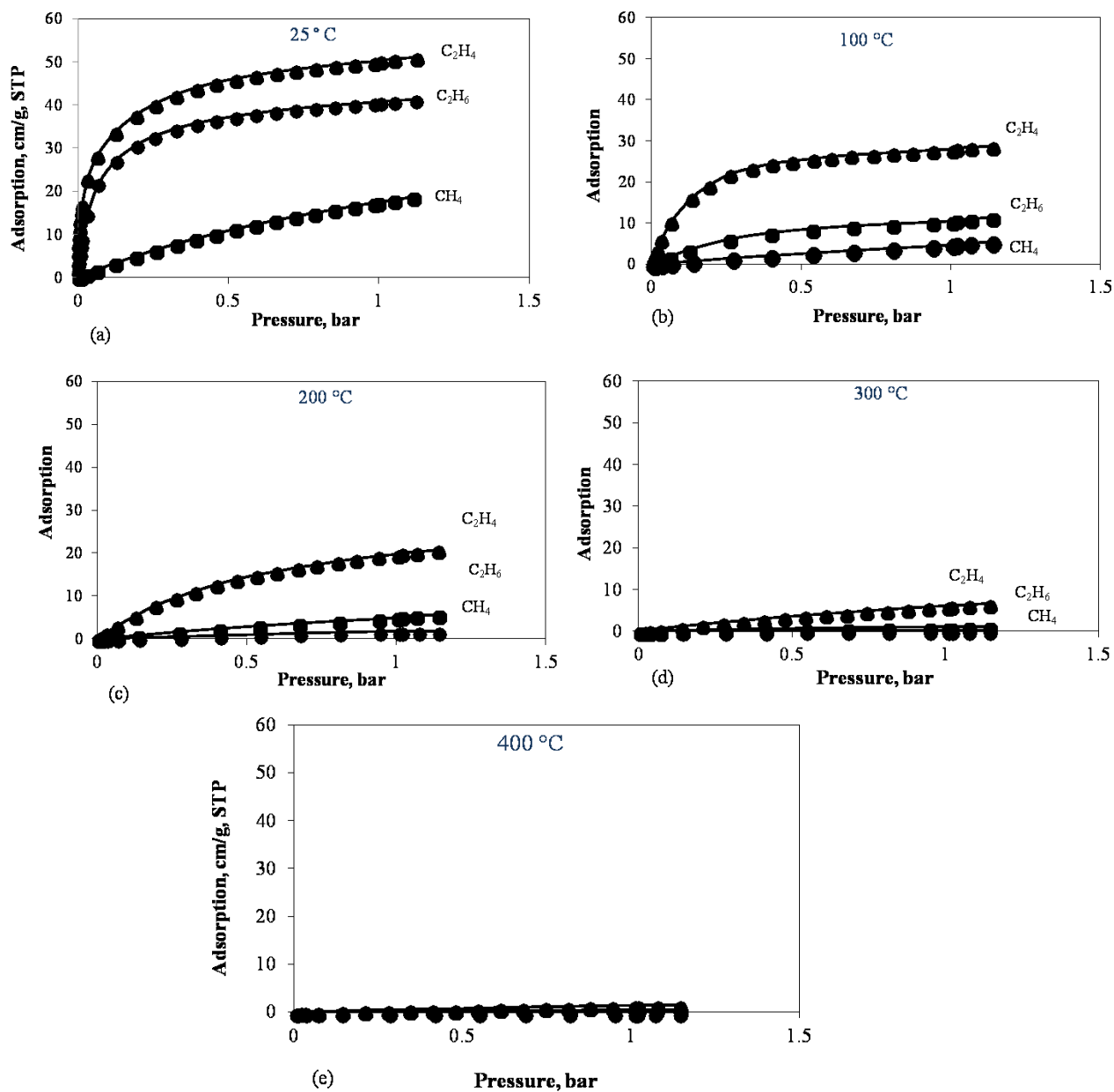


**Figure 7-8.** Adsorption isotherms for ethylene (red), ethane (blue) and methane (green) on as received clinoptilolite at a) 25 °C, b) 100 °C, c) 200 °C, d) 300 °C and e) 400 °C

The load inside the zeolite ( $\theta$ ) is correlated with the partial pressure of component  $i$  by means of an adsorption isotherm model. In this study, Langmuir model is selected due to its simplicity and since it was able to describe H<sub>2</sub> and light hydrocarbons isotherms at low to

moderate pressures. Langmuir model summarizes the pressure reliance of load as following: [20], [21]:

$$\theta_i = \frac{V}{V_{sat}} = \frac{KP_A}{1 + KP_A} \quad (6)$$

Table 7-3 shows the value of adsorption parameters of the various components of the Langmuir adsorption isotherm fit at 25°C, from 0 to 1.2 bars.

**Table 7-3.** Values of the adsorption parameters, for the various components at 70 °C, (Langmuir isotherm)

Component	$V_{sat} K$ , cc/(g.bar)	$V_{sat}$ cc/g	K
H <sub>2</sub>	N/A	N/A	N/A
CH <sub>4</sub>	5.22	15.24	0.0409
C <sub>2</sub> H <sub>6</sub>	21.55	6.13	3.54
C <sub>2</sub> H <sub>4</sub>	243.9	24.4	16

## 7.6 Conclusion

Different observations on mixed gases showed that the behavior for the mixture of the gases was different depending on the operating conditions.

When a gas mixture is studied, depending on its composition in addition to geometrical differences, competitive adsorption has a significant influence on the diffusion of the target permeate. In the zeolite mixed matrix membranes, permeation of hydrogen (at the target permeate) was negatively influenced by the adsorbed hydrocarbons in zeolitic

pores at low temperatures. Increasing the operating temperature, higher than 300 °C, eliminated the adsorption effect. At temperatures higher than 300 °C, geometrical non-similarity and competitive transport among molecules caused deviation from single gas permeance mechanism.

## 7.7 References

- [1] W. An, P. Swenson, L. Wu, T. Waller, A. Ku, and S. M. Kuznicki, "Selective separation of hydrogen from C1/C2 hydrocarbons and CO<sub>2</sub> through dense natural zeolite membranes," *J. Memb. Sci.*, vol. 369, no. 1–2, pp. 414–419, Mar. 2011.
- [2] N. W. Ockwig and T. M. Nenoff, "Membranes for hydrogen separation.," *Chem. Rev.*, vol. 107, no. 10, pp. 4078–110, Oct. 2007.
- [3] N. Nishiyama, M. Yamaguchi, T. Katayama, Y. Hirota, M. Miyamoto, Y. Egashira, K. Ueyama, K. Nakanishi, T. Ohta, A. Mizusawa, and T. Satoh, "Hydrogen-permeable membranes composed of zeolite nano-blocks," *J. Memb. Sci.*, vol. 306, pp. 349–354, 2007.
- [4] H. Verweij, Y. S. Lin, and J. Dong, "Microporous silica and zeolite membranes for hydrogen purification," *MRS Bull.*, vol. 31, pp. 756–764, 2006.
- [5] Z. a E. P. Vroon, K. Keizer, M. J. Gilde, H. Verweij, and a. J. Burggraaf, "Transport properties of alkanes through ceramic thin zeolite MFI membranes," *J. Memb. Sci.*, vol. 113, no. 2, pp. 293–300, 1996.
- [6] W. J. W. Bakker, L. J. P. Van Den Broeke, F. Kapteijn, and J. a Moulijn, "Temperature Dependence of One-Component Permeation through a Silicalite-1 Membrane," *AIChE J.*, vol. 43, no. 9, pp. 2203–2214, 1997.
- [7] Z. A. E. . Vroon, K. Keizer, A. . Burggraaf, and H. Verweij, "Preparation and characterization of thin zeolite MFI membranes on porous supports," *J. Memb. Sci.*, vol. 144, no. 1–2, pp. 65–76, 1998.
- [8] H. Li, K. Haas-Santo, U. Schygulla, and R. Dittmeyer, "Inorganic microporous

- membranes for H<sub>2</sub> and CO<sub>2</sub> separation—Review of experimental and modeling progress,” *Chem. Eng. Sci.*, vol. 127, pp. 401–417, 2015.
- [9] P. Bernardo, E. Drioli, and G. Golemme, “Membrane Gas Separation: A Review/State of the Art,” *Ind. Eng. Chem. Res.*, vol. 48, no. 10, pp. 4638–4663, May 2009.
- [10] M. Sadrzadeh, M. Amirilargani, and K. Shahidi, “Pure and mixed gas permeation through a composite polydimethylsiloxane membrane,” no. June 2009, 2011.
- [11] J. Caro and M. Noack, “Zeolite Membranes – Status and Prospective,” in *Advances in Nanoporous Materials*, vol. 1, Elsevier B.V, 2009, pp. 1–96.
- [12] J. Dong and Y. S. Lin, “Multicomponent Hydrogen / Hydrocarbon Separation by MFI-Type Zeolite Membranes,” vol. 46, no. 10, pp. 1957–1966, 2000.
- [13] D. K. R. Bevington, Philip R., *Data reduction and error analysis for the physical sciences*, 3rd ed. Mc Graw-Hill Companies, Inc., 2003.
- [14] S. Colin, “Rarefaction and compressibility effects on steady and transient gas flows in microchannels,” *Microfluid Nanofluid*, vol. 1, pp. 268–279, 2005.
- [15] *Mason, E. A.; Malinauskas, A. P. Gas Transport in Porous Media: The Dusty-Gas Model; Elsevier: Amsterdam, 1983.*
- [16] S. Thomas, R. Schäfer, J. Caro, and A. Seidel-morgenstern, “Investigation of mass transfer through inorganic membranes with several layers,” vol. 67, pp. 205–216, 2001.
- [17] J. a. Ritter and A. D. Ebner, “State of the Art Adsorption and Membrane Separation Processes for Hydrogen Production in the Chemical and

Petrochemical Industries," *Sep. Sci. Technol.*, vol. 42, no. 6, pp. 1123–1193, Apr. 2007.

- [18] A. M. Tarditi, E. A. Lombardo, and A. M. Avila, "Xylene permeation transport through composite Ba-ZSM-5/SS tubular membranes : modeling the steady-state permeation," *Ind. Eng. Chem. Res.*, vol. 47, pp. 2377–2385, 2008.
- [19] A. H. Shafie, W. An, S. A. Hosseinzadeh Hejazi, J. a. Sawada, and S. M. Kuznicki, "Natural zeolite-based cement composite membranes for H<sub>2</sub>/CO<sub>2</sub> separation," *Sep. Purif. Technol.*, vol. 88, pp. 24–28, Mar. 2012.
- [20] A. E. Principles, "Adsorption Equilibria Adsorption Equilibria."
- [21] a. Wender, a. Barreau, C. Lefebvre, a. Lella, a. Boutin, P. Ungerer, and a. H. Fuchs, "Adsorption of n-alkanes in faujasite zeolites: molecular simulation study and experimental measurements," *Adsorption*, vol. 13, no. 5–6, pp. 439–451, Sep. 2007.

## **Chapter Eight**

---

### **Conclusion and Future Work**

## 8.1 Conclusions

Zeolite molecular sieves have improved the chemical processing industry for applications ranging from membrane technology to adsorption and catalytic reactions. The objective of this research was to develop new molecular sieve materials and study their applications in membrane and adsorptive gas separation processes. Several techniques to employ and modify zeolite molecular sieve materials have been developed, including development of composite disk membranes, dip coated stainless steel tubular membranes and a pore size modification method to create a new rate based adsorbent. The new materials and membranes resulting from the development and modification techniques can be potentially applied to commercial and applied membrane or adsorptive gas separation processes.

In chapter 3 it was shown that the structure of a naturally occurring clinoptilolite was modified through ammonium exchange, calcination, and post-calcination steam treatment. The ammonium exchange removed the structural cations, which caused the framework to expand, while steam treatment at 600 °C caused a contraction in the structure. The effective pore size of the modified clinoptilolite allowed it to adsorb ethylene and exclude ethane in a dynamic adsorption experiment. By incrementally changing the pore size of clinoptilolite, a new rate-based adsorbent for the adsorptive separation of ethylene from ethane was produced.

The study in chapter 5 established the fact that copper can be employed as a metallic sealant in membrane fabrication process to boost the membrane performance. Copper powders were added as a binder and sealant to fill out the non-zeolite region in pressed clinoptilolite disk membranes. However, gas permeance in copper-clinoptilolite

membranes decreased due to reduction of the zeolite volume fraction and the minimization of non-selective flux through inter particle channels. The increase of membrane performance for the copper clinoptilolite composite membranes is attributed to the metallic copper and copper oxide effectively filling a portion of the inter-particle spaces and creating a complete adhesion with the zeolite particles. The natural zeolite disk membrane has the additional aspect of high thermal and chemical stability, which provides the possibility of increasing the permeance at higher temperature.

To enhance the process flexibility and to scale up the disk membrane fabrication process, tubular mixed matrix zeolite membranes were coated on tubular stainless steel supports and discussed in chapter 6. A natural zeolite mixed matrix membrane showed promise in H<sub>2</sub> separation from CO<sub>2</sub> and C<sub>2</sub>H<sub>6</sub>. Multilayer coating method was applied as a post treatment method to improve membrane performance. The improve in selectivity from 8.3 to 10.2 and 6.9 to 8.3 for H<sub>2</sub>/CO<sub>2</sub> and H<sub>2</sub>/C<sub>2</sub>H<sub>6</sub> respectively suggests that the number and size of non-selective, non-zeolite pores reduced after applying the second layer which was also confirmed by the comparative parameter. Total H<sub>2</sub> permeance increased 53% with the increase of temperature due to the larger contribution of the selective compared to the non-selective flux fraction. The study concludes that natural zeolite coated stainless steel tubular membranes have great potential for large-scale hydrogen production at high temperature requirements.

Finally in chapter 7, hydrogen separation mechanism from a mixture of light hydrocarbons was studied and discussed. At room temperature and a feed pressure of 110 kPa large differences for the separation efficiency of hydrogen from lower n-alkanes (CH<sub>4</sub>, C<sub>2</sub>H<sub>4</sub>, C<sub>2</sub>H<sub>6</sub>) were observed for the components under study. After increasing the

temperature up to 600 °C hydrogen permeance increased considerably while the permrance of hydrocarbons slightly increased. Escalating the temperature to 600 °C, enhanced hydrogen permeance significantly, whereas, the permrance of hydrocarbons slightly increased. Experimental analysis showed that at temperatures lower than 300 °C in gas mixture with different adsorption affinities, adsorption caused large deviation from ideal gas behaviour when no geometrical or adsorptive effects play any roles. While coated clinoptilolite membrane separated hydrogen effectively up to 600 °C, hydrogen separation was a factor of 2 lower than the one obtained under ideal single gas permeations.

By means of development of membranes in different shapes with process flexibility or new adsorbents, we have developed several techniques to create new molecular sieve materials for membrane and adsorptive gas separation processes. Further research and development in new micro-porous materials will be critical to the chemical processing industry and should be viewed as an opportunity for the advance of next-generation sustainable membrane or adsorptive gas separation technologies.

## **8.2 Recommendations for Future Work**

In disk membrane preparation, we proposed a new proof of concept based on the use of copper as a binder and sealant agent of clinoptilolite particles to address the cost and scaling-up limitations of zeolite membranes. Knowing that the formed copper and CuO may be also covering active zeolite pores for permeation, the next logical step would be to increase the zeolite volume content in the composite membrane to enhance selectivity and at the same time the permeance. This requires the

modification of heat treatment procedure. Additionally, the preparation method has clear advantages in terms of scaling up. In addition to disks, the preparation method can be applied to other geometries including plates and tubes, which are satisfactory for industrial applications. Besides copper-clinoptilolite disks, more characterization work can be added using other malleable materials like aluminum powder, iron powder or alloys powder.

In coated tubular membranes, understanding the influence of thermal compatibility between the coating slurry and the metallic support on the number of non-zeolite pores requires further study. Since the difference in thermal conductivity results in the appearance of cracks and possibly pinholes, a modified heat treatment at lower temperature or heat treatment at vacuum or supercritical conditions are worth to be further studied. Another method to minimize the effect of thermal conductivity, would be to coat membranes by thermal spray coating method in which melted or heated materials are sprayed onto a surface or the materials are coated onto a heated surface. The benefit of this method is that water is evaporated immediately and the probability of crack formation is reduced.

Presence of any dust or suspended particles facilitates formation of cracks on membranes, it is recommended to perform the coating in a clean room with a low level of environmental pollutants such as dust, airborne or possibly microbes and aerosol particles, and chemical vapours.

Since most of the issues in membrane preparation process were relevant to support as well as compatibility between the zeolite slurry and support, further study of the performance and development of self-supported membranes with the slurry

developed for this research is also encouraged.

Finally, combining a zeolite membrane as a membrane reactor system is another valuable application in which a chemical conversion process is combined with a membrane separation process to add reactants or remove products of the reaction. The zeolite membrane is easily thermally stable to 600 °C, therefore, the membrane reactor system is in particular valuable for endothermic reactions such as dehydrogenation.

## Complete List of references

## Chapter 1:

- [1] C. S. Cundy and P. a. Cox, "The hydrothermal synthesis of zeolites: Precursors, intermediates and reaction mechanism," *Microporous Mesoporous Mater.*, vol. 82, no. 1–2, pp. 1–78, 2005.
- [2] D.W. Breck, "Zeolite Molecular Sieves: Structure, Chemistry, and Use," no. John Wiley & Sons, Ltd, 1974.
- [3] M. W. Ackley, S. U. Rege, and H. Saxena, "Application of natural zeolites in the purification and separation of gases," *Microporous Mesoporous Mater.*, vol. 61, pp. 25–42, 2003.
- [4] G. Gottardi and E. Gallim, "*Natural Zeolites*", Germany: Springer-Verlag Berlin Heidelberg, 1985.
- [5] W. Ackley, Mark, S. U. Rege, and H. Saxena, "Application of natural zeolites in the purification and separation of gases", *Microporous Mesoporous Mater.*, vol. 61, pp. 25–42, Jul. 2003.
- [6] A. W. Thornton, T. Hilder, A. J. Hill, and J. M. Hill, "Predicting gas diffusion regime within pores of different size, shape and composition", *J. Memb. Sci.*, vol. 336, pp. 101–108, Jul. 2009.
- [7] Steven Kuznicki and Kathleen A. Thrush, "Large pored molecular sieves with charged octahedral titanium and charged tetrahedral aluminum", *US005244650A*, 1993.
- [8] L. B. Mccusker and D. H. Olson, "*Atlas of Zeolite Framework Types*". Elsevier,

2007.

- [9] S. M. Kuznicki, V. Bell, S. Nair, H. W. Hillhouse, R. M. Jacobinas, C. M. Braunbarth, B. H. Toby, and M. Tsapatsis, "A titanosilicate molecular sieve with adjustable pores for size-selective adsorption of molecules", *Nature*, vol. 412, no. 6848, pp. 720–4, Aug. 2001.
- [10] F. A. Mumpton, "*Mineralogy and Geology of Natural Zeolites*", Washington, D.C.: Mineralogical Society of America, 1977.
- [11] W. An, P. Swenson, L. Wu, T. Waller, A. Ku, and S. M. Kuznicki, "Selective separation of hydrogen from C1/C2 hydrocarbons and CO2 through dense natural zeolite membranes", *J. Memb. Sci.*, vol. 369, no. 1–2, pp. 414–419, Mar. 2011.
- [12] D. L. Bish and M. D.W., "Natural Zeolites: Occurrence, Properties, Application", *Rev. Miner. Geochemistry*, vol. 45, 2001.
- [13] D. Zhao, K. Cleare, C. Oliver, C. Ingram, D. Cook, R. Szostak, and L. Kevan, "Characteristics of the synthetic heulandite-clinoptilolite family of zeolites", *Microporous Mesoporous Mater.*, vol. 21, no. 4–6, pp. 371–379, 1998.
- [14] S. Satokawa and K. Itabashi, "Crystallization of single phase (K, Na) - clinoptilolite," *Microporous Mater.*, vol. 8, pp. 49–55, 1997.
- [15] A. Ansón, S. M. Kuznicki, T. Kuznicki, T. Haastrup, Y. Wang, C. C. H. Lin, J. A. Sawada, E. M. Eyring, and D. Hunter, "Adsorption of argon, oxygen, and nitrogen on silver exchanged ETS-10 molecular sieve", *Microporous*

*Mesoporous Mater.*, vol. 109, no. 1–3, pp. 577–580, 2008.

- [16] W. T. Schaller and U. S. Geological, “The Mordenite-Ptilolite Group; Clinoptilolite, a New Species”, *Mineral. Soc. Am.*, vol. 8, pp. 128–134, 1923.
- [17] A. Julbe, “Zeolite membranes-synthesis, charactersitic and application” in “*Intorduction to zeolite science and practices*”, Elsevier B.V., 2007.
- [18] A. Dyer, “*An Introduction to Zeolite Molecular Sieves*”, John Wiley, Chichestar, 1988.
- [19] R. Szostak, “*Handbook of Molecular Sieves: Structures*”, New York: Van Nostrand Reinhold, 1992.

## **Chapter 2:**

- [1] D. M. Ruthven, “Principle of adsorption and adsorption processes.” John Wiley & Sons, Inc., 1984.
- [2] Y. Wu, H. Chen, D. Liu, Y. Qian, and H. Xi, “Adsorption and separation of ethane / ethylene on ZIFs with various topologies : Combining GCMC simulation with the ideal adsorbed solution theory ( IAST ),” *Chem. Eng. Sci.*, vol. 124, pp. 1–10, 2014.
- [3] R. Szostak, “*Handbook of Molecular Sieves: Structures*”, New York: Van Nostrand Reinhold, 1992.
- [4] A. Wender, A. Barreau, C. Lefebvre, A. Lella, A. Boutin, P. Ungerer, and A. H. Fuchs, “Adsorption of n-alkanes in faujasite zeolites: molecular simulation study and experimental measurements,” *Adsorption*, vol. 13, no. 5–6, pp. 439–451, 2007.

- [5] A. Ansón, S. M. Kuznicki, T. Kuznicki, T. Hastrup, Y. Wang, C. C. H. Lin, J. A. Sawada, E. M. Eyring, and D. Hunter, “Adsorption of argon, oxygen, and nitrogen on silver exchanged ETS-10 molecular sieve,” *Microporous Mesoporous Mater.*, vol. 109, no. 1–3, pp. 577–580, 2008.
- [6] M. W. Ackley, R. F. Giese, and R. T. Yang, “Clinoptilolite : Untapped potential for kinetic gas separations,” vol. 12, no. April, pp. 780–788, 1992.
- [7] D. M. Ruthven and S. C. Reyes, “Adsorptive separation of light olefins from paraffins,” *Microporous Mesoporous Mater.*, vol. 104, pp. 59–66, 2007.
- [8] M. M. A. Freitas and J. L. Figueiredo, “Preparation of carbon molecular sieves for gas separations by modification of the pore sizes of activated carbons,” *Fuel*, vol. 80, no. 1, pp. 1–6, 2001.
- [9] R. T. Yang, "*Adsorbents: Fundamentals and Applications*". John Wiley and Sons, 2003.
- [10] W. An, P. Swenson, A. Gupta, L. Wu, T. M. Kuznicki, and S. M. Kuznicki, “Improvement of H<sub>2</sub>/CO<sub>2</sub> selectivity of the natural clinoptilolite membranes by cation exchange modification,” *J. Memb. Sci.*, vol. 433, pp. 25–31, 2013.
- [11] C. C. H. Lin, J. A. Sawada, L. Wu, T. Hastrup, and S. M. Kuznicki, “Anion-Controlled Pore Size of Titanium Silicate Molecular Sieves,” *J. Am. Chem. Soc.*, no. 131, pp. 609–614, 2009.
- [12] P. Bartl and W. F. Holderich, “A study of the dealumination methods for zeolite L,” *Microporous Mesoporous Mater.*, vol. 38, no. 38, pp. 279–286, 2000.

- [13] G. E. Keller, R. A. Anderson, and C. M. Yon, "*Handbook of Separation Process Technology*", John Wiley & Sons, 1987.
- [14] D. R. Gaskell, "*Introduction to the Thermodynamics of Materials*", Fifth Edit. Taylor and Francis Books Inc.: London., 2003.

### **Chapter 3:**

- [1] Z. Bao, L. Yu, I. Vasiliev, Q. Ren, X. Lu and S. Deng, "Adsorption of Ethane , Ethylene , Propane , and Propylene on a Magnesium-Based Metal À Organic Framework", *Langmuir.*, vol. 27, pp. 13554–13562, 2011.
- [2] A. Anson, Y. Wang, C.C.H. Lin, T.M. Kuznicki and S.M. Kuznicki, "Adsorption of ethane and ethylene on modified ETS-10", *Chem. Eng. Sci.*, vol. 63, pp. 4171–4175, 2008.
- [3] D. M. Ruthven, "Principle of adsorption and adsorption processes." John Wiley & Sons, Inc., 1984.
- [4] Y. Wu, H. Chen, D. Liu, Y. Qian, and H. Xi, "Adsorption and separation of ethane /ethylene on ZIFs with various topologies : Combining GCMC simulation with the ideal adsorbed solution theory ( IAST )," *Chem. Eng. Sci.*, vol. 124, pp. 1–10, 2014.
- [5] A. Farjoo, F. Khorasheh, S. Niknaddaf and M. Soltani, "Kinetic modeling of side reactions in propane dehydrogenation over Pt - Sn/ $\gamma$  - Al<sub>2</sub>O<sub>3</sub> catalyst", *Sci. Iran.*, vol. 18, pp. 458–464, 2011.

- [6] E. Finocchio, G. Ramis, G. Busca, V. Lorenzelli and R.J. Willey, "On the mechanisms of light alkane catalytic oxidation and an FT-IR study of the n-butane conversion over MgCr<sub>2</sub>O<sub>4</sub> and a Mg-vanadate catalyst", *Catal. Rev.*, vol 28, pp. 381–389, 1996.
- [7] D. Shee and A. Sayari, "Light alkane dehydrogenation over mesoporous Cr<sub>2</sub>O<sub>3</sub>/Al<sub>2</sub>O<sub>3</sub> catalysts", *Applied Catal. A, Gen.* vol. 389, pp. 155–164, 2010.
- [8] M. Lee, B.M. Nagaraja, K. Young and K. Jung, "Dehydrogenation of alkane to light olefin over PtSn/θ-Al<sub>2</sub>O<sub>3</sub> catalyst: Effects of Sn loading", *Catal. Today.*, vol. 232, pp. 53–62, 2011.
- [9] A. Van Miltenburg, W. Zhu, F. Kapteijn and J. A. Moulijn, "Adsorptive Separation of Light Olefin/Paraffin Mixtures", *Chem. Eng. Res. Des.*, vol. 84, pp. 350–354, 2006.
- [10] S. Hosseinpour, S. Fatemi, Y. Mortazavi, M. Gholamhoseini and M.T. Ravanchi, "Performance of CaX Zeolite for Separation of C<sub>2</sub>H<sub>6</sub> , C<sub>2</sub>H<sub>4</sub> , and CH<sub>4</sub> by Adsorption Process; Capacity, Selectivity, and Dynamic Adsorption Measurements', *Sci. Technol.*, vol. 46, pp. 349–355, 2010.
- [11] R.T. Yang and E.S. Kikkinides, "New Sorbents for Olefinparaffin Separations by Adsorption via  $\pi$ -Complexation", *AIChE J.*, vol. 41, pp. 509–517, 1995.

- [12] R. V Jasra and S.G.T. Bhat, "Thermal desorption of normal paraffins from zeolite 5A", *Zeolites.*, vol. 7, pp. 1985–1988, 1987.
- [13] M. Mofarahi and S.M. Salehi, "Pure and binary adsorption isotherms of ethylene and ethane on zeolite 5A", *Adsorption*, vol. 19, pp. 101–110, 2012.
- [14] A. Romero-Perez and G. Aquilar-Armenta, "Adsorption Kinetics and Equilibria of Carbon Dioxide , Ethylene , and Ethane on 4A ( CECA ) Zeolite", *J. Chem. Eng. Data.*, vol. 55, pp. 3625–3630, 2011.
- [15] A. Van Miltenburg, W. Zhu, F. Kapteijn and J. A. Moulijn, "Adsorptive Separation of Light Olefin/Paraffin Mixtures", *Chem. Eng. Res. Des.*, vol. 84, pp. 350–354, 2006.
- [16] D. Hilden and R. F. Stebar, "Evaluation of acetylene as a spark ignition engine fuel", *Energy Res. Soc. Sci.*, vol. 3, pp. 59–71, 1979.
- [17] A. Wehrmeier and B. Dellinger, "Role of Copper Species in Chlorination and Condensation Reactions of Acetylene", *Environ. Sci. Technol.*, vol. 32, pp. 2741–2748, 1998.
- [18] D.W. Breck, "Zeolite Molecular Sieves: Structure, Chemistry, and Use," no. John Wiley & Sons, Ltd, 1974.
- [19] A. Alberti, "The Crystal Structure of Two Clinoptilolites", *Tschermaks Min. Petr. Mitt.*, vol. 22, pp. 25–37, 1975.

- [20] D. L. Bish and M. D.W., "Natural Zeolites: Occurrence, Properties, Application", *Rev. Miner. Geochemistry*, vol. 45, 2001.
- [21] W. An, P. Swenson, L. Wu, T. Waller, A. Ku and S.M. Kuznicki, "Selective separation of hydrogen from C1/C2 hydrocarbons and CO<sub>2</sub> through dense natural zeolite membranes", *J. Memb. Sci.*, vol. 369, pp. 414–419, 2011.
- [22] S. Liu, M. Lim and R. Amal, "TiO<sub>2</sub> -coated natural zeolite : Rapid humic acid adsorption and effective photocatalytic regeneration", *Chem. Eng. Sci.*, vol. 105, pp. 46–52, 2014.
- [23] M. Hasheminejad and A. Nezamzadeh-ejhieh, "A novel citrate selective electrode based on surfactant modified nano-clinoptilolite, *Food Chem.*, vol. 172, pp. 794–801, 2015.
- [24] H. Li and R. Dittmeyer, "Inorganic microporous membranes for H<sub>2</sub> and CO<sub>2</sub> separation-Review of experimental and modeling process", *Chem. Eng. Sci.*, vol. 147, pp. 401-417, 2015.
- [25] M. W. Ackley, S.U. Rege, H. Saxena, "Application of natural zeolites in the purification and separation of gases", *Microporous Mesoporous Mater.*, vol. 61, pp. 25–42, 2003.
- [26] T.C. Frankiewicz and R.G. Donnelly, "Methane/ Nitrogen Gas Separation over the Zeolite Clinoptilolite by the Selective Adsorption", *Ind. Gas Sep.*, pp. 213–233, 1983.

- [27] M.W. Ackley, and R.T. Yang, "Adsorption Characteristics of High-Exchange Clinoptilolites", *Ind. Eng. Chem. Res.*, vol 30, pp. 2523–2530, 1991.
- [28] D.O. Connor, P. Barnes, R. Bates and D.F. Lander, "A hydration-controlled nano-valve in a zeolite", *Chem. Commun.*, pp. 2527–2528, 1998.
- [29] G. Engelhardt and U. Lohse, "High resolution Si n.m.r of dealuminated and ultrastable Y-zeolites", *Zeolites.*, vol. 2, pp. 59–62, 1982.
- [30] G. Engelhardt and U. Lohse, "High resolution Si n.m.r of dealuminated Y-Zeolites", *Zeolites.*, vol. 3, pp. 233–238, 1983.
- [31] G. Engelhardt, and V. Patzelova, "Unit Cell Constants of Zeolites Stabilized by Dealumination", *Cryst. Res. Technol.* vol. 19, pp. 6–8, 1983.
- [32] J. Datka, W. Kolidziejski, J. Klinowski, B. Sulikowski, "Dealumination of zeolite Y by H<sub>4</sub>EDTA", *Catal. Letters.*, vol. 19, pp.159–165, 1993.
- [33] A.T. Steel, "Time dependence of the structural changes occurring in NH<sub>4</sub>-Y zeolite on dealumination: A preliminary study using energy-dispersive X-ray diffraction", *Zeolites.*, vol. 13, pp. 336–340, 1993.
- [34] S. Dzwigaj, M.J. Peltre, P. Massiani, A. Davidson, M. Che and T. Sen, "Incorporation of vanadium species in a dealuminated b zeolite", *Chem. Commun.* pp. 87–88, 1998.

- [35] P. Bartl and W.F. Holderich, "A study of the dealumination methods for zeolite L", *Microporous Mesoporous Mater.*, vol. 38, pp. 279–286, 2000.
- [36] M. Silaghi, C. Chizallet and P. Raybaud, "Challenges on molecular aspects of dealumination and desilication of zeolites", *Microporous and Mesoporous Mater.* vol. 191, pp. 82–96, 2014.
- [37] J.M. Müller, G.C. Mesquita, S.M. Franco, L.D. Borges, J.L. De Macedo and J.A. Dias, , "Solid-state dealumination of zeolites for use as catalysts in alcohol dehydration", *Microporous Mesoporous Mater.*, vol. 204, pp. 50–57, 2015.
- [38] Y. Wang, F. Lin and W. Pang, "Ammonium exchange in aqueous solution using Chinese natural clinoptilolite and modified zeolite", *J. Hazard. Mater.*, vol 142, pp. 160–164, 2007.
- [39] J.B. Lee, H.H. Funke, R.D. Noble, J.L. Falconer, "High selectivities in defective MFI membranes", *J. Memb. Sci.*, vol 321, pp. 309–315, 2008.
- [40] É. Tyrrell, E.F. Hilder, R.A. Shalliker, G.W. Dicoski, R.A. Shellie and M.C. Breadmore, "Packing procedures for high efficiency , short ion-exchange columns for rapid separation of inorganic anions", *J. Chromatogr. A.*, vol. 1208, pp. 95–100, 2008.
- [41] Z. Huang, Q. Subhani, Z. Zhu, W. Guo and Y. Zhu, "A single pump cycling-column-switching technique coupled with homemade high exchange capacity

columns for the determination of iodate in iodized edible salt by ion chromatography with UV detection", *Food Chem.*, vol. 139, pp. 144–148, 2013.

- [42] A. Omegna, M. Haouas, A. Kogelbauer, R. Prins, Realumination of dealuminated HZSM-5 zeolites by acid treatment : a reexamination, *Microporous Mesoporous Mater.*, vol 46, pp. 177–184, 2001.
- [43] M. Roži, S. Cerjan-Stefanovic, S. Kurajica, M. Rozmaric Maefat, K. Margeta and A. Farkas, "Decationization and dealumination of clinoptilolite tuff and ammonium exchange on acid-modified tuff", *J. Colloid Interface Sci.*, vol. 284 pp. 48–56, 2005.
- [44] L.Parker and D. Bibby, "Synthesis and some properties of two novel zeolites, KZ-1 and KZ-2", *Zeolites.*, vol. 3, pp. 8–11, 1983.
- [45] D.C. Organique and D. Recherche, "Hydration of n-Butenes Using Zeolite Catalysts influence of the Aluminium Content on Activity", *J. Catal.*, vol. 89 pp. 60–68, 1984.
- [46] I. Halasz, M. Agarwal, B. Marcus and W.E. Cormier, "Molecular spectra and polarity sieving of aluminum deficient hydrophobic H-Y zeolites", *Microporous Mesoporous Mater.*, vol. 84, pp. 318–331, 2005.
- [47] S. Yasyerli, I. Ar, G. Dogu and T. Dogu, "Removal of hydrogen sulfide by clinoptilolite in a fixed bed adsorber", *Chem. Eng. Process.*, vol. 41, pp. 785–792, 2002.

- [48] O. Korkuna, R. Leboda, J. Skubiszewska-Zieab, T. Vrublevs'ka, V.M. Gun'ko and J. Ryzkowski, "Structural and physicochemical properties of natural zeolites : clinoptilolite and mordenite", *Microporous Mesoporous Mater.*, vol. 87, pp. 243–254, 2006.
- [49] J.A. Kaduk and J. Faber, Crystal structure of zeolite Y as a function of ion exchange, *Rigaku J.*, vol. 12, pp. 14–34, 1995.
- [50] A.L. Myers, "Thermodynamics of Adsorption in porous materials", *AICHE J.*, vol. 48, pp. 145-160, 2002.

#### **Chapter 4:**

- [1] S. Nunes and K. Peinemann, "*Membrane Technology in the Chemical Industry*", John Wiley & Sons., 2006.
- [2] R. W. Baker, "Membrane technology," in "*Encyclopedia Of Polymer Science and Technology*", John Wiley & Sons, pp. 184–249, 2001.
- [3] K. W. Böddeker, "Liquid Separations with Membranes," in "*Liquid Separations with Membranes: An Introduction to Barrier Interference*", Springer, pp. 1–146, 2008
- [4] K. W. Boddeker, "Commentary : Tracing membrane science," *J. Memb. Sci.*, vol. 100, pp. 65–68, 1995.

- [5] D. L. Bish and J. W. Carey, "Thermal Behavior of Natural Zeolites," The Mineralogical Society Of America, pp. 403-452, 2001.
- [6] T. Matsuura, "Synthetic Membranes and membrane separation processes", CRC Press. 1993.
- [7] R. Abedini and A. Nezhadmoghadam, "Application of membranes in gas separation processes: Its suitability and mechanism," *Pet. Coal*, vol. 52, no. 2, pp. 69-80, 2010.
- [8] S. T. Hwang and K. Kammermeyer, "Membranes in separations," in "*Techniques of chemistry*", New York: John Wiley and Sons, p. 442, 1975.
- [9] Y. S. Lin, I. Kumakiri, B. N. Nair, and H. Alsyouri, "Microporous Inorganic Membranes" *Separation & Purif. Rev.*, vol. 31, no. 2., pp. 229-379, 2002.
- [10] S. L. Matson, J. Lopez, and A. Quinn, "Separation of gases with synthetic membranes-Review Article," *Chem. Eng. Sci.*, vol. 38, no. 4, pp. 503-524, 1983.
- [11] S. Sahebdehfar, M. T. Ravanchi, F. Tahriri Zangeneh, S. Mehrazma, and S. Rajabi, "Kinetic study of propane dehydrogenation and side reactions over Pt-Sn/Al<sub>2</sub>O<sub>3</sub> catalyst," *Chem. Eng. Res. Des.*, vol. 90, no. 8, pp. 1090-1097, 2012.
- [12] E. Gobina, K. Hou, and R. Hughes, "Ethane dehydrogenation in a catalytic membrane reactor coupled with a reactive sweep gas," *Chem. Eng. Sci.*, vol. 50, no. 14, pp. 2311-2319, 1995.

- [13] P. Kölsch, D. Venzke, M. Noack, P. Toussaint, and J. Caro, “Zeolite-in-metal membranes: preparation and testing,” *J. Chem. Soc., Chem. Commun*, vol. 2, no. 21, p. 2491, 1994.
- [14] L. Cot, J. Durand, C. Guizard, N. Hovnanian, and A. Julbe, “Inorganic membranes and solid state sciences,” vol. 2, pp. 313–334, 2000.
- [15] J. Caro and M. Noack, “Zeolite membranes – Recent developments and progress,” *Microporous Mesoporous Mater.*, vol. 115, no. 3, pp. 215–233, 2008.
- [16] Y. Gu and G. Meng, “A model for ceramic membrane formation by dip coating,” *J. Eur. Ceram. Soc.*, vol. 19, pp. 1961–1966, 1999.
- [17] H. Maghsoudi, “Defects of Zeolite Membranes: Characterization, Modification and Post-treatment Techniques,” *Sep. Purif. Rev.*, vol. 45, no. 3, pp. 169–192, 2016.
- [18] J. Caro, M. Noack, P. Kolsch, and R. Schafer, “Zeolite membranes ± state of their development and perspective,” *Microporous Mesoporous Mater.*, vol. 38, pp. 3–24, 2000.
- [19] E. E. Mcleary, J. C. Jansen, and F. Kapteijn, “Zeolite based films , membranes and membrane reactors: Progress and prospects,” *Microporous Mesoporous Mater.*, vol. 90, pp. 198–220, 2006.
- [20] J. Caro and M. Noack, “Zeolite Membranes – Status and Prospective,” in “*Advances in Nanoporous Materials*”, Elsevier B.V, vol. 1, pp. 1–96. 2009.

- [21] W. An, P. Swenson, L. Wu, T. Waller, A. Ku, and S. M. Kuznicki, "Selective separation of hydrogen from C1/C2 hydrocarbons and CO<sub>2</sub> through dense natural zeolite membranes," *J. Memb. Sci.*, vol. 369, pp. 414–419, 2011.
- [22] S. T. O. Yama, "Review on Mechanisms of Gas Permeation through Inorganic Membranes," vol. 54, pp. 298–309, 2011.
- [23] A. Julbe, "Zeolite membranes-synthesis, charactersitic and application," in "*Intorduction to zeolite science and practices*", Elsevier B.V., 2007.
- [24] J. Romero, C. Gijiu, J. Sanchez, and G. M. Rios, "A unified approach of gas, liquid and supercritical solvent transport through microporous membranes," *Chem. Eng. Sci.*, vol. 59, no. 7, pp. 1569–1576, 2004.
- [25] R.W. Rousseau, "Handbook of Separation Process Technology", John Wiley & Sons, 1987.
- [26] J. D. Seader, E. J. Henley, and D. K. Roper, "*Separation process principles: Chemical and biochemical operations*", 3rd ed., John Wiley & Sons, 2011.
- [27] J. Xiao and J. We, "Diffusion mechanism of hydrocarbons in zeolites-Analysis of experimental observations," *Chem. Eng. Sci.*, 1992.
- [28] J. Xiao and J. Wei, "Diffusion mechanism of hydrocarbons in zeolites-Theory," *Chem. Eng. Sci.*, vol. 47, pp. 1123-1141, 1992.

- [29] S. A. H. Hejazi, A. M. Avila, T. M. Kuznicki, A. Weizhu, and S. M. Kuznicki, "Characterization of natural zeolite membranes for H<sub>2</sub>/CO<sub>2</sub> separations by single gas permeation.," *Ind. Eng. Chem. Res.*, vol. 50, pp. 12717–12726, 2011.
- [30] R. Krishna and R. Baur, "Modelling issues in zeolite based separation processes," *Sep. Purif. Technol.*, vol. 33, pp. 213–254, 2003.
- [31] S. Thomas, R. Schäfer, J. Caro, and A. Seidel-morgenstern, "Investigation of mass transfer through inorganic membranes with several layers", *Catal. Today*, vol. 67, pp. 205–216, 2001.
- [32] E. A. Mason and A. P. Malinauskas, "*Gas Transport in Porous Media: The Dusty-Gas Model*", *Elsevier: Amsterdam*, 1983.
- [33] Y. S. Lin and M. C. Duke, "Recent progress in polycrystalline zeolite membrane research," *Curr. Opin. Chem. Eng.*, vol. 2, no. 2, pp. 209–216, 2013.
- [34] P. F. Lito, C. F. Zhou, A. S. Santiago, A. E. Rodrigues, J. Rocha, Z. Lin, and C. M. Silva, "Modelling gas permeation through new microporous titanosilicate AM-3 membranes", *Chemical Engineering J.*, vol. 165, pp. 395–404, 2010.
- [35] P. Bernardo, E. Drioli, and G. Golemme, "Membrane Gas Separation: A Review/State of the Art," *Ind. Eng. Chem. Res.*, vol. 48, no. 10, pp. 4638–4663, 2009.

## Chapter 5:

- [1] J. Caro, M. Noack, P. Kolsch, and R. Schafer, "Zeolite membranes  $\pm$  state of their development and perspective," *Microporous Mesoporous Mater.*, vol. 38, pp. 3–24, 2000.
- [2] B. Zornoza, C. Casado, A. Navajas," Renewable hydrogen technologies: production, purification, storage, applications and safety"; Elsevier B.V: Amsterdam,Netherland, 2013.
- [3] R. Abedini and A. Nezhadmoghadam, "Application of membranes in gas separation processes: Its suitability and mechanism," *Pet. Coal*, vol. 52, no. 2, pp. 69–80, 2010.
- [4] R. W. Baker, "Membrane technology," in *Encyclopedia Of Polymer Science and Technology*, vol. 3, Menlo Park; California, pp. 184–249, 2001.
- [5] T. Tomita, K. Nakayama, H. Sakai, "Gas separation characteristics of DDR type zeolite membrane", *Microporous Mesoporous Mater.*, vol. 68, pp. 71-75, 2004.
- [6] C. Hon, P. Li, F. Li, T. Chung and D.R. Paul, "Reverse-selective polymeric membranes for gas separations", *Prog. Polym. Sci.* vol. 38, pp. 740–766, 2013.
- [7] R.T. Yang, "Adsorbents:Fundamentals and Applications",John Wiley and Sons, 2003.
- [8] E. Environ, A.W. Thornton, D. Dubbeldam, M.S. Liu, B.P. Ladewig and J. Hill, "Energy & Environmental Science Feasibility of zeolitic imidazolate framework membranes for clean energy", *R. Soc. Chem.*, vol. 5, pp. 7637–7646, 2012

- [9] N.W. Ockwig, T.M. Nenoff, "Membranes for hydrogen separation", *Chem. Rev.*, vol. 107, pp. 4078–110, 2007.
- [10] M.S. Li, Z.P. Zhao and M.X. Wang, "Controllable modification of polymer membranes by LDDLT plasma flow: membrane module scale-up and hydrophilic stability", *Chem. Eng. Sci.*, vol. 122, pp. 53–63, 2015.
- [11] X. Gu, Z. Tang and J. Dong, "On-stream modification of MFI zeolite membranes for enhancing hydrogen separation at high temperature", *Microporous Mesoporous Mater.*, vol. 111, pp. 441–448, 2008.
- [12] J. Caro and M. Noack, "Zeolite membranes – Recent developments and progress", *Microporous Mesoporous Mater.*, vol. 115, pp. 215–233, 2008.
- [13] Y.S. Lin and M.C. Duke, "Recent progress in polycrystalline zeolite membrane research", *Curr. Opin. Chem. Eng.*, vol. 2, pp. 209–216, 2013.
- [14] M.W. Ackley, R.F. Giese and R.T. Yang, "Clinoptilolite: Untapped potential for kinetic gas separations", *Zeolites*, vol. 12, pp. 780–788, 1992.
- [15] D.L. Bish and J.M. Boak, "Clinoptilolite-Heulandite Nomenclature", Los Alamos National Laboratory, Los Alamos, New Mexico, USA, 2001.
- [16] W. Ackley, Mark, S.U. Rege and H. Saxena, "Application of natural zeolites in the purification and separation of gases", *Microporous Mesoporous Mater.* vol. 61, pp. 25–42, 2003.

- [17] W. An, X. Zhou, X. Liu, P.W. Chai, T. Kuznicki and S.M. Kuznicki, "Natural zeolite clinoptilolite-phosphate composite Membranes for water desalination by pervaporation", *J. Memb. Sci.*, vol. 470, pp. 431–438, 2014.
- [18] D.W. Breck, "Zeolite Molecular Sieves: Structure, Chemistry, and Use," no. John Wiley & Sons, 1974..
- [19] M. Nasrollahzadeh, D. Habibi, Z. Shahkarami and Y. Bayat, "A general synthetic method for the formation of arylaminotetrazoles using natural natrolite zeolite as a new and reusable heterogeneous catalyst", *Tetrahedron.*, vol. 65, pp. 10715–10719, 2009.
- [20] S. Wang and Y. Peng, "Natural zeolites as effective adsorbents in water and wastewater treatment", *Chem. Eng. J.*, 156, pp. 11–24, 2010.
- [21] L.B. Mccusker and D.H. Olson, "Atlas of Zeolite Framework Types", Elsevier, 2007.
- [22] Y. S. Lin, I. Kumakiri, B. N. Nair, and H. Alsyouri, "Microporous Inorganic Membranes," in "*Separation and Purification Methods*", vol. 31, no. 2, pp. 229–379, 2002.
- [23] R. Szostak, "Handbook of Molecular Sieves", New York: Van Nostrand Reinhold, 1992.
- [24] <http://www.iza-structure.org>.

- [25] A.W. Thornton, T. Hilder, A.J. Hill and J.M. Hill, "Predicting gas diffusion regime within pores of different size, shape and composition", *J. Memb. Sci.*, vol. 336, pp. 101–108, 2009.
- [26] J. Dong, Y.S. Lin, M. Kanezashi and Z. Tang, "Microporous inorganic membranes for high temperature hydrogen purification", *J Applied Phycis*, vol. 104, pp. 1-17, 2013.
- [27] F. Gallucci, E. Fernandez, P. Corengia and M. van Sint Annaland, "Recent advances on membranes and membrane reactors for hydrogen production", *Chem. Eng. Sci.*, vol. 92, pp. 40–66, 2013.
- [28] N. Nishiyama, M. Yamaguchi, T. Katayama, Y. Hirota, M. Miyamoto and Y. Egashira, "Hydrogen-permeable membranes composed of zeolite nano-blocks", *J. Memb. Sci.*, vol. 306, pp. 349–354, 2007.
- [29] S. Battersby, T. Tasaki, S. Smart, B. Ladewig, S. Liu and M.C. Duke, "Performance of cobalt silica membranes in gas mixture separation", *J. Memb. Sci.*, vol. 329, pp. 91–98, 2009
- [30] W. An, P. Swenson, L. Wu, T. Waller, A. Ku and S.M. Kuznicki, "Selective separation of hydrogen from C1/C2 hydrocarbons and CO<sub>2</sub> through dense natural zeolite membranes", *J. Memb. Sci.*, vol. 369, pp. 414–419, 2011.

- [31] W. An, P. Swenson, A. Gupta, L. Wu, T.M. Kuznicki and S.M. Kuznicki, "Improvement of H<sub>2</sub>/CO<sub>2</sub> selectivity of the natural clinoptilolite membranes by cation exchange modification", *J. Memb. Sci.*, vol. 433, pp. 25–31, 2013.
- [32] T.F. Narbeshuber, H. Vinek and J.A. Lercher, "Monomolecular conversion of light alkanes over H-ZSM-5", *J. Catal.*, vol. 157, pp. 388-395, 1995.
- [33] A. Farjoo, F. Khorasheh, S. Niknaddaf and M. Soltani, "Kinetic modeling of side reactions in propane dehydrogenation over Pt - Sn/ $\gamma$  - Al<sub>2</sub>O<sub>3</sub> catalyst", *Sci. Iran.*, vol. 18, pp. 458-464, 2011
- [34] A.M. Avila, Z. Yu, S. Fazli, J.A. Sawada, S.M. Kuznicki, "Hydrogen-selective natural mordenite in a membrane reactor for ethane dehydrogenation", *Microporous Mesoporous Mater.*, vol. 190, pp. 301–308, 2014.
- [35] A.H. Shafie, W. An, S.A. Hosseinzadeh Hejazi, J. a. Sawada, S.M. Kuznicki, "Natural zeolite-based cement composite membranes for H<sub>2</sub>/CO<sub>2</sub> separation", *Sep. Purif. Technol.* 88 (2012) 24–28. doi:10.1016/j.seppur.2011.11.020.
- [36] R.D. Noble, "Perspectives on mixed matrix membranes", *J. Memb. Sci.*, vol. 378 pp. 393–397, 2011.
- [37] A.M. Abyzov, S. V. Kidalov and F.M. Shakhov, "High thermal conductivity composites consisting of diamond filler with tungsten coating and copper (silver) matrix", *J. Mater. Sci.*, vol. 46, pp. 1424–1438, 2011.

- [38] C. Joyce, L. Trahey, S.A. Bauer, F. Dogan and J.T. Vaughey, "Metallic copper binders for lithium-ion battery silicon electrodes", *J. Electrochem. Soc.* vol. 159, pp. 909–914, 2012.
- [39] D.K.R. Bevington and Philip R., "Data reduction and error analysis for the physical sciences", 3rd ed., Mc Graw-Hill Companies, 2003.
- [40] S.A.H. Hejazi, A.M. Avila, T.M. Kuznicki, A. Weizhu and S.M. Kuznicki, "Characterization of natural zeolite membranes for H<sub>2</sub>/CO<sub>2</sub> separations by single gas permeation", *Ind. Eng. Chem. Res.*, vol. 50, pp. 12717–12726, 2011.
- [41] J. A. Ritter and A.D. Ebner, "State of the Art Adsorption and Membrane Separation Processes for Hydrogen Production in the Chemical and Petrochemical Industries", *Sep. Sci. Technol.*, vol. 42 , pp. 1123–1193, 2007.
- [42] A.M. Tarditi, E.A. Lombardo and A.M. Avila, "Xylene permeation transport through composite Ba-ZSM-5/SS tubular membranes : modeling the steady-state permeation", *Ind. Eng. Chem. Res.*, vol. 47, pp. 2377–2385, 2008.
- [43] R.M. Barrer, "Porous Crystal Membranes", *J. Chem. Soc.*, vol. 86, pp. 1123–1130, 1990.
- [44] S. W. Webb, "Gas Phase Diffusion in Porous Media: Comparison of Models", Sandia National Laboratories, New Mexico, 1998.
- [45] E. A. Mason and A. P. Malinauskas, "*Gas Transport in Porous Media: The Dusty-Gas Model*", Elsevier: Amsterdam, 1983.

- [46] H. Li and R. Dittmeyer, "Inorganic microporous membranes for H<sub>2</sub> and CO<sub>2</sub> separation-Review of experimental and modeling process", Chem. Eng. Sci., vol. 127, pp. 401-417, 2015.
- [47] S. Colin, "Rarefaction and compressibility effects on steady and transient gas flows in microchannels", Microfluid Nanofluid., vol. 1, pp. 268–279, 2005.
- [48] S. Thomas, R. Schäfer, J. Caro and A. Seidel-Morgenstern, "Investigation of mass transfer through inorganic membranes with several layers", Catal. Today, vol. 67, pp. 205–216, 2001.
- [49] V.A. Alekseevich, V.V. Kurbatkina, A.A. Zaitsev, D. Andreevna, Sidorenko and S.I. Rupasov, "Copper based binder for the fabrication of diamond tools", US0325049, 2012.
- [50] K.S. Rothenberger, A. V Cugini, B.H. Howard, R.P. Killmeyer, M. V Ciocco and B.D. Morreale, "High pressure hydrogen permeance of porous stainless steel coated with a thin palladium film via electroless plating", J. Memb. Sci. vol. 244, pp. 55–68, 2004.
- [51] B. Sea and K. Lee, "Molecular sieve silica membrane synthesized in mesoporous  $\gamma$ -alumina layer", Bull. Korean Chem. Soc., vol. 22, pp. 1400–1402, 2001.
- [52] S. Yan, H. Maeda, K. Kusakabe and S. Morooka, "Thin palladium membrane formed in support pores by metal-organic chemical vapor deposition method and

application to hydrogen separation", *Ind. Eng. Chem. Res.*, vol. 33, pp. 616–622, 1994.

- [53] A. Huang, Y. Chen, Q. Liu, N. Wang, J. Jiang and J. Caro, "Synthesis of highly hydrophobic and permselective metal organic framework Zn(BDC)(TED)0.5 membranes for H<sub>2</sub>/CO<sub>2</sub> separation", *J. Memb. Sci.*, vol. 454, pp. 126–132, 2014.
- [54] R.M. De Vos and H. Verweij, "Improved performance of silica membranes for gas separation", *J. Memb. Sci.*, vol. 143, pp. 37–51, 1998.
- [55] H. Bux, F. Liang, Y. Li, J. Cravillon and M. Wiebcke, "Zeolitic imidazolate Framework molecular sieving membrane titania support", *J. Am. Chem. Soc.*, vol. 131, pp. 16000–16001, 2009.

## Chapter 6:

- [1] Y. Yampolskii, "Polymeric gas separation membranes," *Macromol. (ASC Publ.)*, vol. 45, no. 8, pp. 3298–3311, 2012.
- [2] R. W. Baker, "Membrane technology," in "*Encyclopedia of Polymer Science and Technology*", Jone Wiley and Sons, pp. 184–249, 2001.
- [3] S. Yan, H. Maeda, K. Kusakabe, and S. Morooka, "Thin palladium membrane formed in support pores by metal-organic chemical vapor deposition method and application to hydrogen separation", *Ind. Eng. Chem. Res.*, vol. 33, pp. 616–622, 1994.

- [4] K. S. Rothenberger, A. V Cugini, B. H. Howard, R. P. Killmeyer, M. V Ciocco, B. D. Morreale, R. M. Enick, F. Bustamante, I. P. Mardilovich, and Y. H. Ma, "High pressure hydrogen permeance of porous stainless steel coated with a thin palladium film via electroless plating," *J. Memb. Sci.*, vol. 244, pp. 55–68, 2004.
- [5] Y. Huang and R. Dittmeyer, "Preparation and characterization of composite palladium membranes on sinter-metal supports with a ceramic barrier against intermetallic diffusion," vol. 282, pp. 296–310, 2006.
- [6] D. Q. Vu, W. J. Koros, and S. J. Miller, "Mixed matrix membranes using carbon molecular sieves II. Modeling permeation behavior," *J. Memb. Sci.*, vol. 211, pp. 335–348, 2003.
- [7] S. Rafiq, Z. Man, S. Maitra, N. Muhammad, and F. Ahmad, "Kinetics of Thermal Degradation of Polysulfone/Polyimide Blended Polymeric Membranes," *J. Appl. Polym. Sci.*, vol. 123, pp. 3755-3763, 2012.
- [8] B. Zornoza, B. Seoane, J. M. Zamaro, C. Tøllez, and J. Coronas, "Combination of MOFs and Zeolites for Mixed-Matrix Membranes," *ChemphysChem*, vol. 12, pp. 2781–2785, 2011.
- [9] C. Casado-coterillo, J. Soto, M. T. Jimare, S. Valencia, A. Corma, C. Tellez, and J. Coronas, "Preparation and characterization of ITQ-29/polysulfone mixed-matrix membranes for gas separation: Effect of zeolite composition and crystal size," *Chem. Eng. Sci.*, vol. 73, pp. 116–122, 2012.

- [10] L. Cot, J. Durand, C. Guizard, N. Hovnanian, and A. Julbe, “Inorganic membranes and solid state sciences”, *Solid States Sciences*, vol. 2, pp. 313–334, 2000.
- [11] S. Battersby, T. Tasaki, S. Smart, B. Ladewig, S. Liu, M. C. Duke, V. Rudolph, and J. C. Diniz, “Performance of cobalt silica membranes in gas mixture separation”, *J. Memb. Sci.*, vol. 329, pp. 91–98, 2009.
- [12] J. B. Miller, B. D. Morreale, M. W. Smith, and W. Virginia, “Pd-Alloy membranes for hydrogen separation,” in “*The chemistry and physics of separation by dense metal membranes*”, Elsevier B.V., pp. 135–161, 2014.
- [13] N. Nishiyama, M. Yamaguchi, T. Katayama, Y. Hirota, M. Miyamoto, Y. Egashira, K. Ueyama, K. Nakanishi, T. Ohta, A. Mizusawa, and T. Satoh, “Hydrogen-permeable membranes composed of zeolite nano-blocks,” *J. Memb. Sci.*, vol. 306, pp. 349–354, 2007.
- [14] W. Ackley, Mark, S. U. Rege, and H. Saxena, “Application of natural zeolites in the purification and separation of gases”, *Microporous Mesoporous Mater.*, vol. 61, pp. 25–42, 2003.
- [15] D.W. Breck, “Zeolite Molecular Sieves: Structure, Chemistry, and Use,” no. John Wiley & Sons, Ltd, 1974.
- [16] R. Szostak, “Handbook of Molecular Sieves”, New York: Van Nostrand Reinhold, 1992.

- [17] R. M. Barrer, "Porous Crystal Membranes", *J. Chem. Soc.*, vol. 86, no. 7, pp. 1123–1130, 1990.
- [18] E. E. Mcleary, J. C. Jansen, and F. Kapteijn, "Zeolite based films , membranes and membrane reactors: Progress and prospects", *Microporous Mesoporous Mater.*, vol. 90, pp. 198–220, 2006.
- [19] K. Kusakabe, S. Yoneshige, A. Murata, and S. Morooka, "Morphology and gas permeance of ZSM-5-type zeolite membrane formed on a porous  $\alpha$ -alumina support tube," *J. Memb. Sci.*, vol. 116, pp. 39–46, 1996.
- [20] J. Dong, Y. S. Lin, M. Z. Hu, R. A. Peascoe, and E. A. Payzant, "Template-removal-associated microstructural development of porous-ceramic-supported MFI zeolite membranes," *Microporous mesoporous Mater.*, vol. 34, pp. 241–253, 2000.
- [21] G.V.Tsitsishvili, N.S.Skhirtladze, T.G.Andronikashvili, V.G.Tsitsishvili, and A.V.Dolidze, "Natural zeolites of Georgia: occurrences, properties, and application," in "*Porous Materials in Environmentally Friendly Processes*", vol. 125, Elsevier Science B.V., 1999, pp. 715–722.
- [22] A. S. Zarchy, Amawalk, R. Correia, Elmsford, C. C. Chao "Process for the adsorption of hydrogen sulfide with clinoptilolite molecular sieves", US005164076, 1992.

- [23] M. Nasrollahzadeh, D. Habibi, Z. Shahkarami, and Y. Bayat, “A general synthetic method for the formation of arylaminotetrazoles using natural natrolite zeolite as a new and reusable heterogeneous catalyst”, *Tetrahedron*, vol. 65, no. 51, pp. 10715–10719, 2009.
- [24] S. Wang and Y. Peng, “Natural zeolites as effective adsorbents in water and wastewater treatment,” *Chem. Eng. J.*, vol. 156, no. 1, pp. 11–24, 2010.
- [25] M. P. Pina, M. Arruebo, M. Felipe, F. Fleta, M. P. Bernal, and J. Santamar, “A semi-continuous method for the synthesis of NaA zeolite membranes on tubular supports,” *J. Memb. Sci.*, vol. 244, pp. 141–150, 2004.
- [26] G. Yang, X. Zhang, S. Liu, K. Lun, and J. Wang, “A novel method for the assembly of nano-zeolite crystals on porous stainless steel microchannel and then zeolite film growth,” *J. Phys. Chem. Solids*, vol. 68, pp. 26–31, 2007.
- [27] J. Caro, M. Noack, P. Kolsch, and R. Schafer, “Zeolite membranes  $\pm$  state of their development and perspective,” *Microporous Mesoporous Mater.*, vol. 38, pp. 3–24, 2000.
- [28] W. T. Schaller and U. S. Geological, “the Mordenite-Ptilolite Group; Clinoptilolite, a New Species,” *Mineral. Soc. Am.*, vol. 8, pp. 128–134, 1923.
- [29] F. A. and Mumpton, “The american mineralogist, vol. 45, march\_april, 1960,” *Am. Mineral.*, vol. 45, pp. 351–369, 1960.

- [30] W. An, P. Swenson, L. Wu, T. Waller, A. Ku, and S. M. Kuznicki, "Selective separation of hydrogen from C1/C2 hydrocarbons and CO<sub>2</sub> through dense natural zeolite membranes," *J. Memb. Sci.*, vol. 369, pp. 414–419, 2011.
- [31] A. H. Shafie, W. An, S. A. Hosseinzadeh Hejazi, J. Sawada, and S. M. Kuznicki, "Natural zeolite-based cement composite membranes for H<sub>2</sub>/CO<sub>2</sub> separation," *Sep. Purif. Technol.*, vol. 88, pp. 24–28, 2012.
- [32] A. Farjoo, F. Khorasheh, S. Niknaddaf, and M. Soltani, "Kinetic modeling of side reactions in propane dehydrogenation over Pt - Sn/ $\gamma$ -Al<sub>2</sub>O<sub>3</sub> catalyst," *Sci. Iran.*, vol. 18, no. 3, pp. 458–464, 2011.
- [33] A. M. Avila, Z. Yu, S. Fazli, J. A. Sawada, and S. M. Kuznicki, "Materials Hydrogen-selective natural mordenite in a membrane reactor for ethane dehydrogenation," *Microporous mesoporous Mater.*, vol. 190, pp. 301–308, 2014.
- [34] M. Rajiv, D. Q. Vu, and W. J. Koros, "Mixed Matrix Membranes Materials: An Answer to the Challenges Faced by Membrane Based Gas Separations Today," *J. Chin. Inst. Chem. Engrs.*, vol. 33, pp. 77-86, 2002.
- [35] Y. Gu and G. Meng, "A model for ceramic membrane formation by dip coating," *J. Eur. Ceram. Soc.*, vol. 19, pp. 1961–1966, 1999.
- [36] M. Norio, Y. Okamoto, J. Tamaki, K. Morinaga, and N. Yamazoe, "Oxygen semipermeability of mixed conductive oxide thick-film prepared by slip casting," *Solid State Ionics*, vol. 79, pp. 195–200, 1995.

- [37] “The preparation and characterization of alumina membranes with ultrafine pores,” *J. Colloid Interface Sci.*, vol. 105, no. 1, pp. 27–40, 1985.
- [38] “<http://www.accumetmaterials.com/refractobond.htm>.” .
- [39] B. L. Krasnyi, V. P. Tarasovskii, and A. B. Krasnyi, “Study of the effect of Aluminosilicate binder chemical composition on physicochemical properties of porous permeable ceramic,” *Refract. Ind. Ceram.*, vol. 52, no. 6, pp. 405–408, 2012.
- [40] A. S. Wagh and S. Y. Jeong, “Chemically Bonded Phosphate Ceramics: III, Reduction Mechanism and Its Application to Iron Phosphate Ceramics,” *J. Am. Ceram. Soc.*, vol. 55, pp. 1850–1855, 2003.
- [41] J. H. . Hampton, S. B. Savage, and D. R.A.L, “Experimental analysis and modeling of slip casting,” *J. Am. Ceram. Soc.*, vol. 71, no. 12, pp. 1040–1045, 1988.
- [42] F. M. Tiller and C. Tsai, “Theory of filtration of ceramics : I , slip casting,” *J. Am. Ceram. Soc.*, vol. 69, no. 12, pp. 882–87, 1986.
- [43] D. S. Adcock and I. Mcdowall, “The mechanism of filter pressing and slip casting,” *J. Am. Ceram. Soc.*, vol. 40, no. 10, pp. 355–360, 1956.
- [44] W. An, P. Swenson, A. Gupta, L. Wu, T. M. Kuznicki, and S. M. Kuznicki, “Improvement of H<sub>2</sub>/CO<sub>2</sub> selectivity of the natural clinoptilolite membranes by cation exchange modification,” *J. Memb. Sci.*, vol. 433, pp. 25–31, 2013.

- [45] Y. S. Lin, I. Kumakiri, B. N. Nair, and H. Alsyouri, "Microporous Inorganic Membranes," in "*Separation and Purification Methods*", vol. 31, no. 2, pp. 229–379, 2002.
- [46] S. A. H. Hejazi, A. M. Avila, T. M. Kuznicki, A. Weizhu, and S. M. Kuznicki, "Characterization of natural zeolite membranes for H<sub>2</sub>/CO<sub>2</sub> separations by single gas permeation," *Ind. Eng. Chem. Res.*, vol. 50, pp. 12717–12726, 2011.
- [47] E. A. Mason and A. P. Malinauskas, "*Gas Transport in Porous Media: The Dusty-Gas Model*", Elsevier: Amsterdam, 1983.
- [48] S. W. Webb, "Gas Phase Diffusion in Porous Media: Comparison of Models", Sandia National Laboratories, New Mexico, 1998.
- [49] S. Colin, "Rarefaction and compressibility effects on steady and transient gas flows in microchannels," *Microfluid Nanofluid*, vol. 1, pp. 268–279, 2005.
- [50] R. Krishna and R. Baur, "Modelling issues in zeolite based separation processes," *Sep. Purif. Technol.*, vol. 33, pp. 213–254, 2003.
- [51] J. Xiao and J. Wei, "Diffusion mechanism of hydrocarbons in zeolites-Theory," *Chem. Eng. Sci.*, *Chem. Eng. Sci.*, vol. 47, pp. 1123-1141, 1992.
- [52] M. Kanezashi and Y. S. Lin, "Gas permeation and diffusion characteristics of MFI-type zeolite membranes at high temperatures", *J. Phys. Chem. C*, vol. 113, pp. 3767–3774, 2009.

- [53] A. M. Avila, H. H. Funke, Y. Zhang, J. L. Falconer, and R. D. Noble, "Concentration polarization in SAPO-34 membranes at high pressures," *J. Memb. Sci.*, vol. 335, pp. 32–36, 2009.
- [54] A.J. Burggraaf, "Important characteristics of inorganic membranes," in "Fundamentals of Inorganic Membrane Science and Technology", Elsevier Science B.V., 1996.
- [55] H. Li, K. Haas-Santo, U. Schygulla, and R. Dittmeyer, "Inorganic microporous membranes for H<sub>2</sub> and CO<sub>2</sub> separation—Review of experimental and modeling progress," *Chem. Eng. Sci.*, vol. 127, pp. 401–417, 2015.
- [56] O. Korkuna, R. Leboda, J. Skubiszewska-Zieab, T. Vrublevs'ka, V. M. Gun'ko, and J. Ryczkowski, "Structural and physicochemical properties of natural zeolites : clinoptilolite and mordenite," *Microporous Mesoporous Mater.*, vol. 87, pp. 243–254, 2006.
- [57] S. Yasyerli, I. Ar, G. Dogu, and T. Dogu, "Removal of hydrogen sulfide by clinoptilolite in a fixed bed adsorber," *Chem. Eng. Process.*, vol. 41, pp. 785–792, 2002.
- [58] J. Xiao and J. We, "Diffusion mechanism of hydrocarbons in zeolites-Analysis of experimental observations," *Chem. Eng. Sci.*, 1992.

- [59] A. M. Tarditi, E. A. Lombardo, and A. M. Avila, "Xylene permeation transport through composite Ba-ZSM-5/SS tubular membranes : modeling the steady-state permeation," *Ind. Eng. Chem. Res.*, vol. 47, pp. 2377–2385, 2008.
- [60] J. a. Ritter and A. D. Ebner, "State of the Art Adsorption and Membrane Separation Processes for Hydrogen Production in the Chemical and Petrochemical Industries," *Sep. Sci. Technol.*, vol. 42, no. 6, pp. 1123–1193, Apr. 2007.
- [61] M. Kanezashi, J. O. Brien-Abraham, and Y. S. Lin, "Gas Permeation Through DDR-Type Zeolite Membranes at High Temperatures," *AIChE J.*, vol. 54, no. 6, pp. 1478–1486, 2008.

## **Chapter 7:**

- [1] W. An, P. Swenson, L. Wu, T. Waller, A. Ku, and S. M. Kuznicki, "Selective separation of hydrogen from C1/C2 hydrocarbons and CO<sub>2</sub> through dense natural zeolite membranes," *J. Memb. Sci.*, vol. 369, no. 1–2, pp. 414–419, Mar. 2011.
- [2] N. W. Ockwig and T. M. Nenoff, "Membranes for hydrogen separation.," *Chem. Rev.*, vol. 107, no. 10, pp. 4078–110, Oct. 2007.
- [3] N. Nishiyama, M. Yamaguchi, T. Katayama, Y. Hirota, M. Miyamoto, Y. Egashira, K. Ueyama, K. Nakanishi, T. Ohta, A. Mizusawa, and T. Satoh, "Hydrogen-permeable membranes composed of zeolite nano-blocks," *J. Memb. Sci.*, vol. 306, pp. 349–354, 2007.
- [4] H. Verweij, Y. S. Lin, and J. Dong, "Microporous silica and zeolite membranes for hydrogen purification," *MRS Bull.*, vol. 31, pp. 756–764, 2006.

- [5] Z. a E. P. Vroon, K. Keizer, M. J. Gilde, H. Verweij, and a. J. Burggraaf, "Transport properties of alkanes through ceramic thin zeolite MFI membranes," *J. Memb. Sci.*, vol. 113, no. 2, pp. 293–300, 1996.
- [6] W. J. W. Bakker, L. J. P. Van Den Broeke, F. Kapteijn, and J. a Moulijn, "Temperature Dependence of One-Component Permeation through a Silicalite-1 Membrane," *AIChE J.*, vol. 43, no. 9, pp. 2203–2214, 1997.
- [7] Z. A. E. . Vroon, K. Keizer, A. . Burggraaf, and H. Verweij, "Preparation and characterization of thin zeolite MFI membranes on porous supports," *J. Memb. Sci.*, vol. 144, no. 1–2, pp. 65–76, 1998.
- [8] H. Li, K. Haas-Santo, U. Schygulla, and R. Dittmeyer, "Inorganic microporous membranes for H<sub>2</sub> and CO<sub>2</sub> separation—Review of experimental and modeling progress," *Chem. Eng. Sci.*, vol. 127, pp. 401–417, 2015.
- [9] P. Bernardo, E. Drioli, and G. Golemme, "Membrane Gas Separation: A Review/State of the Art," *Ind. Eng. Chem. Res.*, vol. 48, no. 10, pp. 4638–4663, May 2009.
- [10] M. Sadrzadeh, M. Amirilargani, and K. Shahidi, "Pure and mixed gas permeation through a composite polydimethylsiloxane membrane," no. June 2009, 2011.
- [11] J. Caro and M. Noack, "Zeolite Membranes – Status and Prospective," in *Advances in Nanoporous Materials*, vol. 1, Elsevier B.V, 2009, pp. 1–96.
- [12] J. Dong and Y. S. Lin, "Multicomponent Hydrogen / Hydrocarbon Separation by MFI-Type Zeolite Membranes," vol. 46, no. 10, pp. 1957–1966, 2000.
- [13] D. K. R. Bevington, Philip R., *Data reduction and error analysis for the physical*

*sciences*, 3rd ed. Mc Graw-Hill Companies, Inc., 2003.

- [14] S. Colin, "Rarefaction and compressibility effects on steady and transient gas flows in microchannels," *Microfluid Nanofluid*, vol. 1, pp. 268–279, 2005.
- [15] *Mason, E. A.; Malinauskas, A. P. Gas Transport in Porous Media: The Dusty-Gas Model; Elsevier: Amsterdam, 1983.*
- [16] S. Thomas, R. Schäfer, J. Caro, and A. Seidel-morgenstern, "Investigation of mass transfer through inorganic membranes with several layers," vol. 67, pp. 205–216, 2001.
- [17] J. a. Ritter and A. D. Ebner, "State of the Art Adsorption and Membrane Separation Processes for Hydrogen Production in the Chemical and Petrochemical Industries," *Sep. Sci. Technol.*, vol. 42, no. 6, pp. 1123–1193, Apr. 2007.
- [18] A. M. Tarditi, E. A. Lombardo, and A. M. Avila, "Xylene permeation transport through composite Ba-ZSM-5/SS tubular membranes : modeling the steady-state permeation," *Ind. Eng. Chem. Res.*, vol. 47, pp. 2377–2385, 2008.
- [19] A. H. Shafie, W. An, S. A. Hosseinzadeh Hejazi, J. a. Sawada, and S. M. Kuznicki, "Natural zeolite-based cement composite membranes for H<sub>2</sub>/CO<sub>2</sub> separation," *Sep. Purif. Technol.*, vol. 88, pp. 24–28, Mar. 2012.
- [20] A. E. Principles, "Adsorption Equilibria Adsorption Equilibria."
- [21] a. Wender, a. Barreau, C. Lefebvre, a. Lella, a. Boutin, P. Ungerer, and a. H. Fuchs, "Adsorption of n-alkanes in faujasite zeolites: molecular simulation study and experimental measurements," *Adsorption*, vol. 13, no. 5–6, pp. 439–451, Sep. 2007.